WYLE LABORATORIES

WYLE LABORATORIES RESEARCH STAFF

REPORT WR 70 - 6

VIBRO - ACOUSTIC STUDIES OF BUILDING 49A FOR FUTURE NASA MSC MISSIONS

FOR

MANNED SPACECRAFT CENTER
HOUSTON, TEXAS

JUNE 1970

NASA CR 108490

WYLE LABORATORIES RESEARCH STAFF
REPORT WR 70 - 6

VIBRO - ACOUSTIC STUDIES OF BUILDING 49A FOR FUTURE NASA MSC MISSIONS

FOR

MANNED SPACECRAFT CENTER
HOUSTON, TEXAS

JUNE 1970

WYLE LABORATORIES RESEARCH STAFF
REPORT WR 70-6

VIBRO-ACOUSTIC STUDIES OF BUILDING 49A FOR FUTURE NASA MSC MISSIONS

FOR

MANNED SPACECRAFT CENTER
HOUSTON, TEXAS

Prepared By:

Wyle Laboratories
128 Maryland Street
El Segundo, California

Under Contract Number NAS 9-7484

JUNE 1970

COPY NO. 2

FOREWORD

This report was prepared by the Research Staff of Wyle Laboratories, El Segundo, California, under Contract No. NAS9-7484, for NASA, Manned Spacecraft Center, Houston, Texas.

Contributing members included Richard Potter, Fancher Murray, Ben Sharp, Victor Mason, and Kenneth Eldred.

SUMMARY

Environmental testing of spacecraft during the 1970's will involve expansion of existing facilities. Building 49A of the Manned Spacecraft Center will be used for some combined loads testing of large vehicles. Test requirements are projected into the next decade to predict dimensions and capability requirements to be imposed upon Building 49A.

Expected pressure and thermal and dynamic loads are defined, and the requirements for simulation of these loads are discussed.

Testing concepts and philosophies are used to lay a basic groundwork, particularly as applied to acoustic testing. Specific numbers are then derived to describe modifications to Building 49A and test methods to be used therein. These include comparisons of reverberant versus progressive wave sound fields.

It is recommended that a steel or concrete liner be used to decrease room absorption. The height of the building is to be increased and both dimensions of the specimen access door will be increased to allow entrance of foreseeable vehicle components.

The modified building will be designed primarily to test the vehicles of the 1970's in a reverberant acoustic field, with local positive and negative enhancement where required on the specimen.

TABLE OF CONTENTS

LIST OF TABLES

LIST OF FIGURES

1.0 INTRODUCTION

This report has been prepared for NASA, Manned Spacecraft Center (MSC), under Contract Number NAS 9-7484. It represents an attempt to assess environmental testing requirements for the 70's as they pertain to the Spacecraft Acoustic Laboratory (SAL), Building 49A, at MSC in Houston. Since there are many unknowns in such an assessment, several decisions (particularly relating to the size of the facility) were necessary to enable the development of specific recommendations for the SAL. Wyle Laboratories gratefully acknowledges the assistance of MSC personnel in these decisions and in developing the vehicle sizes and general test requirements.

This report contains a discussion of the test requirements for the 70's, with emphasis on the types of vehicles of principal concern for manned space flights, the types of loads, and considerations related to interaction of these loads. It develops the general requirements for the acoustic test facility in terms of the estimated vehicle flight environments which may be simulated on the ground by acoustic testing, and discusses the tradeoffs between acoustic test methods for these purposes. Finally, it recommends general and detailed modifications to Building 49A to enable it to accomplish these potential test objectives.

2.0 COMBINED LOAD TESTING CONSIDERATIONS

An environmental test consists of three basic elements. They are:

- The failure or potential failure which the test is designed to investigate or against which the specimen is to be qualified.
- The loads which produce or contribute to the failure mode.
- The specimen or structure under investigation.

For illustration in this section, the structure is assumed to be a space launch vehicle and its environment is that encountered during launch and subsequent flight. However, the general conclusions drawn from the illustrations will be applicable to the much wider environmental test problem.

2.1 Failure Modes

In some ways, the failure mode is the most important of the three elements since it generally provides the reason for performing an environmental test. Failure modes are many and varied. Some of the more common examples have been listed by Eldred, Roberts and White (Reference 1), Crede (Reference 2), and Piersol (Reference 3). They cite a multitude of failures and malfunctions which can be classified under the broad heading of structural failures. This classification is a reasonable generalization since all the failures could be eliminated if the structure (be it part of the rocket main structure or a component in an electronic subsystem) were built with greater strength or rigidity. This can be illustrated by considering a few examples.

- Failure in buckling of the main structure of a rocket is obviously due to overstressing.
- Fatigue failures, whether of a support bracket or an electrical connecting wire, are overstressing structural failures.
- Microphonic effects in electronic circuitry could be overcome by building the circuits more ruggedly so they would not respond to the sound.
- Chatter in relays, although due basically to excess acceleration, could be corrected by increasing the structural stiffness of the relevant component in the relay.
- Misalignment of components due to relative displacement under load could be corrected by increased rigidity.

- Thermal stresses causing buckling or failure result because the structure is not strong enough to withstand its environment.

The list is endless, although it is possible to find some exceptions in the field of electronics. For example, the mutual interference between two electronic circuits due to electromagnetic radiation is in no way a structural failure. Practically without exception, however, majority of the failures encountered in an environmental test are structural in character.

2.2 Loads

The failures discussed above occur because of the structure's response to its environment. The environmental loads can be divided into four main categories.

(1) Static Loads.
These arise due to gravity, acceleration loads and rocket engine thrust, steady symmetrical or unsymmetrical aerodynamic forces, and the pressurization of various parts of the rocket structure. These loads produce static stresses in the vehicle.

(2) Direct Dynamic Structural Loads.
These result mainly from unsteady rocket thrust and oscillation in the propulsion system, with smaller contributions from auxiliary motors. They also result from engine start and shut-off, and shock associated with staging and landing. These loads produce dynamic stresses and displacements directly in the vehicle structure which, in turn, radiate noise into the vehicle.

(3) External Surface Pressure Fluctuations.
These include sound radiated from rocket combustion and unsteady aerodynamic forces such as boundary layer turbulence or oscillating shock waves. They produce exactly the same type of structural response as the dynamic structural loads.

(4) Thermal Loads.
These can result from aerodynamic heating, cryogenic cooling of the liquid fuels, or the burning of the rocket propellant. They produce dimensional changes in the structure which result in a complex static stress distribution. In addition, the resulting temperature changes may affect the structure's strength and fatigue properties.

It should be emphasized that these loads are time-varying quantities throughout flight, and their relative importance and interrelations are also time-varying. If any one load is severe enough, it can cause a structural failure. In practice, however, the loads act simultaneously and the structure may or may not be more sensitive to the combined load situation than to each load acting singly. As far as the structure is concerned, these four loads produce two types of stresses and deflections - static and dynamic. Thus, it is the static-dynamic interaction which is of prime interest and received the most attention.

A simple example of load interaction is the combination of end loads on the lateral vibration of a simply supported beam or plate. These problems were investigated by Eldred and Spice (Reference 4). They showed that the beam's natural frequencies increased with increasing tension and decreased with increasing compression loads until the fundamental beam frequency dropped to zero at the buckling load.

For the plate, the calculated effect was similar, except that with the application of compressive loads to one pair of opposite edges of the plate and tensile loads on the other pair, the results indicated no effect on the plate resonant frequencies under certain circumstances. However, experiments conducted on the response of a plate under compression across two opposite edges indicated that the practical effects were more complicated than the theory indicated. This work is also reported in Reference 4. It shows that the effective plate stiffness did indeed decrease as the load was increased from zero, but at a certain load the stiffness began to increase again until the effective stiffness was greater than the unloaded stiffness. This presumably indicates that the effect of the initial buckling of the plate was to increase its effective stiffness. With further increase in load, the stiffness again decreased. Additional tests, which included a pressure differential across the plate, indicated that the response problem became nonlinear under these conditions since the order in which the pressurization and compression loads were applied affected the ultimate response of the panel.

Other work has investigated the effect of static loads on cylinders and conical frustrums. In 1962, Weingarten (Reference 5) examined the effect of a bending moment on the vibration of a cylinder. He found that the modal resonant frequencies both decreased and increased in frequency with applied load. Later, Bozich (Reference 6) presented the results of a comprehensive theoretical analysis of the vibration characteristics of cylinders under the combined action of axial compression and external pressure. The data he presents is intended for use by a design engineer.

More recently, Mixson and Naumann (Reference 7) studied the vibration of a conical frustrum under axial load from both theoretical and practical aspects. References 6 and 7 both show that the natural frequencies of the structure are reduced with increasing compressive axial load, and that the effect on the higher modes having many radial and longitudinal nodal lines is proportionally much greater than the effect on the lower modes. All three references, i.e., 5, 6, and 7, indicate it is these higher modes that constitute the buckling modes of both the cylinder and conical frustrum. The other fact that consistently appears from these dynamic buckling tests (and from static buckling experiments) is that the practical buckling loads are always much less than the theoretically predicted buckling loads.

In the papers discussed above, the practical experiments were conducted on models. A paper by Kennedy and Saint (Reference 8), which discusses the results of a combined loads experiment on a full sized Saturn IV B Forward Skirt, Instrument Unit and Spacecraft Adapter, conducted at Wyle Laboratories in Huntsville, shows yet another side to the problem. Analysis of the results of this experiment showed that the response of the structure was nonlinear with increasing excitation levels unless a certain minimum static load was applied to the structure. The reason for this was not clear.

The above examples have shown that the application of static loads on a structure can significantly affect the structure's dynamic response. The principal effect is a reduction in the structure's resonant frequencies with increasing compressive loads, with the effect greater for the higher modes. Thus, the static loads will alter the vibration response characteristics of the structure and its subsystems.

2.3 Structural Test Specimen

The characteristics of the test specimen is the third element for an environmental test. It is necessary to choose enough structure around the intended test specimen to ensure that the specimen is being subjected to as near the correct loads as possible. This consideration has been discussed in some detail by Eldred (Reference 9) and is termed the "Structural Sufficiency Concept." This concept gives the basic criteria required for a decision on the size of the test structure to be used for the test and is outlined in Chart 1.

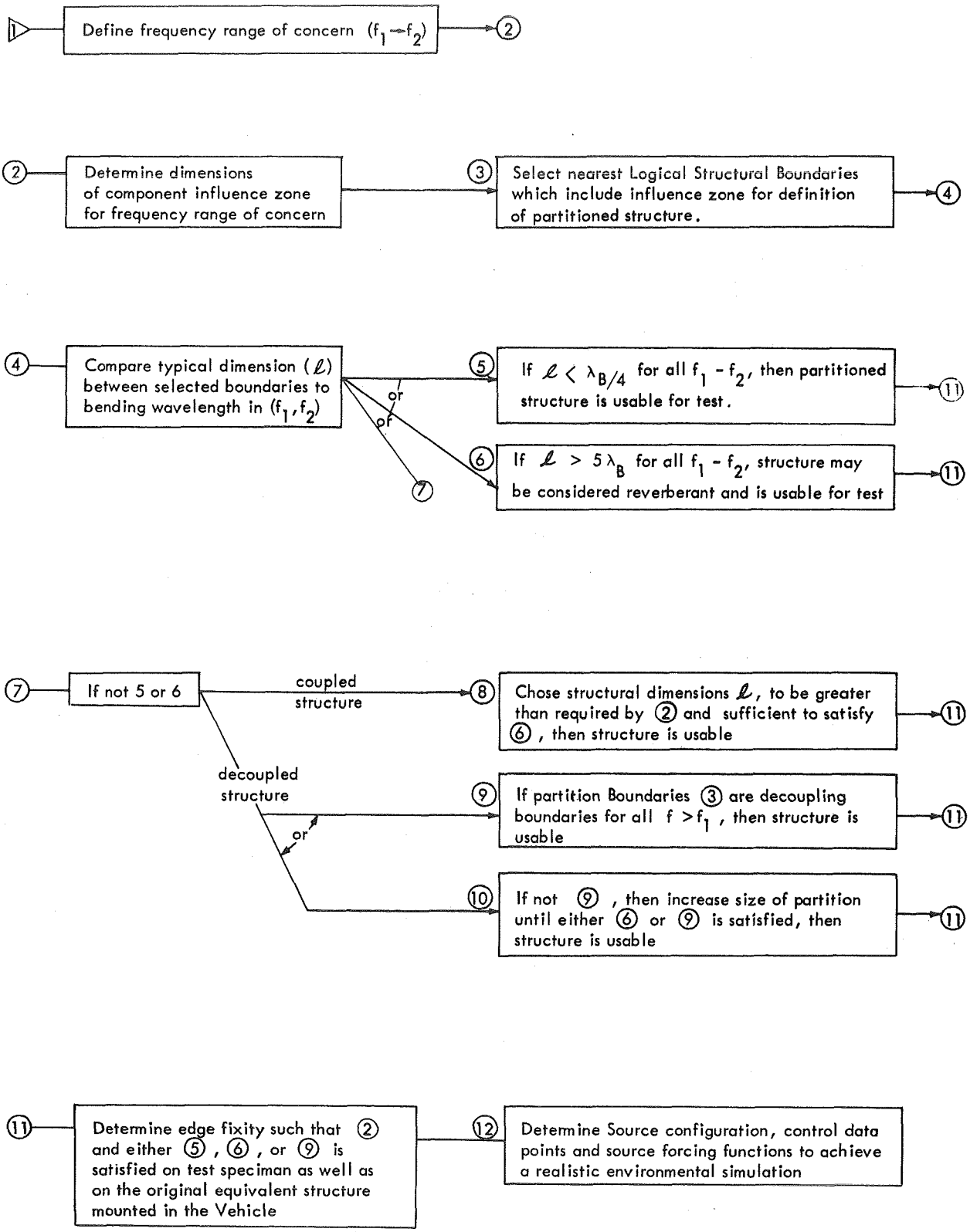

note: Values of ℓ / λ_B are only very approximate and are included for orientation only.

Chart 1: SUMMARY OF STRUCTURAL SUFFICIENCY CRITERIA CONCEPT

Reduced to its simplest form, the concept states that when a section of a large structure is removed from an environmental test, the test conditions will be inaccurate in the frequency range containing the lower resonances of the sectioned structure on its test mountings. These are the resonances introduced due to the removal of the test structure from the complete structure and mounting it in the test stand. Therefore, they are resonances which do not occur on the complete structure and hence will cause erroneous stress levels in their frequency region, even if the correct excitation spectra are applied.

Below the lowest of these artificial resonances, the correct vibration environment can be simulated by forcing the test structure in rigid body motion (i.e., all points in phase) of the appropriate amplitude.

Well above the frequency of the artificial resonances, the sectioned structure response will become a better approximation of the true response. The effect of the difference between the test mountings and the actual structural mountings will be important only in the region near the test mountings.

The concept therefore shows that a given specimen guarantees realistic structural test conditions only in certain restricted frequency regions, unless care is taken to ensure that the impedance of the mountings of the test specimen is the same as the impedance of the specimen connections to the complete structure. In practice, the situation is often eased considerably by careful choice of the dimensions of the test specimen so that the test specimen boundaries effectively decouple the test specimen from the rest of the structure. As an example, such a decoupling boundary could be a large stiff structural frame member.

The structural sufficiency concept, as described in the preceding paragraphs, has ignored many detailed points. In addition, practical considerations such as the size of the available test area must often override the recommendations deduced from the concept. Nevertheless, application of the concept can yield important conclusions. In particular, it will indicate the frequency regions in which the test results will be valid and those in which they probably will be invalid.

2.4 Combined Loads Requirements

The design of combined loads tests is necessarily far more sophisticated than the design of tests involving a single load. It involves all the considerations of the latter, and in addition requires a knowledge of possible failure modes to assess the requirements and tolerances for each of the loads to be combined. Some of the considerations for test design are illustrated in Chart 2.

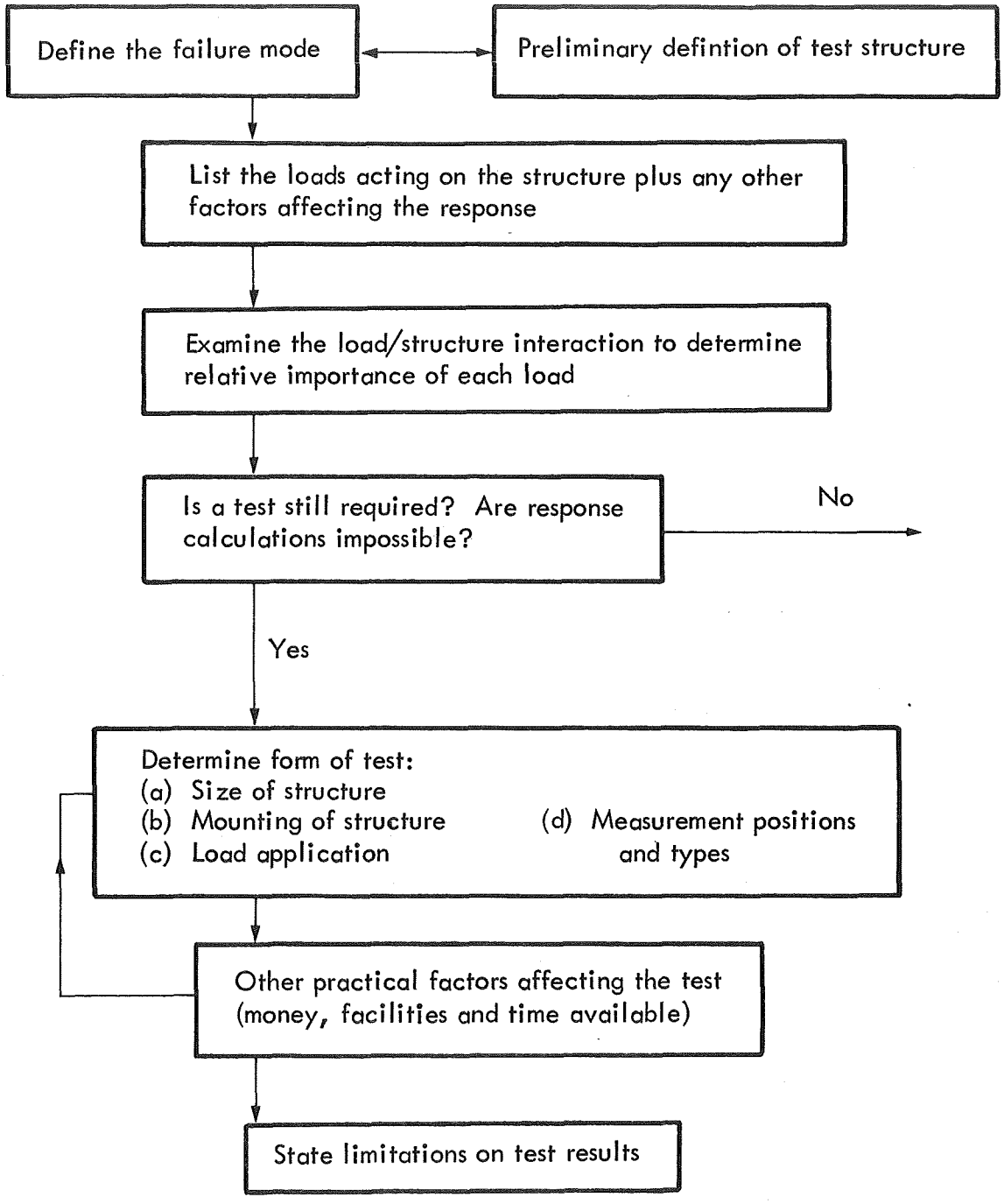

Chart 2: DESIGN OF A COMBINED LOADS TEST

It is anticipated that combined loads testing will become more prevalent in the 70's, particularly in view of the reduced number of flight test vehicles and the corresponding increased responsibility accruing to the ground test results. Therefore, modifications to Building 49A should be made with the possibility of future combined loads requirements, including static, vibration, and thermal loads.

3.0 GENERAL ENVIRONMENTAL TEST REQUIREMENTS FOR THE 70's

Environmental testing has a most important role in assuring reliability of manned space vehicles. During the 60's, environmental testing was used extensively in both qualification and acceptance testing of space vehicles. During this period, testing capability was extended to large structural sections of space vehicles and to the application of loads in combination, rather than singly. These advances have particular significance for the 70's, since generally fewer vehicles will be produced for given missions. Thus, the number of vehicles available for flight testing will be decreased and a greater emphasis must necessarily be placed on ground testing to assure reliability.

The following subsections briefly outline present types and sizes of manned vehicles under consideration and the loads to which these vehicles will be exposed.

3.1 Types and Sizes of Manned Space Vehicles

It is our understanding that there are four (4) principal classes of vehicles to be utilized for manned space flight in the 70's. These are:

- Apollo - lunar landing missions.
- Skylab - early orbital space station experiments.
- Space Base - prolonged operational space station.
- Space Shuttle - recoverable personnel and cargo vehicle for missions between earth and space.

The stages of the Apollo vehicle, the major interest of MSC, are shown in Figure 1. Building 49A was originally configured for acoustically testing this vehicle, utilizing an assembly of sixteen (16) progressive wave ducts.

The current configuration of the Skylab is illustrated in Figure 2. Its dimensions are compatible with Building 49A. It is orbited by Saturn S-1C and S-2 booster stages and subjected to a flight environment which is generally similar to that of the Apollo vehicle.

The proposed configuration of the Space Base is shown in Figure 3. This configuration consists of a long axial hub with two spokes. The nuclear power

module will be at the end of the hub, approximately 300 feet from the normal working area. The two spokes will extend 176 feet from the axis and will rotate about this axis approximately three times each minute. This will give a maximum artificial gravity of .54 G at the outer end.

The major segments of the Space Base are launched in the configurations shown in Figure 4. These launch configurations are all 33 feet in diameter; they vary in height from 92.5 feet to 99.5 feet and cannot be conveniently tested in Building 49A. Each of the components will be orbited by the basic Saturn rockets consisting of the S-1C and S-2 stages plus instrumentation sections.

Several of the proposed configurations for the Space Shuttle are illustrated in Figure 5. It is anticipated the Shuttle will consist of two separable vehicles, the larger used for initial boost and the smaller used for space flight. It is obvious from the figure that the total combined vehicle is very large, and that its configuration is not precisely defined. It would appear impracticable to reconfigure Building 49A to handle the entire combined vehicle. However, a modified Building 49A could probably be used to test significant sections of the boost vehicle, and perhaps the entire orbiter.

3.2 Types of Loads

The loads which will be experienced by these vehicles in the various phases of flight are summarized in Table I.

All flight phases involve dynamic loads of some type, and five of the eight phases involve external pressure fluctuations. The primary purpose of the acoustic facility is to simulate external pressure fluctuations which are the most significant source of vibration for space vehicles. However, the effect of the vehicle vibratory response and the resulting structural reliability often may be influenced by the presence of other loads. Thus, for some test requirments the acoustic facility must be capable of simulating other loads simultaneously with the acoustic loads.

It is not possible to develop detailed requirements for all of the load combinations which might be required for future vehicles. It is sufficient to note that some of the combinations in Table I may prove critical for segments of future vehicles, and the facility may be required to simulate some of these loads together with the fluctuating pressures. The remainder of this report will consider only the acoustic loads and recommendations for their simulation.

TABLE I

ENVIRONMENTAL LOADS AND CONDITIONS WHICH MAY INTERACT TO EFFECT VIBRATION INDUCED FAILURES AS A FUNCTION OF FLIGHT PHASE

Flight Phase	Loads
Lift-off	Acoustic, engine vibration, internal temperature distribution
Transonic	Unsteady aerodynamics including buffet, static acceleration, internal temperature distribution, static pressure differential
Supersonic Flight	Unsteady aerodynamics related to vehicle geometry and protuberances, static acceleration, static pressure differential, non-symmetric surface pressure distribution from angle of attack, aerodynamic heating, internal temperature distribution
End of Boost/ Separation	Shock from engine shut-off and separation, engine vibration, static acceleration, residual aerodynamic heating, internal temperature distribution
Space Flight	Shock from engine start and shut-downs, variable static acceleration, radiant heat loads, static pressure differential, external space vacuum, internal temperature distribution
Re-entry	Unsteady aerodynamics, aerodynamic heating
Deceleration	Unsteady aerodynamics, shock associated with deployable deceleration devices, aero heating and cooling, static acceleration, static pressure differential
Landing	Landing shocks

3.3 Requirements for Simulation of Fluctuating Pressure Loads

There are two types of fluctuating pressure loads to be simulated. These are: acoustic noise from the rocket at launch, and aerodynamic pressure fluctuations associated with the transonic and maximum dynamic pressure flight phases. This section contains an estimate of these environments for space vehicles of the 70's.

3.3.1 Estimate of the Acoustic Environment at Launch.

The following estimates are in accordance with Potter and Crocker, Reference 10. The assumed distribution consists of five nozzles, each with an exit diameter of 11.2 feet. The nozzle exit velocity (V_e) is 8800 feet per second, and the thrust is 7.5×10^6 pounds. Gas density (ρ) $_e$ computes to 0.000393 slugs/ft^3. The equivalent diameter (D_e) of the nozzles is 25 feet. These parameters give an Acoustic Power Level (PWL) of 217.5 decibels (re: 10^{-13} watts) for the overall level.

This total output power will be distributed over the frequency spectrum, and each band of frequencies will have a different apparent source along the rocket exhaust. The frequency and spatial distributions have been estimated to determine source-receiver distances and then multiplied by source directivity indices to obtain the data of Table 2 and Figure 6. The table lists the octave band center frequencies from 1 to 4000 Hz and shows the power level of each source generating energy in the respective bands. The next column gives the distance along the exhaust where each octave band is predominant. The following columns show the source distances and levels for a deflected exhaust radiating to three different points on the vehicle. These points are at 450, 350, and 250 foot heights above the base of the vehicle. Since most of the acoustic energy is radiated downstream away from the vehicle, the total power has been corrected by a directivity index ranging from -5 decibels at low frequencies to +2 decibels at high frequencies. Table 2 also gives 148, 149, and 151 dB overall sound pressure levels (re: 0.0002 microbar) at the 450, 350, and 250 foot levels, respectively.

3.3.2 Estimate of the Acoustic Environment due to Aerodynamic Loading. (Reference 11)

The trajectory for a typical Space Base launch is tabulated in Table 3. This table shows that the maximum "Q" at 82 seconds after takeoff is 34,243 newtons/meter^2, or 717 pounds per square foot. Figure 7 is an outline drawing of a typical launch configuration with empirically derived coefficients from References 11 and 12, giving the ratio of the dynamic to static pressures found at various points.

TABLE 2

ESTIMATED LAUNCH NOISE

Octave Band Center Frequency	Power Level (re: 10^{-13})	Source Distance Along Exhaust	Source Distance 450 ft Level	SPL 450 ft Level	Source Distance 350 ft Level	SPL 350 ft Level	Source Distance 250 ft Level	SPL 250 ft Level
1	196	925	895	122	875	122	873	122
2	203	880	863	128	845	128	837	129
4	208	850	838	134	815	134	805	134
8	211	780	778	138	755	138	734	138
16	211	675	696	139	660	139	635	139
32	210	510	590	140	540	140	490	140
63	208	365	518	141	450	141	370	142
125	206	240	485	140	400	141	290	143
250	203	128	480	139	385	141	250	143
500	200	44	490	137	395	138	252	142
1000	197	10	490	134	395	135	252	139
2000	194	10	490	131	395	132	252	136
4000	191	10	490	128	395	129	252	133
Overall	217			148		149		151

TABLE 3

TYPICAL TRAJECTORY INFORMATION
FOR A LARGE LAUNCH VEHICLE

Time (seconds)	Altitude (meters)	Velocity (meters/sec.)	Mach No.	Q (newtons/meter^2)
0	0	0	0	0
10	110	23	.066	310
20	480	52	.15	1547
30	1179	89	.26	4217
40	2288	135	.3999	8713
50	3889	193	.579	15061
60	6058	265	.8155	22645
70	8835	351	1.128	29802
80	12230	459	1.5527	34068
82	13024	484	1.658	34243
89	15818	578	2.03	32208
99	24016	739	2.53	23669

These coefficients, applied to the 717 psf given previously, give a range of 3.5 to 35.0 psf as the dynamic pressures operating on the vehicle at maximum "Q" and a range of 2.9 to 29 psf in the transonic flight phase.

Some of the spectra associated with these values are given in Figure 8, which is based on Reference 11. Although these spectra probably will not apply exactly to any specific vehicle, they are believed to portray the range of spectra which may be encountered in the launch of vehicles during the 1970's. It should be noted that the very high levels associated with separated flow apply over limited axial distances on the vehicle.

4.0 ACOUSTICAL TESTING CONCEPTS

There are several methods which may be employed to accomplish an acoustical test for a segment of the space vehicle. The choice of method, or combination of methods, depends on the purpose of the test, the vehicle configuration, and the type of environment to be simulated. Thus, unless the facility is designed for a specific type of test (a single vehicle in a unique mission), it is undesirable to specialize the facility for only one method of testing. Hence, the facility design must provide its operators with flexibility in the choice and use of various test methods.

4.1 General Test Objectives

Although there are innumerable terms for the objectives of acoustic test utilized by various agencies on various programs, the majority can be grouped under one of the following three general categories:

- Structural Qualification
- System Qualification
- Acceptance Test

In general, the structural qualification test objective requires the most detailed simulation of the environment. Here, detail is especially important if the outer shell structural integrity may be impaired by vibration fatigue and if the pressure fluctuations over the shell vary significantly with position in terms of intensity, spectra, and correlation properties. In such cases, it is generally undesirable to test the entire structure in the uniform acoustic field, since such a test would under-test local areas which are subjected to high intensity pressure fluctuations in flight. Conversely, if the test were designed to be adequate for the high intensity area, it could seriously over-test the lower intensity areas. Consequently, the result from a uniform acoustic field in this case would often be meaningless.

On the other hand, both the system and acceptance tests may not require as detailed a duplication of the environment as required in the structural qualification test. Here, the judgment depends upon the importance of the local variation in the external shell vibration to the vibration response of the system under test. In general, it may be assumed that if the system under test consists of black boxes mounted to the primary structure, the structure will perform a sufficient averaging of the vibration inputs from all other external shells. However, if the system

includes components which are directly mounted to the external shell and which may be exposed to significantly higher level local vibration because of the local variation in intensity, additional detail must be accounted for in simulation.

It should be noted that the optimum test of a system mounted within a vehicle which is exposed to external pressure fluctuations during flight is to subject an appropriate segment of the vehicle to external acoustic pressure fluctuations in the laboratory. As long as the segment of the vehicle is of sufficient size, it can be assumed that it will present to the internal system a vibration environment which is well related to the actual flight vibration environment. On the other hand, if the internal system is directly exposed to an acoustic field which has been calculated to be of an intensity similar to that anticipated inside the vehicle, the test will be of far less value since the structural filtering and the resultant structural vibration input to the specimen will be absent. Thus, in tests of internal systems, the vehicle serves primarily as a loading fixture with the unique property that it is identical to the loading fixture utilized in flight.

It should be recognized that there are differences in the vibration response of the structure to external pressure fluctuations, depending upon whether they are the result of aerodynamic turbulence or acoustic waves. These differences depend primarily on the spatial variations of the phase of the pressure fluctuations in narrow bands of frequency over the vehicle. These differences in phase, generally expressed in terms of spatial correlation, can be approximately accounted for by suitable adjustment in the spectrum and intensity of the acoustic simulation. However, for such adjustment to be practical, the acoustic field must have at least some of the important correlation properties for the flight environment. For example, it is exceedingly difficult to excite structural bending waves around the circumference of a cylinder if the acoustic pressures are in phase and of the same amplitude over the entire circumference.

4.2 Acoustic Test Methods

There are two pure types of acoustic fields which can be employed for acoustic testing. These are the reverberant field and the progressive plane wave field. The ideal reverberant field is diffuse when excited by a wide band acoustic source, in that the field is continuous in both narrow-band frequency spectrum and angular distribution of energy. A practical reverberation room does not fulfill this definition at low frequencies, but sometimes approaches the ideal diffuse condition at high frequencies. The reverberation room furnishes a test tool of high utility for tests in which the spectrum and level are constant over the entire specimen surface.

The progressive plane wave field is generally contained in a duct over the surface of the vehicle, as in Building 49A. In the ideal plane wave case, the power flows through the duct without reflections, with the particle velocity and pressure in phase; the spectrum is continuous and directly proportional to that of the acoustic source. Progressive wave ducts offer high efficiency and utility for testing a vehicle which requires continuous variation in level over a portion or all of its surface.

In addition to the two pure forms of testing, there are many combinations which include:

- Reverberation room plus plane wave duct
- Reverberation room plus contoured wave horn
- Reverberation room plus direct radiation

These latter configurations generally are utilized for vehicles which have distinct zones in which the spectrum and level requirements differ significantly. As will be discussed later, the most efficient of these combinations is considered to be the reverberant room with either plane wave duct or contoured horn. Both of these configurations lend themselves to the tailoring of very high level sound fields over specific areas, such as regions of shock wave impingement, wakes, and other unsteady aerodynamic flow. The combination of reverberation room and direct radiation is less efficient since it requires a considerably greater number of noise sources or power to achieve a given result, although it has the advantage of requiring no special ducting for the sound.

4.3 Reverberation Rooms

Many of the acoustical tests carried out in reverberation rooms assume that the sound field is "diffuse" and can be treated using statistical methods. The word "diffuse" implies that the sound pressure is constant throughout the volume of the room and that all directions of propagation are equally probable. Under these conditions, the relatively simple Sabine Equation (Reference 13) can be used to determine the sound level and other quantities of importance. However, it is found that serious errors can be introduced by making this assumption in the case where the sound field cannot be treated statistically, as is the case at low frequencies and in symmetrically shaped rooms. These errors result because the simple diffuse field theory neglects the wave nature of the sound waves which, of course, is important when the wavelength is of the same order of magnitude as the room dimensions.

A striking example of the errors that can occur is shown in Figures 9 and 10. The first figure is a plot of the octave band sound pressure levels at a point in a small reverberation room (Reference 14) when excited with pink noise. The frequency response of the same room is shown in Figure 10, where the irregular nature of the curve at low frequencies is immediately obvious. This result clearly demonstrates the way in which steady-state measurements using bands of noise can hide the actual room response. Therefore, it is not sufficient to use the simpler statistical approach under all conditions, and the wave theory must be employed.

4.3.1 Acoustic Modes.

It is a well known fact that the sound energy from a small source in free space is radiated uniformly in all directions in the form of spherical waves. When such a source is placed in an enclosure, the space into which it radiates is bounded. Hence, reflections of the sound waves occur and an exceedingly complex field is set up consisting of an infinite set of standing waves. The frequency response of the enclosure is thus characterized by an infinite number of discrete resonances called modes, the frequencies of which are determined by the dimensions. For a rectangular enclosure, these frequencies are given by the expression (Reference 13):

$$f_N = \frac{c}{2}\left[\left(\frac{n_x}{\ell_x}\right)^2 + \left(\frac{n_y}{\ell_y}\right)^2 + \left(\frac{n_z}{\ell_z}\right)^2\right]^{1/2} \qquad (1)$$

where c is the velocity of sound,

ℓ_x, ℓ_y, ℓ_z are the dimensions of the enclosure,

$n_x, n_y, n_z = 0, 1, 2 \ldots\ldots$ et cetera, are the mode orders,

and N represents the trio of integers, n_x, n_y, n_z.

Only at frequencies given by f_N is there any substantial enclosure response to excitation. It can be seen that there are three types of modes in which 1, 2, and 3 mode orders have non-zero values. These are called the axial, tangential, and oblique modes, respectively, where the direction of propagation is in one, two, and three dimensions. The lowest modal frequency is an axial mode corresponding to the longest dimension of the enclosure, i.e., $c/2\ell_x$, where $\ell_x > \ell_y$ and ℓ_z. For two enclosures having maximum dimensions of 10 feet and 50 feet, the lowest modal frequencies are 56 Hz and 11 Hz, respectively. If the enclosure is

rectangular, or approaches a rectangular shape, the spatial variation of the sound pressure for any one particular mode is represented by a cosine function. The pressure in the room may therefore vary considerably from point to point, having a maximum value at the surface of the enclosure. Also, since the sound pressure at a point in the enclosure at a frequency close to a modal frequency behaves in a manner similar to that of a tuned electrical circuit, the width of the acoustical resonance curve can be seen analogously to be dependent on the amount of damping. In other words, the greater the damping present in the enclosure, the wider will be the resonance curve.

It can be seen in Equation (1) that it may be possible for modes of different orders (n_x, n_y, n_z) to result in the same value of modal frequency, f_N. Such modes are termed "degenerate," and the enclosure will respond strongly at these frequencies. Also, the fact that two or more of the modes coincide in frequency results in a reduction in the number of discrete modes and leaves large gaps in the frequency response.

4.3.2 Modal Density.

It can be shown (Reference 15) that the number of modes per unit frequency range, called the modal density, is given approximately by:

$$G(f) = \left(\frac{4\pi V}{c^3}\right) f^2 + \left(\frac{\pi A}{2c^2}\right) f + \left(\frac{L}{8c}\right) \qquad (2)$$

where $V = \ell_x, \ell_y, \ell_z,$

$A = 2(\ell_x \ell_y + \ell_y \ell_z + \ell_z \ell_x),$

and $L = 4(\ell_x + \ell_y + \ell_z).$

Thus, the modal density is largely dependent on the dimensions of the enclosure as well as the frequency. At low frequencies, the density is small and hence the relative spacing is large. As the frequency is increased, however, the spacing is reduced until eventually the individual modes overlap. At frequencies greater than this, the sound field can be considered on the statistical basis mentioned previously.

In order that the acoustical response at the low frequencies can be optimized, it is necessary to investigate the effect of various room dimension ratios. Obviously, if the room is square or if the various dimensions are commensurate, many degeneracies will occur and the frequency response will be poor. Figure 11 is a computer plot of the modes in a room having dimension ratios of 1 : 0.513 : 0.513, where the vertical distance at any particular mode represents the frequency range between the two adjacent modes. It can be seen that the modal density varies irregularly with frequency, usually a good sign of a poor room. Sepmeyer (Reference 16) has proposed the ratios 1 : 0.82 : 0.72 as being optimum from a trial and error computer method. Figure 12 gives the result. Wyle Laboratories also has investigated and designed a 100,000 cubic foot chamber having dimension ratios of 1 : 0.79 : 0.63 for its testing facility in Huntsville, Alabama; the modal density is as shown in Figure 13. This ratio results in a fairly good modal density variation with frequency and has the added advantage that the major dimension can be halved while still retaining the same dimension ratios. More recently, Wyle derived a set of dimension ratios, 1 : 0.816 : 0.707, that produce a very uniformly decreasing modal density with frequency as shown in Figure 14. It is interesting to note that the optimum Wyle ratio is only slightly different from that proposed by Sepmeyer, but even this minor change definitely produces an observable difference in the uniformity.

When the purpose of a room is to test tall and narrow specimens, then the use of the above dimension ratios requires excessive floor space. Also, the extra wall space involved increases the absorption and necessitates more acoustical power to attain a specified test level. Because of these problems, it may be desirable in some cases to use a "tower" ratio for the room dimensions, i.e., the major dimension remains unaltered with the other two dimensions being halved. In the case of the optimum Wyle dimensions, this results in a ratio set of 1 : 0.408 : 0.353, the modal density of which is shown in Figure 15. Although the response is irregular at the lowest frequencies, it smooths out at the higher frequencies.

When an acoustic chamber is utilized to test a specimen at high sound levels, the results will lose a good deal of their meaning unless all the structural modes of the specimen are excited to some extent. Because of this requirement, it is usually arranged that one of two conditions apply:

- That there are at least twenty modes in the lowest octave band in which testing is to be carried out. This is rather an arbitrary condition, but is often a sufficient one, especially when the lowest octave band is at very low frequencies.

- That there are a certain number of room modes lying within the bandwidth of the lowest structural mode of the specimen to be tested. Eldred (Reference 17) has shown that it is possible to relate the number of modes in any desired bandwidth to a parameter $f_o V^{1/3}$, where f_o is the center frequency of the band. This relationship is shown in Figure 16 for bandwidths of $0.02 f_o$ (corresponding to values for Q of the specimen of 50 and 25 at 100 Hz). It is therefore possible to define a lower bound frequency f_{LB} for a reverberation room as the lowest frequency at which the room has a required modal density. A reasonable condition would appear to be that there should be at least one room mode lying within the bandwidth of the lowest structural mode. If this is so, Eldred shows that for a 90 percent probability of finding a room mode within a frequency range $0.02 f_{LB}$, the lowest usable frequency in the room is given approximately by:

$$f_{LB} = \frac{2120}{V^{1/3}} \text{ Hz}$$

This demonstrates that a room of volume V should be used to test a specimen only if the lowest modal frequency of the latter is at least f_{LB}, and the Q not greater than 50. Figure 17 is a replot of the information given in Figure 16, and shows the lower bound frequency as a function of room volume for various modal density limits. It is clear that large volumes are required to obtain low lower bound frequencies, and hence, to test structures having low fundamental frequencies.

4.3.3 Power Requirements.

If it is assumed that the sound field in the room can be treated statistically, then the relationship between the power input to the room and the sound pressure level can be written as:

$$PWL = SPL + 10 \log a - 6.4 \text{ dB}$$

where PWL = power level of source

$$= 10 \log \frac{W}{W_o}$$

W = rated power of source in watts,

W_o = reference power of 10^{-13} watts,

a = total amount of absorption present in room in square feet,

and SPL = sound pressure level in room with respect to 0.0002 dynes/cm^2.

Note that this equation relates the power delivered by a source to a reverberation room with sound pressure level. For air modulator noise sources, the coupling efficiency between source and room is approximately 33 percent, so that the rated power of the source in an anechoic termination must be three times (or 5 dB) greater than the delivered power requirement.

The total absorption in the room consists of contributions from two main effects:

- The absorption presented by the surface of the room. This is dependent on the area and absorption coefficient of the surface which is usually of painted concrete, and therefore has a coefficient of approximately 0.01 - .015. It is necessary to provide a smooth, hard finish to the walls to achieve this low value of absorption, which entails stone-grinding the surface and using a very hard-drying paint. To this absorption has to be added that due to the horn openings which, incidentally, should be sealed off when not used during a test. Also, the exhaust outlet from the room will act as an absorber, and therefore should be placed at a low impedance point in the room. This can be achieved by placing it at or near the center points of the walls, away from the corners and edges, and allowing the outlet duct to actually enter the room a foot or so.

- The absorption presented by the air itself. This is due to the natural vibrations of the oxygen molecules in the air and is of importance only at frequencies greater than 1000 Hz. At higher frequencies and in large rooms, air absorption accounts for majority of the absorption and presents a problem when high sound levels are required. This effect can be reduced greatly if the air is replaced by nitrogen, which has a low molecular absorption at audio frequencies. In this case, time must be allowed before any test so that the room may be completely filled with nitrogen. This may slightly increase the cost of testing; however, it is more than compensated for in the saving due to the lower power requirements at high frequencies.

The total absorption in a room due to both effects is shown in Figure 18 for the optimum dimension Wyle room mentioned previously. The importance of the air absorption at high frequencies can be clearly seen. Figure 19 enables a calculation to be made of the power required to produce a specified sound pressure level assuming the absorption at various volumes given in the previous figure. When the room is filled with nitrogen, the curve "absorption due to surfaces alone" should be applied to all frequencies.

An extremely important point which is often ignored concerns the use of non-coherent sources. If more than one source is used to excite the room and the acoustic outputs are coherent (as would be the case if all the driving units were fed from the same signal generator), then interference effects will cause cancellation of several modes. Similar interference effects will occur if the sources have any fixed relative phase difference between their outputs. The only means of avoiding this effect is to use separate random noise generators for each source such that there is no existing fixed phase relationship.

4.4 Close-Coupled Configurations

In order to provide sound pressure level gradients over a specimen so as to take into account the effect of local variations, it is necessary to utilize a close-coupled configuration. There are two principal methods by which these variations have been produced in previous experiments; the advantages and disadvantages are discussed below.

4.4.1 Progressive Wave Testing.

A progressive wave test configuration consists of a series of ducts which cover the vehicle. One side of each duct is the outer skin of the vehicle. A detailed example of the applications of this configuration to the Apollo is given by Wren, et al, in Reference 18.

In this configuration, the specimen is loaded by progressive plane acoustic waves propagating along the length of the duct. In general, the duct is terminated by an acoustic absorber whose cutoff frequency is designed consistent with the lowest frequency to be utilized in the test. When the ducts are properly designed to minimize reflections, the frequency spectrum attained in the duct can be smooth and continuous, directly proportional to the spectrum input to the driving noise source. This result is in sharp contrast to the irregular spectrum that is attained in reverberation rooms at low frequencies.

One of the major advantages of the progressive wave duct is its efficient use of power. For example, to achieve 150 dB over the surface of the Apollo (forward of the S IVB), requires approximately 4,000 watts for the progressive wave system. To achieve the same result in a reverberation room, sized to accommodate the stack, would require approximately 21,000 watts rated noise source power. For this example, the reverberation room is assumed to be 100 x 41 x 35 feet, with a total volume of approximately 144,000 cubic feet.

Another major advantage in the duct system is that it provides the ability to vary the level of the sound throughout the length of the duct simply by varying the cross-sectional area of the duct. Two examples of the variation that were achieved in the Apollo duct system are given in Figure 20 which was taken from Reference 18. As can be seen in the figure, when the duct spacing was flared over the surface module from an initial value of 4.5 inches to 15 inches, and maintained constant at 15 inches over the SLA, the variation in sound pressure level over the vehicle was very close to that calculated in accordance with the area expansion. However, when the spacing was kept at 4.5 inches over the entire vehicle, the sound pressure level for frequencies below 500 Hz was attenuated along the length of the duct by as much as 10 dB more than would be expected from the area variation. This attenuation is believed to be the result of the absorption of sound by the vehicle. Thus, it is necessary in designing a duct system to provide sufficient initial area, as in Figure 20(a), such that unwanted additional attenuation will not occur. This ability to vary the actual sound pressure level along the duct during test enables approximate matching of the sound pressure level gradients which exist on the vehicle during its mission, thus avoiding the compromise between over-test and under-test inherent for some vehicles in the reverberation room approach.

The duct system also enables control over the spatial correlation, spectrum, and level from duct to duct. This ability for independent control further enhances the potential realism which may be attained during the test.

The principal disadvantage of the progressive wave duct is the expense of the duct system which must be tailor-made for each vehicle. Further, the test setup is much more complex than the reverberation room approach.

4.4.2 Direct Impingement.

An alternative method of obtaining high localized sound levels is to use direct radiation from a source that is close to the specimen. This method has the advantage of both localization of power and ease of adjustment. However, it entails having the driving units, together with their associated horns, in the immediate vicinity of the specimen, which reduces the working space if (as is usual) many such sources are required. Also, the fact that the source is directed towards the specimen makes possible the formation of standing waves due to reflection, which produces an irregular exciting force on the specimen. However, the main disadvantage associated with this method is that it is extremely inefficient at producing the high testing levels required when compared to that using progressive waves. An example will clearly explain the reason for this.

Figure 21 shows the power required to produce a sound pressure level of 160 dB at the surface of a specimen as a function of the distance of the source from the specimen. The useful area of excitation of the specimen can be defined by the -3 dB points on the directivity curve of the source. For the low frequencies, it is assumed that the appropriate horn has a mouth diameter of 6 feet, whereas for higher frequencies (1000 Hz), the diameter is assumed to be 1 foot. For these conditions, the area of specimen over which the sound pressure is sensibly constant is plotted in Figure 21 for three frequencies: 60 Hz, 300 Hz, and 1000 Hz. These curves demonstrate that increasing the distance between source and specimen necessitates an increase in power to produce the same sound pressure level, and also increases the effective area of excitation. The power required per unit of effective area remains constant.

The power required to excite the specimen at a 160 dB sound pressure level using progressive waves, assuming the ducts are 3 feet wide and 3 inches deep, is also plotted in Figure 22. Absorption by the specimen at low frequencies, together with leakage losses at high frequencies, will result in slightly higher power requirements, but not as high as for the direct radiation method. The above calculation clearly shows the difference in power required for the two methods of excitation, and is good evidence for not using the direct radiation approach on this basis.

4.5 General Conclusion Relative to Building 49A

Building 49A was originally designed to enable test of the Apollo stack with a progressive wave system employing 16 ducts, as discussed in Reference 18. As a secondary objective, it was hoped that reverberant testing up to 155 dB also could be achieved with the power available. This limit in upper level was determined by the structural fatigue properties estimated for the PEAF panels which formed the outer wall of the building.

Although no horns were provided to achieve full level in the room, it has been estimated that the maximum level for the room, as built, is approximately 147 dB because of the absorption of the platform gratings, air conditioning ducts, and numerous other equipment. Furthermore, because of the large volume of the room, approximately 440,000 cubic feet, the air absorption results in a significant degradation of the high frequency end of any desired test spectrum. For these reasons, it is impractical to utilize this room for high intensity reverberant testing. Therefore, the facility, as it exists, must be considered primarily a progressive wave test facility.

The principal advantages and disadvantages of progressive wave and reverberant field testing are summarized in Table 4. In general, it may be concluded that the progressive wave facility has far greater technical versatility than the reverberant room, but at a cost in test fixturing and setup time. For some test objectives, as discussed in the preceding, this additional cost is both warranted and mandatory if the test is to have any validity. For other objectives, however, the simpler reverberant test may be technically acceptable. In such cases, it would be desirable to have this capability in Building 49A.

Therefore, the general conclusion is that any modifications to Building 49A, required to enable it to accommodate the larger vehicles of the 70's, should be made in a manner which will enhance the building's capabilities for reverberant testing. Such modifications should still allow the utilization of progressive wave ducts for those tests where they are necessary, thus making Building 49A a more versatile facility. The remainder of this report will discuss and give recommendations for this purpose.

TABLE 4

COMPARISON OF MAJOR FACTORS BETWEEN
REVERBERATION ROOM AND PROGRESSIVE WAVE TESTING

Function	Reverberation Room	Progressive Wave Ducts
Typical power ratio $\left(\frac{\text{Reverberation Requirements}}{\text{Progressive Wave Requirements}}\right)$	5-10	1
Spectrum regularity	Irregular below $f = \frac{2120}{V^{1/3}}$	Regular over entire design frequency range
Spatial variation of sound pressure level	Very little	Controllable along duct for variations of at least 10-15 dB: completely controllable from duct to duct
Spatial correlation	$\sin \frac{kx}{kx}$ at higher frequencies: complex function of room modes at low frequencies	cos kx along duct: controllable between ducts
Vehicle contact with other structures	none except support fixture	Slight contacts between duct and vehicle with gaskets which separate ducts: may give problem on vehicles which have much thinner skins than Apollo
Test setup difficulty	minimal	May be complex, requiring tailor-made duct system and careful positioning during setup

5.0 ACOUSTIC FACILITY - GENERAL CONFIGURATION AND REQUIREMENTS

5.1 Basic

The purpose of the recommended modifications will be to enable reverberant testing of large Space Base components, particularly launch configurations of these components, in Building 49A. This purpose may be achieved by constructing a reverberation room inside the building.

At present, the SAL is capable of operating as a reverberant chamber up to the order of 150 - 155 dB, depending upon the spectrum. It is possible to increase this maximum level by lining the inside surface of the walls with an additional layer of steel to reduce the loading on the existing walls. This alteration would leave all the platforms with their attendant wires, pipes, ducts, grilles, hoses, stairways, and lighting fixtures inside the chamber. It has been shown that all of this material inside the chamber causes considerable absorption of sound. Indeed, the average absorption coefficient inside the chamber is presently of the order of 20 percent and would not be likely to change a good deal with the steel liner mentioned above.

A second method of building the reverberation room inside the building would be to build steel or concrete walls just inside the lines defining the platforms themselves. This will result in a reverberation room 45' 6" deep by 49' 10" wide, minus whatever space was taken by the walls. Existing beams inside the room would be used to support the steel walls. These walls would be of 1/4 inch steel plate and would be backed by 1/4 inch of a good vibro-damping compound to increase transmission loss and fatigue life.

In view of the height of the Space Base launch configurations (Figure 4), it will be necessary to add some height to the existing building. Since the present working height of the building is about 90 feet, it will be necessary to add at least 10 feet if each of the launch configurations are to be tested. It should also be noted that the existing 75-ton hoist has been derated to approximately 25 tons because of modifications that became necessary to slightly increase the working height of this hoist. While this derated hoist proved adequate for previous tests, the heavier payloads associated with the Space Base will make it imperative that the hoist be restored to its normal capacity. This will mean some additional height must be added to the building, and it is recommended that a total of 20 feet be added.

It will also be necessary to increase the door size to accommodate the larger Space Base components. The present door opening is 32' 8" wide and will not accommodate the components which are 33 feet wide. It is possible to increase the door width to 33' 2" with a minimum of effort, but this would result in a very tight squeeze with possible damage to the specimen if an emergency arises. The present door is supported on concrete footings which cannot be considered movable. It will be possible to install new footings beside the existing footings and the door widened to fit these new footings. This will result in a door 42 feet wide. While this is wider than necessary for the Space Base components, the Space Shuttle, which has not been designed as of this writing, will undoubtedly require more room. It is therefore recommended that 42 feet be accepted as the minimum width.

The steel beams across the top of the door will have to be replaced, and it will also be necessary to increase the door height to accommodate the 57 foot height of the components of the launch configuration. Again, it is desirable that an additional 10 feet be allowed for growth of either of these components or of the Space Shuttle.

In summary, then, it is recommended that an inner shell approximately 45.5 x 49.8 x 120 feet be built inside Building 49A, and that the present door opening be increased to 42 x 67 feet.

5.2 Design Calculations

The absorption of sound by a steel panel used as part of a wall of a reverberation room is discussed in Appendix A. This discussion shows that for low frequencies the panel can be considered analogous to a lumped constant RLC series electrical circuit having a radiation damping load as well as any damping which may be inherent in the panel. This is a reasonably simple analog and needs little further explanation other than reference to Figure 3 of the Appendix. This figure plots the absorption coefficient for the 1, 1 mode of a 4' x 4' x 1/4" panel, assuming this mode might appear at any frequency on the chart. The actual resonance appears at 22 Hz with an absorption coefficient of 80 percent, but this drops very rapidly to 2.5 percent at 30 Hz. Other modes shown for the panel show very little absorption, and then over very narrow ranges.

5.2.1 Reverberation Room Design.

The reverberation chamber described in the previous section has a plan of 49.8 x 45.5 feet and a height of 120 feet maximum dimensions. Such a reverberation

room shape will exhibit two longitudinal resonances before any of the cross modes excite. The first resonant frequency will fall at 4.69 Hz; the second will be just two times that frequency. At higher frequencies, cross modes and resonances will appear. The relationship governing the allowed frequencies of excitation is given in Equation (1). This equation may be used to determine the spacing on the frequency scale of each allowed frequency. The ratios:

$$\frac{\ell_y}{\ell_x} \quad \text{and} \quad \frac{\ell_z}{\ell_x}$$

determine the shape of a given rectangular room and thereby determine the uniformity of the spacing of the solutions to Equation (1).

A computer program, Reference 19, has been written to plot the positions on the frequency scale of all modes in the first decade of response. It is used to optimize the shape of any given reverberation room so that large gaps are not left in the frequency response of the room (Figures 11 - 14). Through the use of this program, it has been found that the room shape above will display a large gap between 15 and 20 Hz, and that considerable improvement in frequency distribution can be obtained with any of several slight variations of this size. Ideal dimensions for these variations would be 121 x 49.5 x 42.8 feet. This shape and size uses the full depth of the available space, but 3 feet of the width of the room is lost. It is probable that the cost of constructing the steel wall some 3 feet from the supporting beams may be prohibitive, in which case it may be desirable to use the dimensions of 121 x 49.5 x 45.5 feet, making two of the lengths in a "correct" ratio and allowing the third length to fit the present configuration. Another possible configuration would be to use dimensions of 128.9 x 49.8 x 45.5 feet. In this configuration the height and width are "correct" and the depth is 3 feet less than it should be.

Each of the above configurations has a reasonably good distribution. The "ideal" shape of 121 x 49.5 x 42.8 feet shows some advantage, but probably cannot justify the additional cost of constructing steel support beams inside the existing ones to support the wall. It would seem that the best compromise shape would be the 128.9 x 49.8 x 45.5 foot room since it adds additional height to the building and this will add to the working space rather than detract from it as the "ideal" shape will do.

From the above discussion, it is recommended that the building height (inside) be increased to 128.9 feet and that 1/4 inch steel walls be built as close to the existing platforms as possible to form the reverberation room for testing in the 70's.

This proposed room will have a volume of 282,000 cubic feet, a total inside surface area of 29,000 square feet, and an edge length of 897 feet.

Experiments performed at Wyle Laboratories indicate that an absorption coefficient of 1.6 - 2.0 percent for damped steel plates is reasonable. The absorption varies with frequency, as shown in Figure 23. Using 1.75 percent as an average, the total absorption in the room will be:

$$a = S\bar{\alpha}$$
$$= (29{,}000)\ (.0175)$$
$$= 510 \text{ square feet}$$

Air absorption will add to the high frequency end by the equation: (Reference 20)

$$a = 4mV$$

where V = room volume,

and m = absorption parameter for air and is frequency dependent.

The measured values for m are linear with frequency and vary between 0027 m^{-1} at 2 K Hz to 0313 m^{-1} at 12.5 K Hz at 70 percent relative humidity. These values, applied to the proposed room, would give 930 square feet at 2,000 Hz and 10,800 square feet at 12,500 Hz. Figure 23 illustrates these estimates as functions of frequency in the proposed room. Other factors within the room will, of course, affect the detailed structure of these curves, but this shows the general effect.

Reference 13 gives the reverberation time of the room by the equation:

$$T = \frac{.049V}{a + 4mV}$$

and this function is plotted in Figure 24 using the information of Figure 23. It may be seen that the reduced wall absorption makes the air absorption a much larger factor of consideration than has been previously necessary.

Figure 25 shows power levels that will be required to produce the sound pressure levels of Figures 6 and 8 in the proposed facility. These data reflect the effects of wall and air absorption shown in Figure 23, and it is seen that the high frequency

air absorption causes tremendous increases in required sound power even though pressure levels are dropping. Also included in Figure 25 are the power output capabilities of one WAS 3000 Airstream Modulator.

It must be noted that the maximum transducer power shown in Figure 25 does not represent power that may be generated into a reverberant field. Rather, this curve was taken from calibration tube measurements wherein the transducer was terminated by an anechoic wedge. No airstream modulator will generate its full rated power into a reverberant field. The actual power delivered to such a field must be derated about 3 decibels for a semi-reverberant room to 5 decibels for a fully reverberant room. Since the room becomes semi-reverberant above 1000 Hz or so, it is possible that the high frequency region will transfer most of its energy into the room. At low frequencies, greater losses would be expected - probably 4 decibels.

A nitrogen atmosphere will result in a "harder" room at the higher frequencies and will therefore reduce the coupling efficiency of high frequency transducers. It will also cause the room to respond more strongly to the energy that is coupled, and the high frequency levels will be as much as 4 or 5 decibels higher than they are in air. Thus, the nitrogen filling causes two effects, one bad and one good, at the same time.

5.2.2 Horn Design.

5.2.2.1 Low Frequency Horns - Figure 26 is a sketch of the proposed horn configuration for the lower frequencies. It is expected that an engineering prototype of this horn will be produced on another program (Reference 21) and some evaluation of it will be made before others like it are built. The data of Figure 25 shows that one low frequency transducer of the WAS 3000 type could come very close to producing sufficient power to drive the low frequency portion of the required spectra, with the exception of the separated flow spectrum. However, experience has shown that reverberant chambers will not accept all of the power available from an airstream modulator, and it is therefore recommended that four low frequency drivers be considered for this task.

5.2.2.2 High Frequency Horns - The sound generation equipment presently available in Building 49A includes 18 high frequency air modulators of the EPT-200 design. These transducers should be used to provide all high frequency requirements of the reverberation chamber. It is expected that some high frequency gains can be obtained if a recirculating 100 percent nitrogen atmosphere can be used in the chamber, but the exact effect of this can only be evaluated during chamber checkout.

It is recommended that a total of eight horns be constructed having lower cutoff frequencies of 100 Hz. These horns will be connected to eight of the existing EPT-200 transducers and driven in the frequency range of 150 to 550 Hz. The horns would be mounted through the wall of the reverberation chamber, conveniently near an edge of the room. The mouth openings of these horns would be 1/6 th wavelength at 100 Hz, or 22.5 inches in diameter. The remaining ten transducers would then be allowed to radiate directly into the room through holes 3.57 inches in diameter. These entrance holes would be flush mounted in a wall of the chamber, sufficiently separated to prevent phase coupling of the acoustic signals. The transducers would be operated in the range of 550 Hz to 1200 Hz. Verbal communication with NASA and Brown Root & Northrop (BRN) personnel has indicated that the EPT-200 radiates better in this frequency range without any type of horn.

5.2.3 Estimate of the Sound Pressure Level on the Work Platforms.

Since the existing permanent work platforms will be accessible to personnel during tests, it is reasonable that some estimate be available as to the sound pressure level that will be expected in this area during testing. The 1/4-inch steel wall separating the work platforms and the actual test chamber will have a transmission loss as shown in Figure 27, from Reference 22. Curve (b) will be appropriate for the damping level expected with the proposed design. While this wall has a reasonably good transmission loss characteristic, the sound reduction through it will be dependent entirely upon the absorption characteristics of the space between it and the outer wall of the building. Fortunately, considerable absorption does exist in this region. The sound power leaving the reverberation chamber will be equal to the sound power entering it, less the power actually absorbed by the walls and air. The walls will absorb very little energy and the air will only absorb energy above 500 Hz, so the total energy passing through the walls is estimated at 179 decibels (re: 10^{-13} watts) during testing to simulate the separated flow spectrum. Previous measurements of the absorption in Building 49A probably indicate a good estimate of the absorption that will be available to reduce sound levels in the work platform space of the new facility. These measurements show an average of about 4200 Sabines. From this, the sound pressure level in the work space can be computed directly as 149 decibels. This level is too high for any but emergency entrance into the work area, and even then complete ear protection must be afforded.

5.3 Trade-Off Considerations

Examination of Figures 6 and 8 shows three significant spectra which must be approximated in Building 49A in order to accomplish the desired testing of the Space Base

launch configurations. The liftoff spectra are characterized by very broad band energy, essentially flat between 100 and 5,000 Hz. The overall level of this energy will be of the order of 150 decibels (re: 0.0002 microbar) with some additional high frequency energy if testing is to be performed at or below 250 feet on the boost vehicle.

Attainment of such a flat spectrum will be very difficult within the present state-of-the-art. It may be noted that the levels represented by the separated flow region of Figure 8 are higher than the levels of Figure 6. It may also be noted that this separated flow spectrum shape is within the state-of-the-art since the peak energy occurs at 500 Hz and below, and it is only necessary to produce sufficient power to produce the desired spectrum. Indeed, the separated flow spectrum of Figure 8 represents a "good" application of low frequency airstream modulators. It is probable that the low frequency portion of the spectrum would have to be supplied by transducers operating into low frequency horns, and the high frequency (150 Hz and above) would best be supplied by transducers driving horns having 100 Hz lower cutoff frequencies. In any case, a relatively large number of transducers will be required. (See Section 5.2.)

It must be recognized, however, that the separated flow spectrum represents an over-test for most of the vehicle, and it may not be realistic to consider a reverberant field of this level. This particular spectrum exists only during conditions of maximum Q and then only near the shoulder regions where the conical section meets the straight section. The boundary layer spectrum of Figure 8 is more representative of the acoustic levels that will be found over the body of the vehicle; the more realistic test procedure would be to produce this spectrum in the reverberant field, and then apply local excitation to the shoulder regions through horns coupling directly to the shoulder.

The boundary layer noise is characterized by the air noise of airstream modulators and this might be suitable for simulating these spectra. Low frequency horns operating between 25 and 150 Hz would be suitable for simulating the low frequency portions of the liftoff and separated flow spectra. The middle frequency portions of these two spectra would then be produced through horns having a low cutoff frequency of 100 Hz, as mentioned above. The high frequency portion of the liftoff spectrum would be accomplished using EPT-200 transducers operating without horns, radiating directly into the room through holes cut in the wall.

A primary trade-off decision, then, would be concerned with the development of the separated flow spectrum in the entire reverberation room. It has been shown in Section 5.2 that this spectrum (from examination of its power requirements) is

within reason. The question then becomes whether this amount of over-test for the larger part of the vehicle is desirable. It is expected that this spectrum would actually be produced for a few seconds which would simulate passage through maximum Q conditions, and there may be no serious problem exposing the boost vehicle for these few seconds. The alternative to this type of test would be the construction of a number of complicated horns to fit around the vehicle shoulder so that the increased levels can be placed directly on the shoulder and not elsewhere. The complexity of such a system would be slightly simpler than the duct work used on previous Apollo tests.

It may be possible to arrive at some compromise spectrum that would simulate the launch, the boundary layer, and the separated flow by use of an extended time. The launch spectrum will exist on the vehicle for a short time, and the boundary layer will build up from a low level to a high level during the flight profile. A compromise spectrum and level could be established which would apply approximately the same total energy at a lower level for a longer time (say 155 decibels peaking at 250 Hz for two or three times the normal flight time) for qualification of the vehicle. This program would depend entirely upon the customer's engineering staff and would result in over-test of some parts of the vehicle and under-test of other parts.

6.0 MODIFICATIONS TO THE EXISTING ACOUSTIC TEST BUILDING 49A

6.1 Height Addition to Basic Structure

In view of the reduced floor area in the interior reverberation chamber recommended for Building 49A, it will not be necessary or desirable to increase the height of the entire building. Figure 28 is an outline sketch of the north and east elevations of the proposed new design. This sketch shows the central parts of the north and south walls extended upward 26 feet. The width of this extension of the north and south walls is approximately 50 feet and is intended to accommodate an increase in height of existing beams within the building. The entire width of the east elevation is shown with its height increased by the required 26 feet. This will allow extension of the existing stairway to the top of the building, and it will also allow placement of the existing bridge crane in the same relative position that it now occupies. It is recommended that the narrow extensions of the north and south walls be of the same PEAF panel exterior construction as is used on the existing building. The east and west set-back walls might well have an exterior surface consisting of vinyl covered steel as is used on many other buildings at the NASA site.

Figures 29, 30, and 31 are interior photographs of Building 49A taken from the 75 foot level. Figure 29 clearly shows the circular bridge crane centered at the top of the building. This crane and its associated supports will be lifted to a new roof height of 128 feet. Figure 30, looking at the east wall, shows the interior columns that will be extended upward and will define the new reverberation room wall. Figure 31, also looking east, more fully discloses the plane to be covered by the steel wall of the reverberation room. Also shown is the north door which will be increased in height to a level above the air conditioning ducts shown. The elevator will not be extended by the additional 26 feet unless other considerations prevail. It is anticipated that construction cranes will move all material to the top of the building during construction and that no further requirement will exist for moving freight to the 100 foot level by the elevator.

6.2 Modify Existing Building

Details of the increased height can be seen by reference to the Launch Environment Test Facility, Acoustic Test Facility, Building Number 49A, by Bovay Engineers, Inc. Invitation Number Eng-(NASA)41-443-65-1, File Number NASA-101-19.

Page S-49A-10 of these plans shows an interior column schedule. Columns C-7, F-7, C-2, and F-2 define the east and west walls of the proposed interior chamber. These columns are presently 102' 5" tall and will be extended to a height of 128' 11". The new interior walls will be placed between these columns so that the columns themselves will be "outside" the new chamber. Columns G-6 and G-3 will define the south wall of the new chamber in the same way. These columns are presently 74' 10-1/2" high. Thus, they do not interfere with motion of the circular bridge crane, and this crane can bring objects to and place them on the top work platform. These two columns are to be extended to a height of 102' 5" where they will support a new work platform placed at the same level as the existing roof. This work platform will receive the uppermost extension of the existing stairway and will be 51' 6" wide and 13' 4" deep. The wall of the reverberation chamber will extend up to the roof and will be altered to include a door through which the 5-ton hoist can travel for clearance and for material transfer to the top work platform. It will also be necessary to make the floor of the new top platform removable in order that the 5-ton hoist can also reach the work platform at the 75 foot level. This will remove any requirement that the elevator be altered to operate above the 75 foot level since material may be transferred to the crane from this level.

In order to provide clearance for the rotating bridge crane (5-ton hoist), reference is made to Page S-49A-14 of the plans. Clearance Plan 1-14-14 shows the operating plan of this crane. Section 2-14-14, just below the plan, shows an elevation of this crane. Considering the crane to be 26 feet higher than shown in this section, it may be seen that a slot 34 feet wide extending from projections of beam G-3 to G-6 will just clear the rotating bridge of the crane. This slot will be 6 feet in the vertical dimension and will extend from the elevation station 116' 10-1/2" to 122' 10-1/2". The slot must be covered by some reflecting surface during operations in the reverberation room. The top of the slot will intersect the circular beam supporting the bridge and may be sealed to it. This may be accomplished by use of steel doors that open whenever the bridge is turned.

The material-handling doors associated with this crane may be as narrow as 6 to 8 feet and should be centered over Column G-5. This will allow transfer of material of most descriptions to be picked up at the 102 or 75 foot level. The structure of these doors will be of the same 1/4-inch steel plate as the rest of the walls. A steel frame around the doors will facilitate acoustic sealing of the door.

The main door to the building is shown on the north elevation as greatly enlarged over the present door design. This new door is 42 feet wide and 67 feet high.

As described in Section 4, this door will allow entrance of all foreseeable space vehicles and components. The 67 foot height is not as tall as these vehicles, but it will be possible to bring a given top section of any component in through the door, raise it with the 75-ton hoist in the center of the room, and then bring the lower part of the component and drop the top section down to it with the hoist. Detailed plans for the new door structure are being developed by the LTV Aerospace Corporation and will not be elaborated here.

6.3 Additional Details

Details associated with the design of the reverberation chamber within Building 49A include such items as access panels from the work platforms, viewing windows, lighting, electrical service, pneumatic supply, acoustic horn entrances, et cetera.

6.3.1 Access Panels.

In order to provide access to a potential test specimen at various heights, it will be desirable that a worker can obtain access through the reverberation chamber wall at each of the existing and new levels of the work platforms. A scheme recommended for accomplishment of this access is shown in Figure 32. This figure shows a "drawbridge" type door opening from one of the work platform levels. The drawbridge is supported by cables and includes a chain railing around it. Existing fishbelly beams will be placed across the reverberation chamber during work sessions; these doors will open out onto the beams in order that a worker needing closer access to the vehicle may use a combination of fishbelly beam and drawbridge to gain access. The drawbridge doors should be installed at each level, and there should be a minimum of three such doors at each level.

6.3.2 Viewing Windows.

A minimum of six viewing windows should be installed at each work platform level to allow viewing of the specimen just before and immediately after test operations. It would even be possible to view the specimen under test through these windows, but this is not recommended in view of the high sound pressure levels expected in this area. However, television cameras could well view the specimen through these windows, and it is desirable that they be of high quality. It is recommended that the windows be placed flush with the inside surface of the reverberation chamber and that they be about 1 foot square. They should be placed about 5 feet above the floor and should be of 1 inch thick plexiglass. Plexiglass is chosen for this use because of its inherent internal damping, but glass of a like thickness could

also be used if the optical qualities of the plexiglass are not suitable for television viewing. The windows should be placed so as to be out of direct exposure to the work platform lights so that reflections will not spoil the visibility through the plexiglass or glass.

6.3.3 Lighting Inside the Reverberation Chamber.

It is necessary that lights be installed in the reverberation chamber to allow work on the various specimens to be tested. These lights should be of the flush-mounted design to maintain the acoustical integrity of the chamber. It is recommended that they be of the mercury vapor type since these have shown consistent good service during past years in high intensity acoustic fields. Lighting should be well distributed over the inside surface of the reverberation chamber, and it should result in an interior light level of about 50 foot candles on and around the specimen. It is recommended that the interior of the reverberation room be painted white to enhance the light distribution.

6.3.4 Electrical Service.

Since workers will require the use of hand-carried tools and lights, it is necessary that adequate electrical service be provided. Electrical outlets will be required near all access doors and these will be capable of supplying 110 and 220 volt power to electrical tools and lights. It is recommended that four double outlets for 110 volts and one 3-phase, 220 volt outlet be provided near each opening into the room.

6.3.5 Pneumatic Supply.

Because of their non-hazardous nature, it is expected that some extensive use will be made of air-operated tools around future spacecraft. It is therefore recommended that air pressure lines be made available to each of the access doors so that air-operated tools can be used at the discretion of the operators. These air lines should be terminated by quick-disconnect couplings as is standard practice in many locations where such tools are used. One double connection is recommended for each access door.

6.3.6 Acoustic Horn Entrances.

The four low frequency horns will have mouth openings of 90 inch diameter. The horns will not have integral flanges, but metal slip-on flanges are recommended to attach the horns to their respective openings. These flanges will accommodate

bolts which will pass through matching holes in flanges mounted in the 1/4 inch steel wall. Nuts will then secure the bolts in place.

The four horns will be mounted in the four lower corners of the chamber, as shown in Figure 26. The two horns shown on the west wall of the chamber will be overlapped and it may be necessary to adjust the two of them to avoid conflict with the existing structure and each other. Horn entrances for the eight EPT-200 transducers using horns will be 22.5 inches in diameter. These horns, too, should be attached by slip-on flanges to the outer surface of the chamber wall. They may be located at convenient locations along the edges of the chamber wall corners. The openings should be at least 5 feet from each other to prevent phase coupling between transducers, but otherwise no restriction need be placed on their location. The eight EPT-200 transducers not using horns will radiate directly into the chamber through holes in the wall far removed from edges or corners or from each other. Again, "far removed from each other" may be defined as 5 feet or further to prevent phase coupling. The entrance holes will be 3.57 inches in diameter and a hole pattern may be cut into the 1/4 inch steel to match the mounting holes of the EPT-200, or a special flange may be mounted on the wall, whichever is considered convenient.

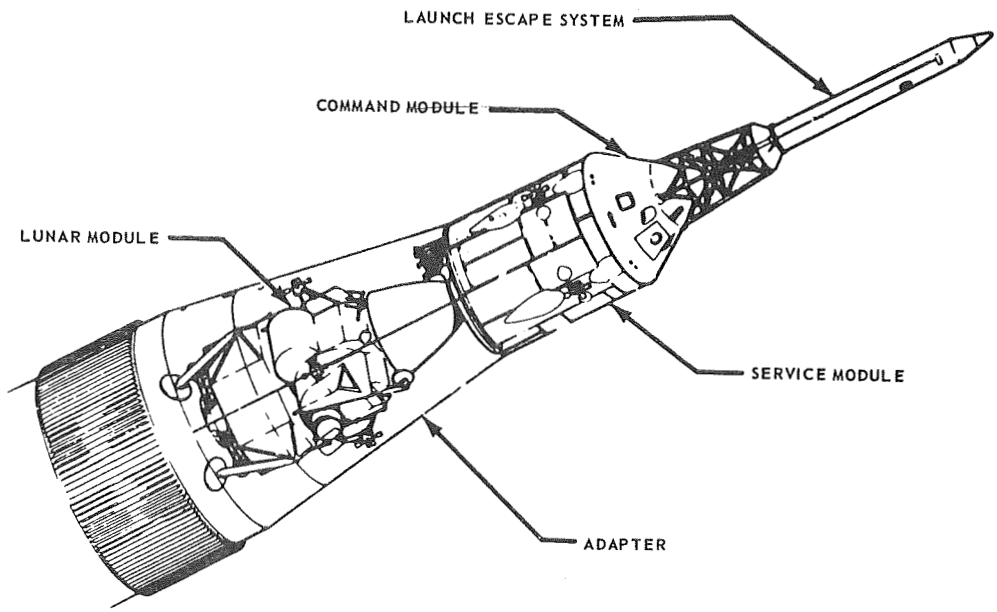

Figure 1. APOLLO SPACECRAFT AND INSTRUMENT UNIT

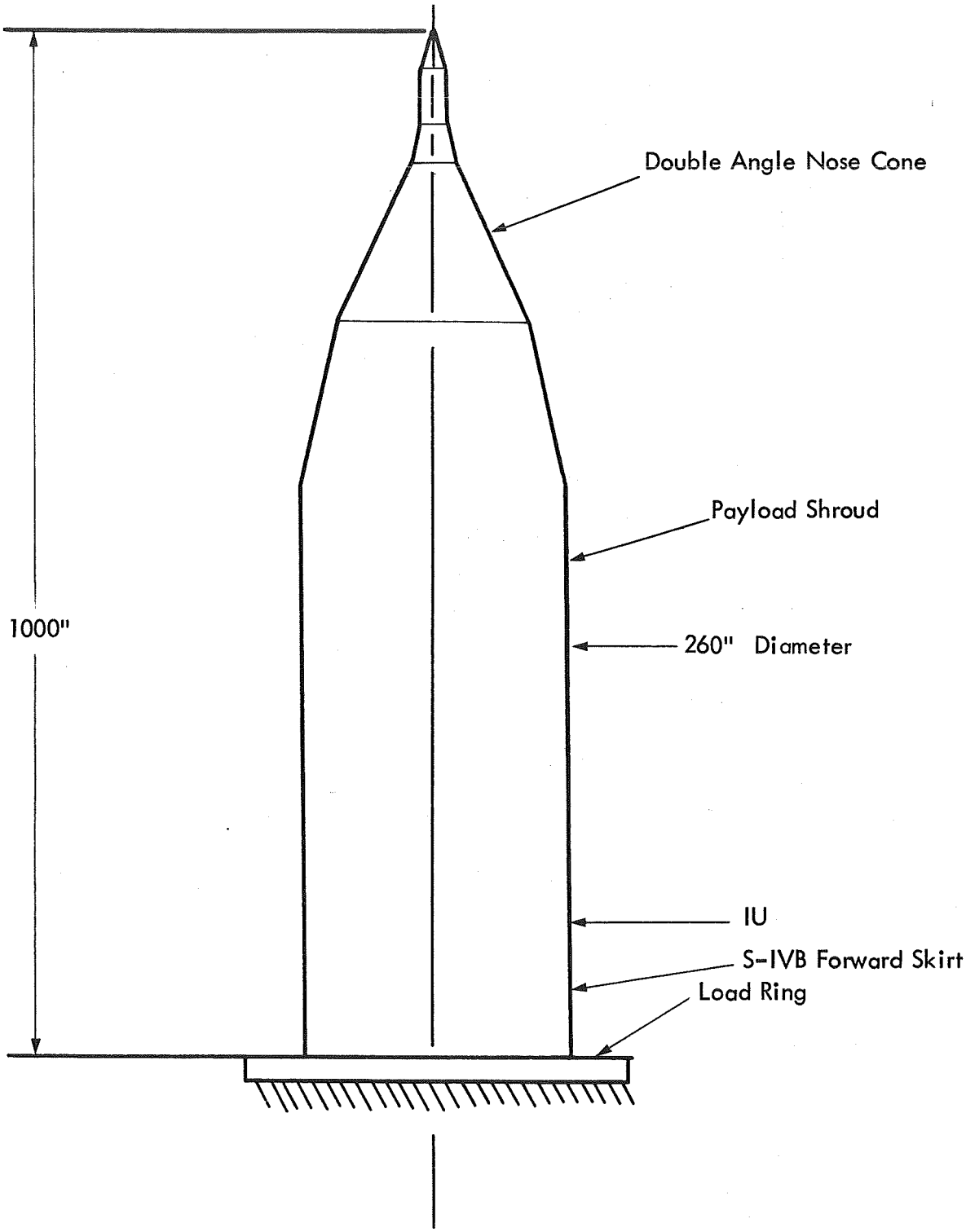

Figure 2. AAP PAYLOAD CLUSTER CONFIGURATION

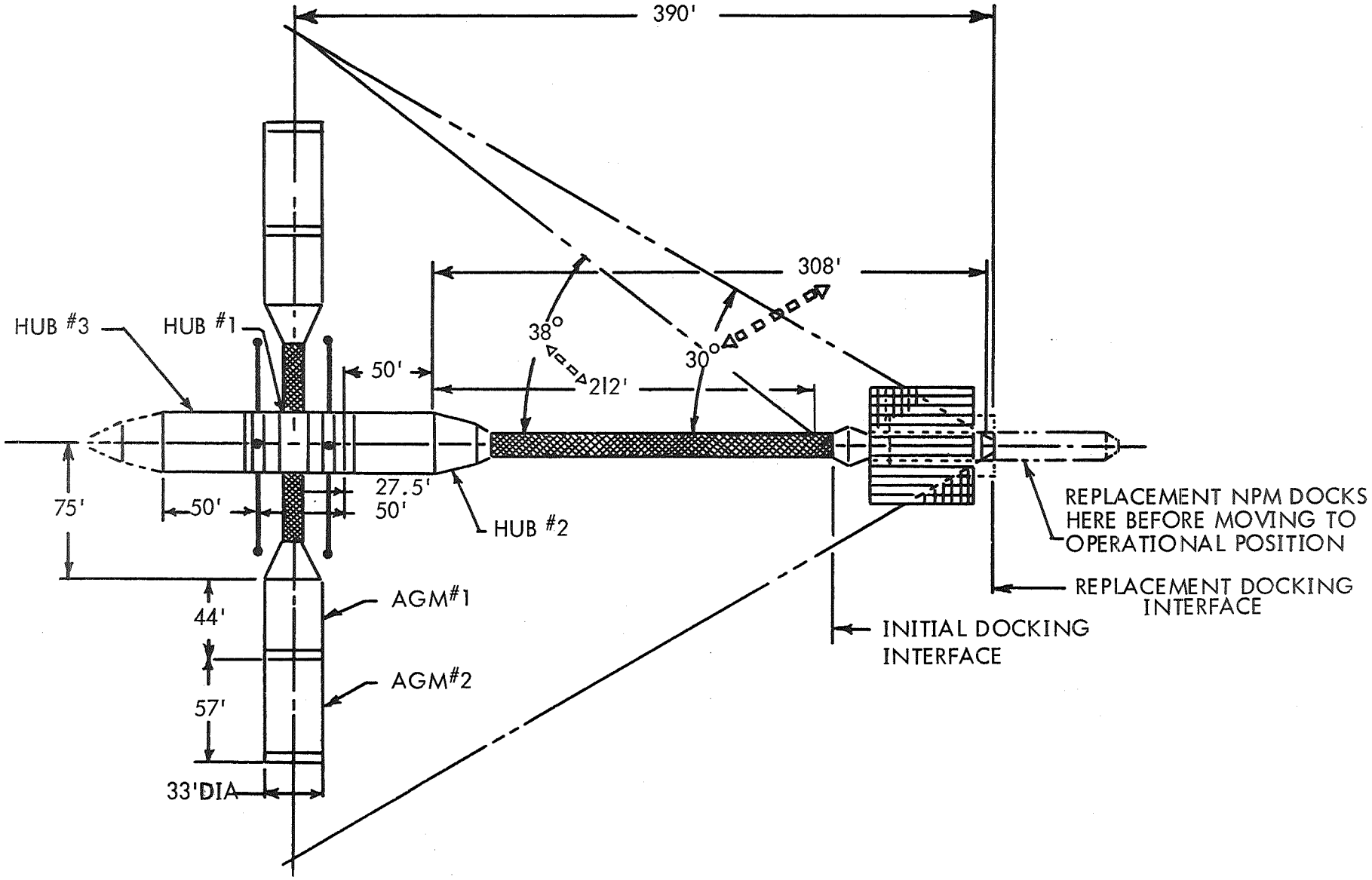

Figure 3. SPACE BASE CONFIGURATION

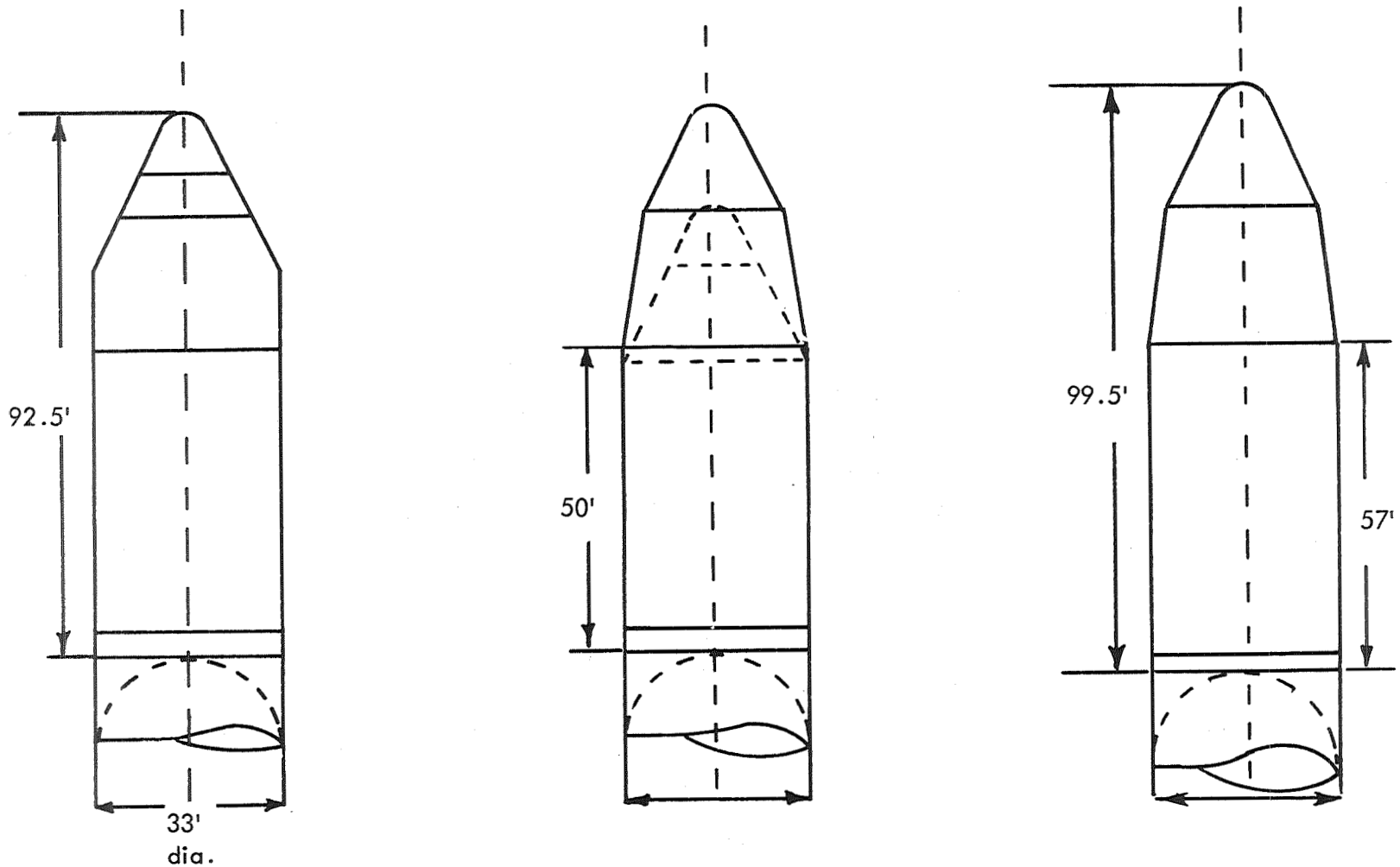

Figure 4. LATEST LAUNCH CONFIGURATIONS FOR SPACE BASE STRUCTURE

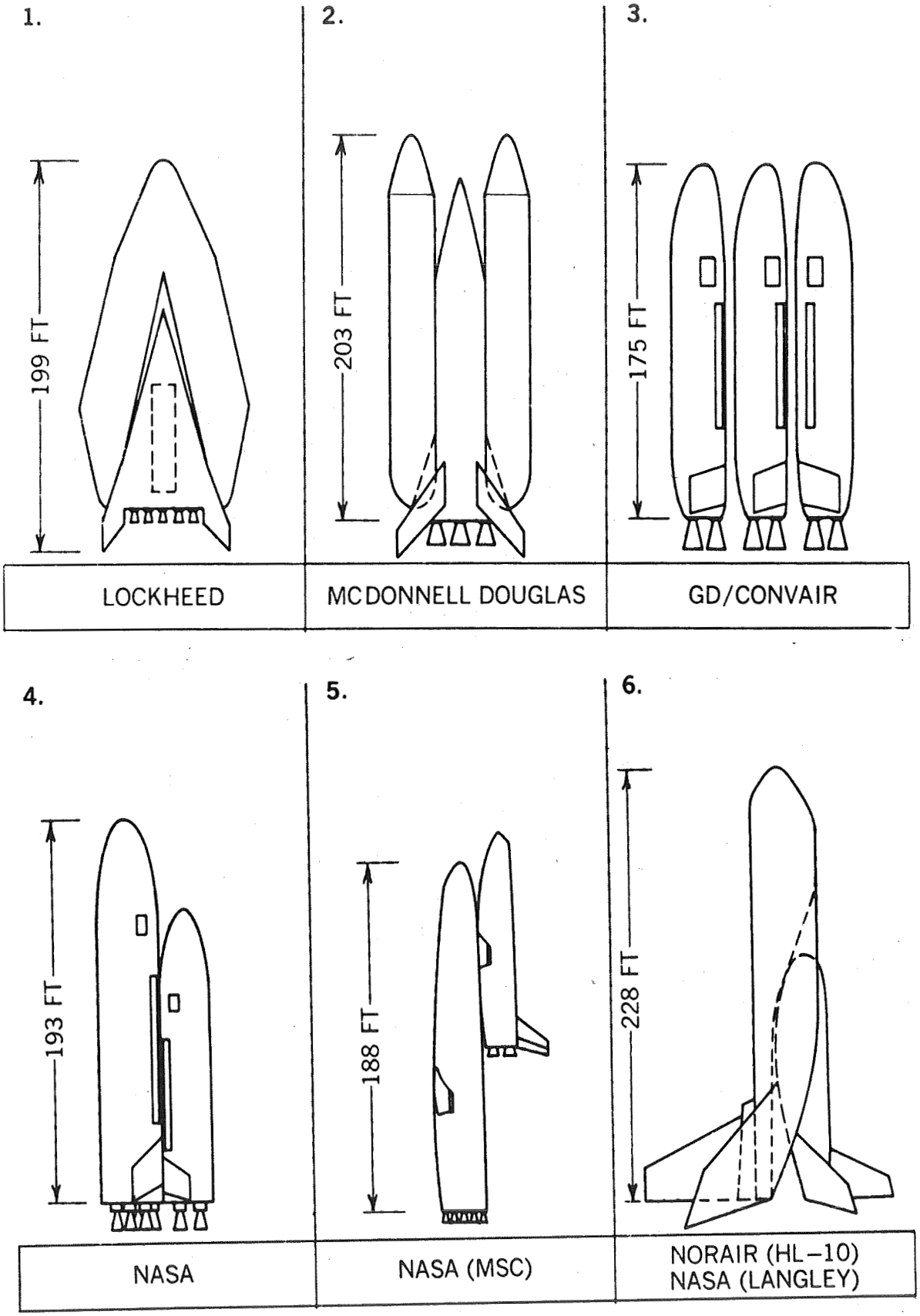

Figure 5. SOME POSSIBLE SPACE SHUTTLECRAFT CONFIGURATIONS (SPACE/AERONAUTICS, SEPTEMBER 1969)

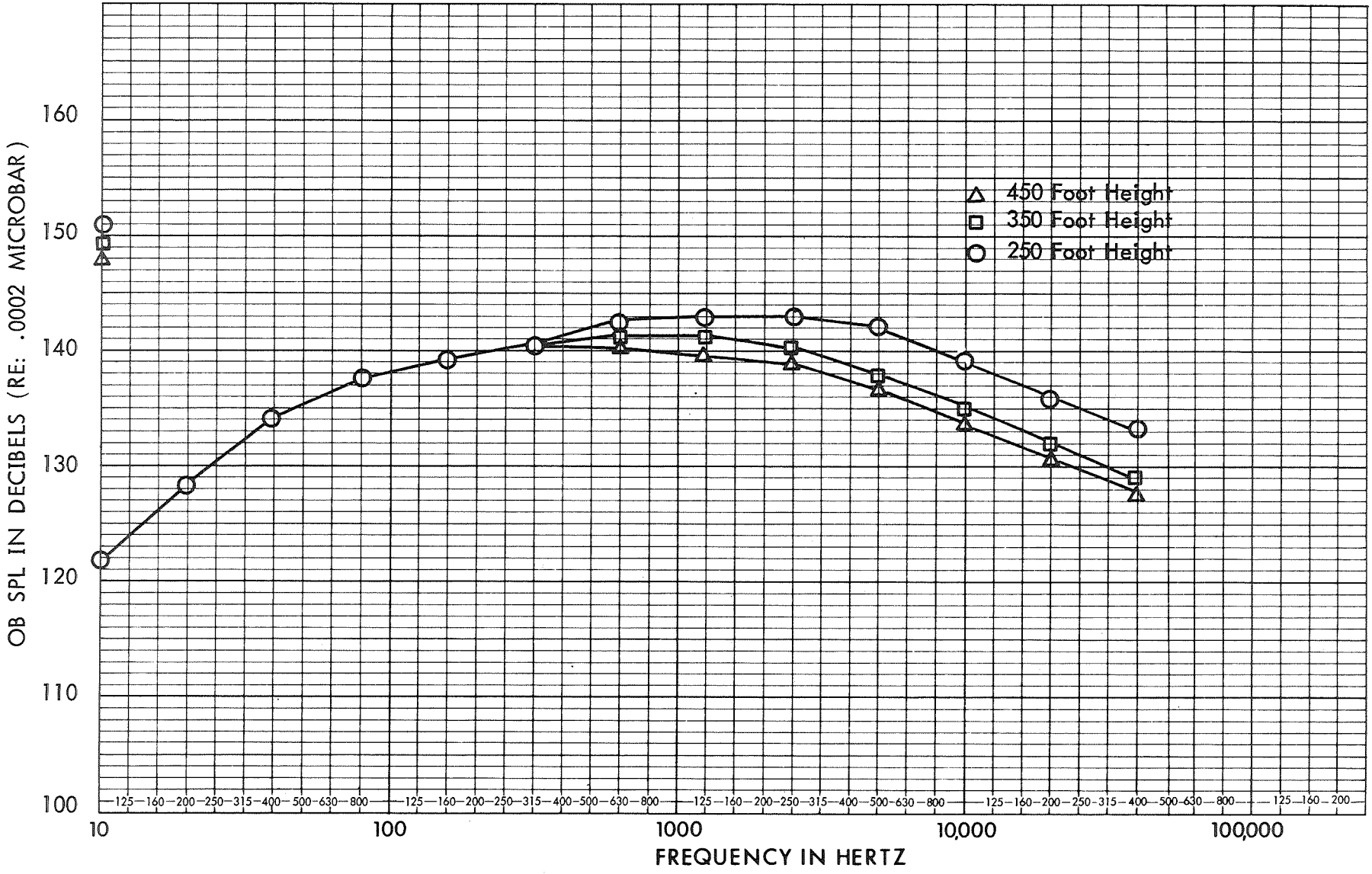

Figure 6. LIFTOFF OCTAVE BAND SPECTRA

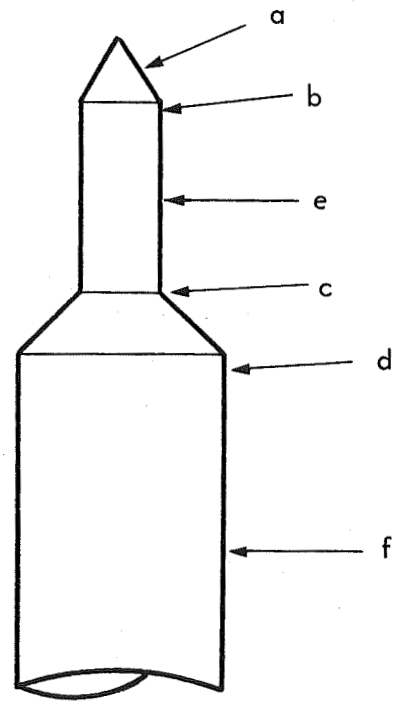

Positions	Coefficients P/Q		Pounds Per Square Foot		Pressure Fluctuations in dB (re: .0002 dynes/cm^2)	
	M = 1	M = 1.6	M = 1	M = 1.6	M = 1	M = 1.6
a (with wake)	.05	.05	29	35	157	158
a (without wake)	.005	.005	2.9	3.5	137	138
b	.05	.05	29	35	157	158
c	.015	.015	8.5	10.5	145	147
d	.025	.05	14.4	42	150	158
e (with wake)	.025	.015	14.4	10.5	150	147
e (without wake)	.005	.005	2.9	3.5	137	138
f	.015	.015	8.5	10.5	145	147

Figure 7. FLUCTUATING PRESSURE COEFFICIENTS FOR TYPICAL VEHICLE

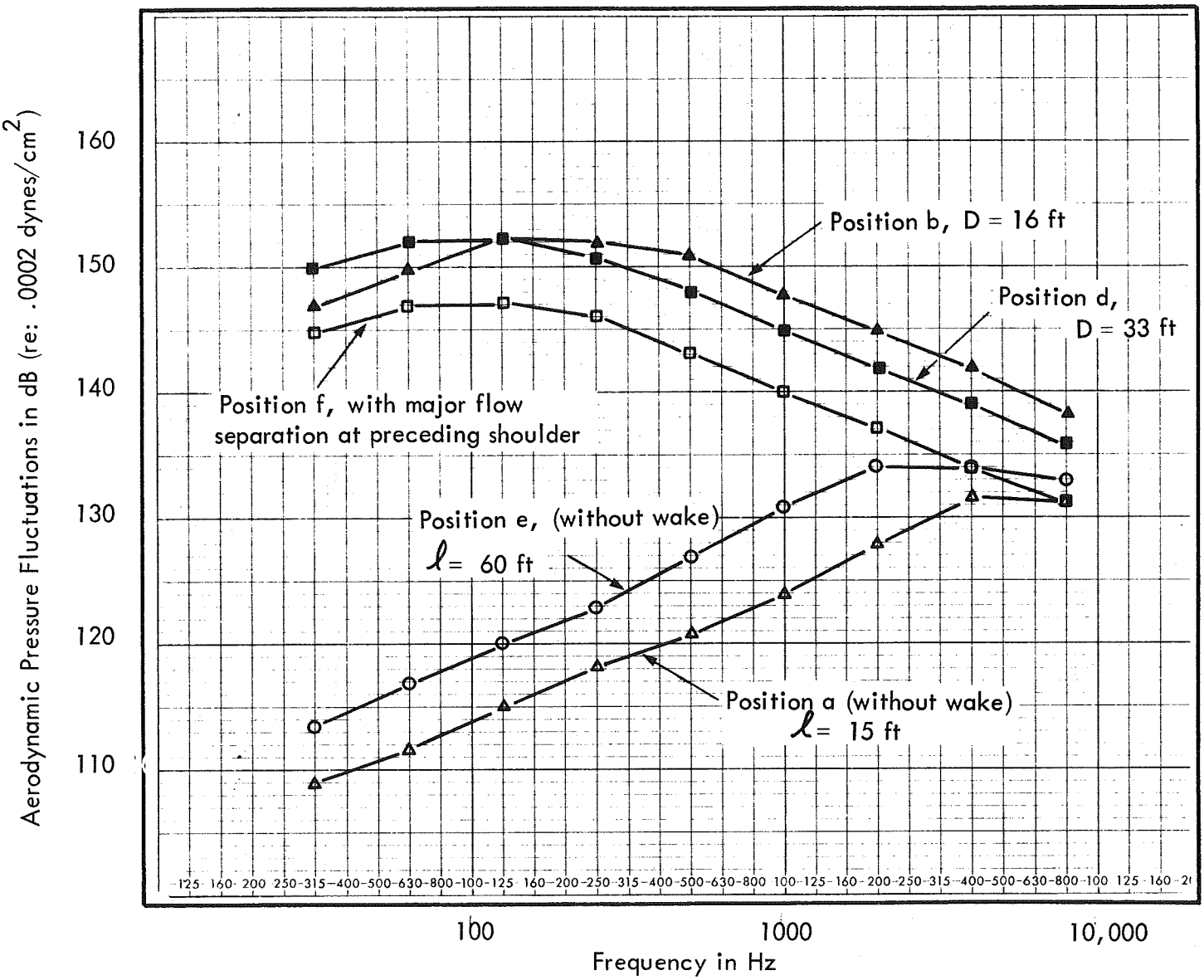

Figure 8. TYPICAL AERODYNAMIC PRESSURE FLUCTUATIONS FOR SPACE BASE LAUNCH FOR MAX Q

(POSITIONS REFER TO FIGURE 7.)

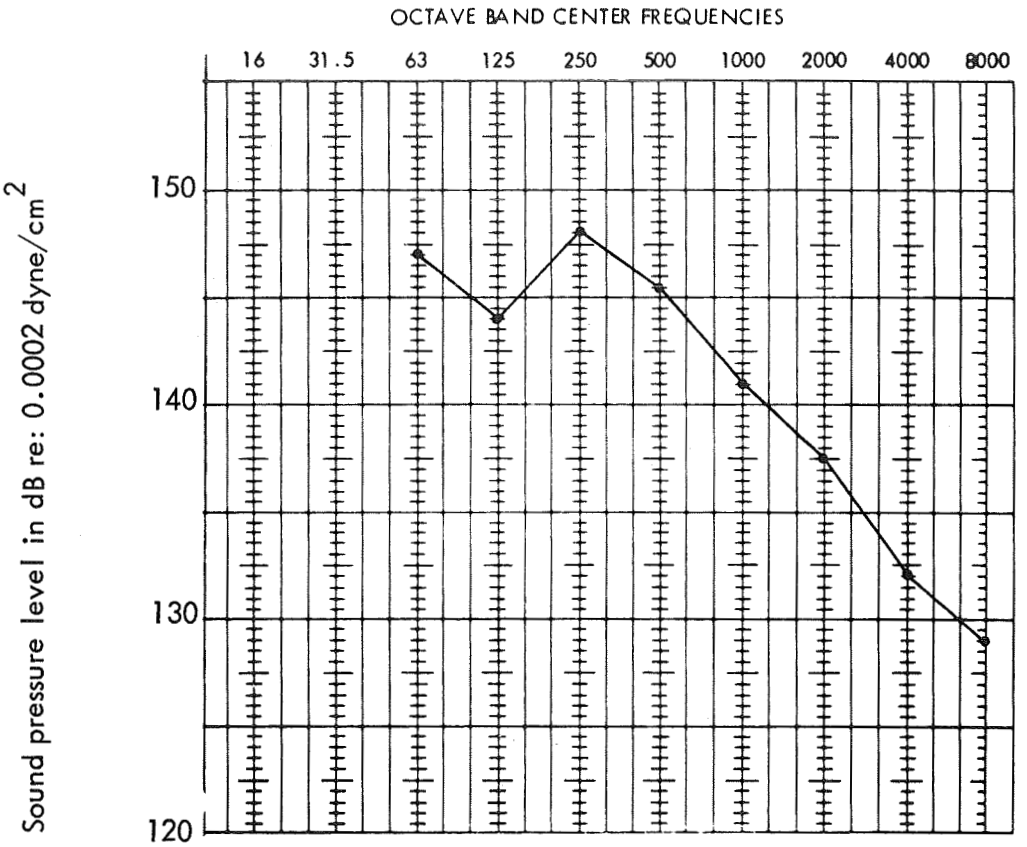

Figure 9. OCTAVE BAND SOUND PRESSURE LEVELS AT ONE POSITION IN A SMALL REVERBERATION ROOM

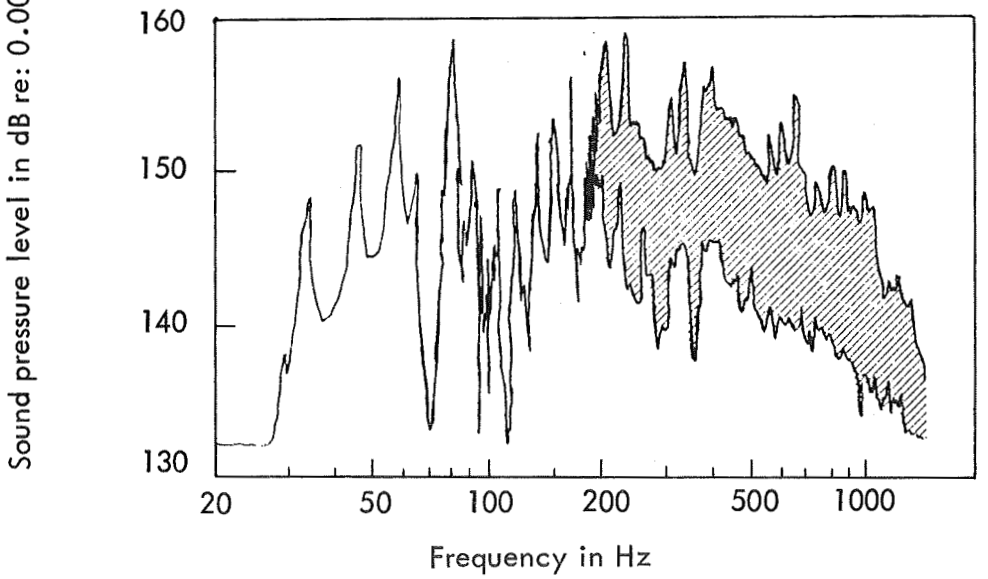

Figure 10. FREQUENCY RESPONSE OF A REVERBERATION ROOM TAKEN AT THE SAME POSITION AS THAT IN FIGURE 9

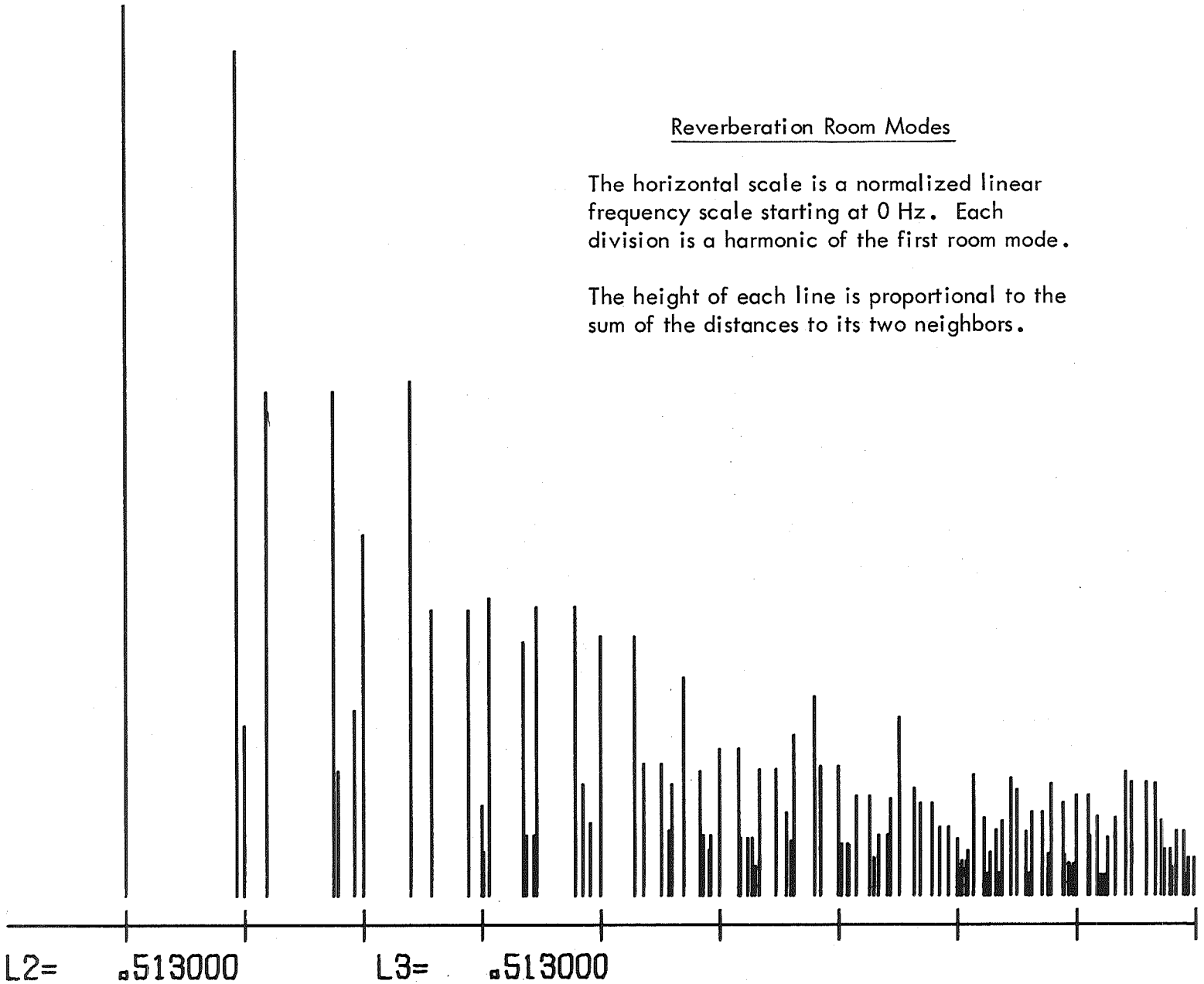

Figure 11. MODAL DENSITY FOR A ROOM HAVING DIMENSION RATIOS 1 : 0.513 : 0.513

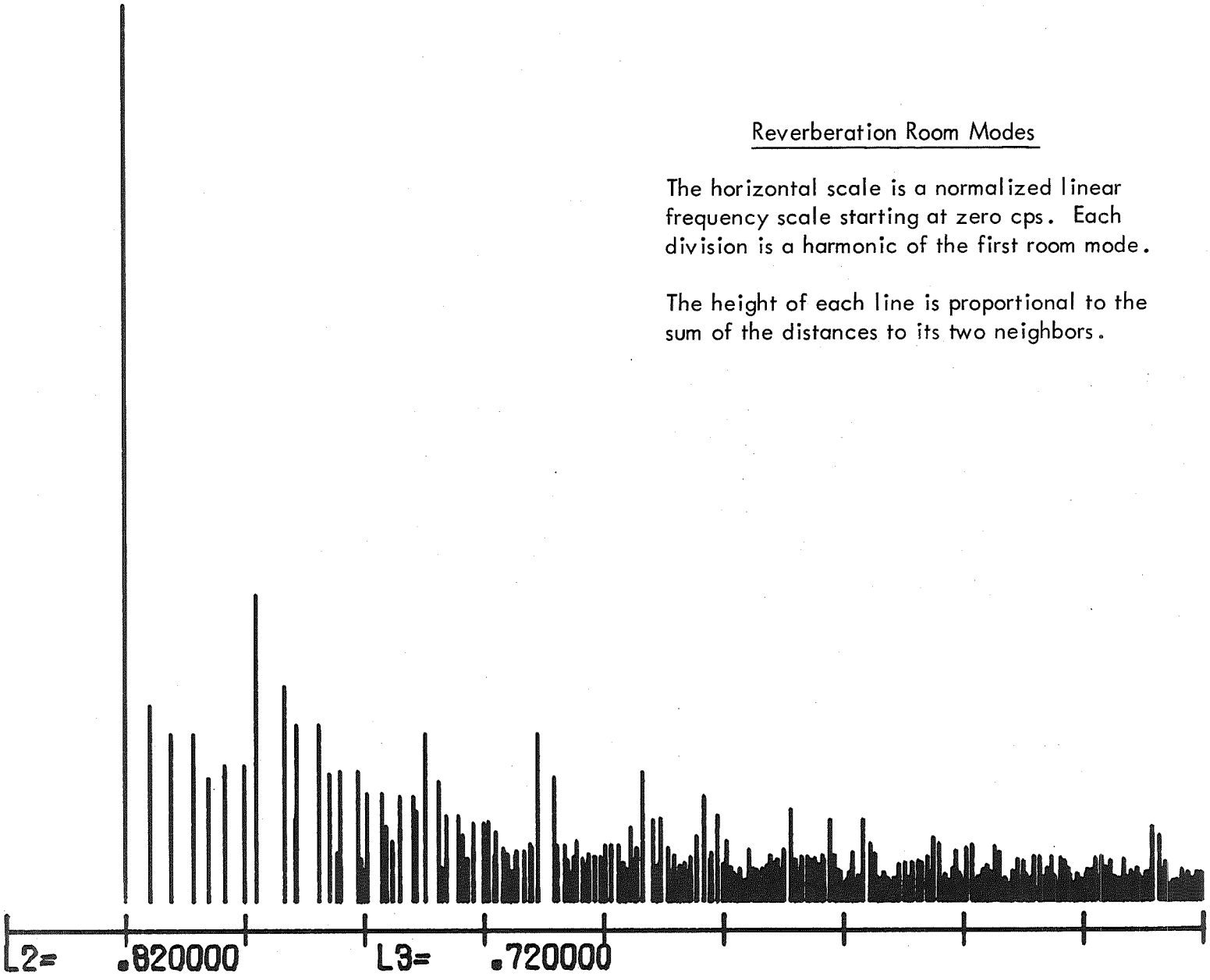

Figure 12. MODAL DENSITY FOR A ROOM HAVING DIMENSION RATIOS 1: 0.82 : 0.72

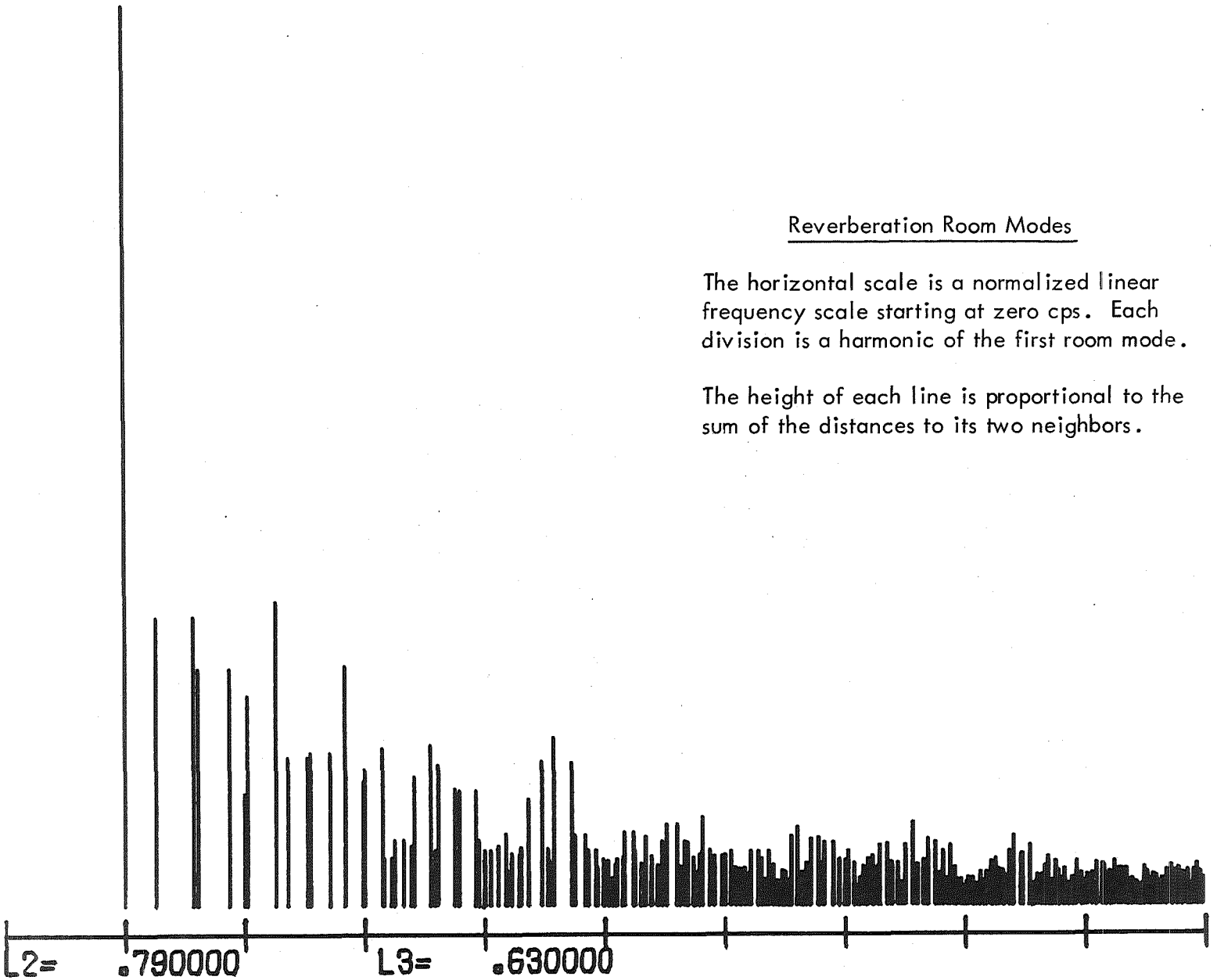

Figure 13. MODAL DENSITY FOR A ROOM HAVING DIMENSION RATIOS 1 : 0.79 : 0.63

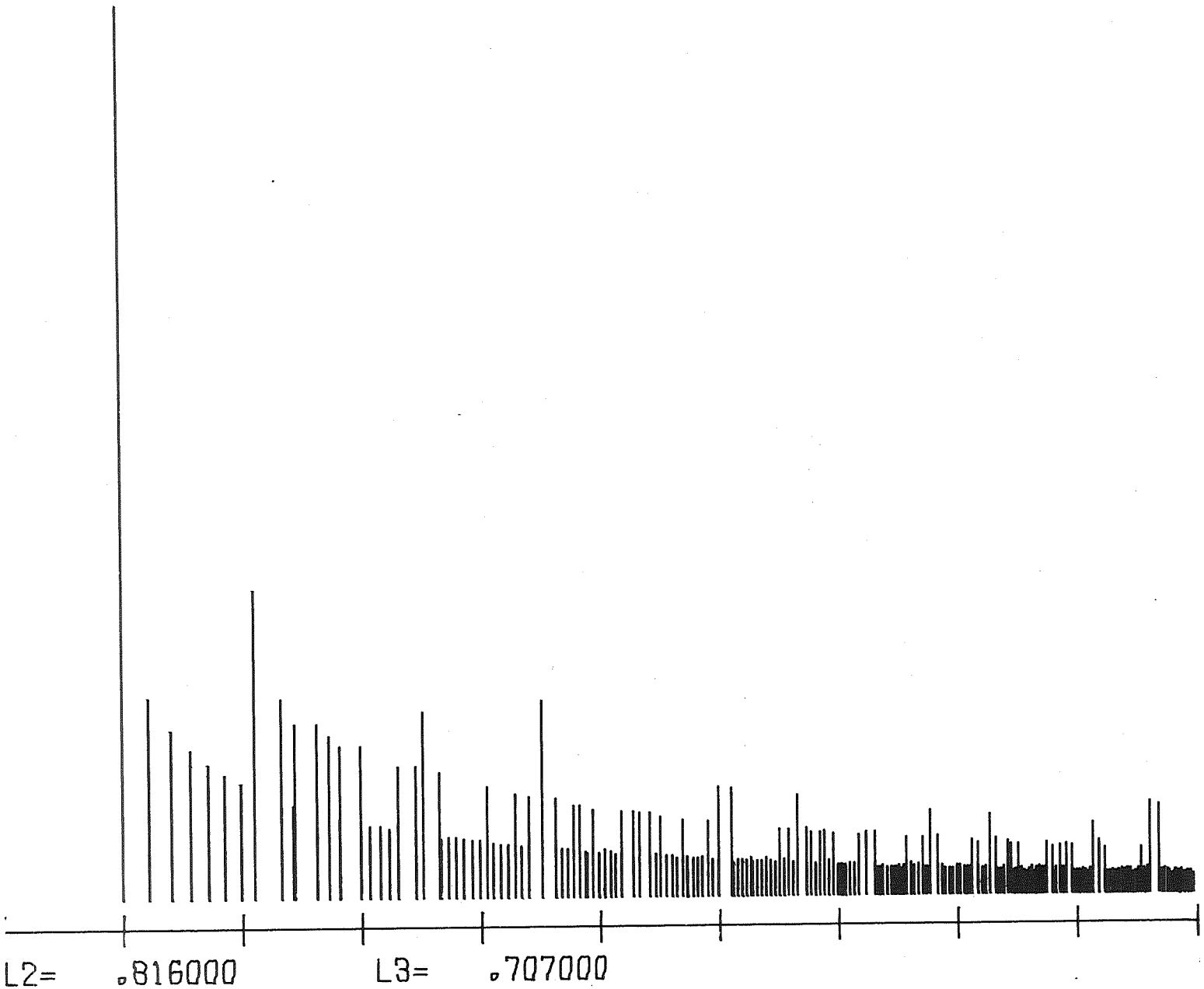

Figure 14. MODAL DENSITY FOR A ROOM HAVING DIMENSION RATIOS 1 : 0.816 : 0.707

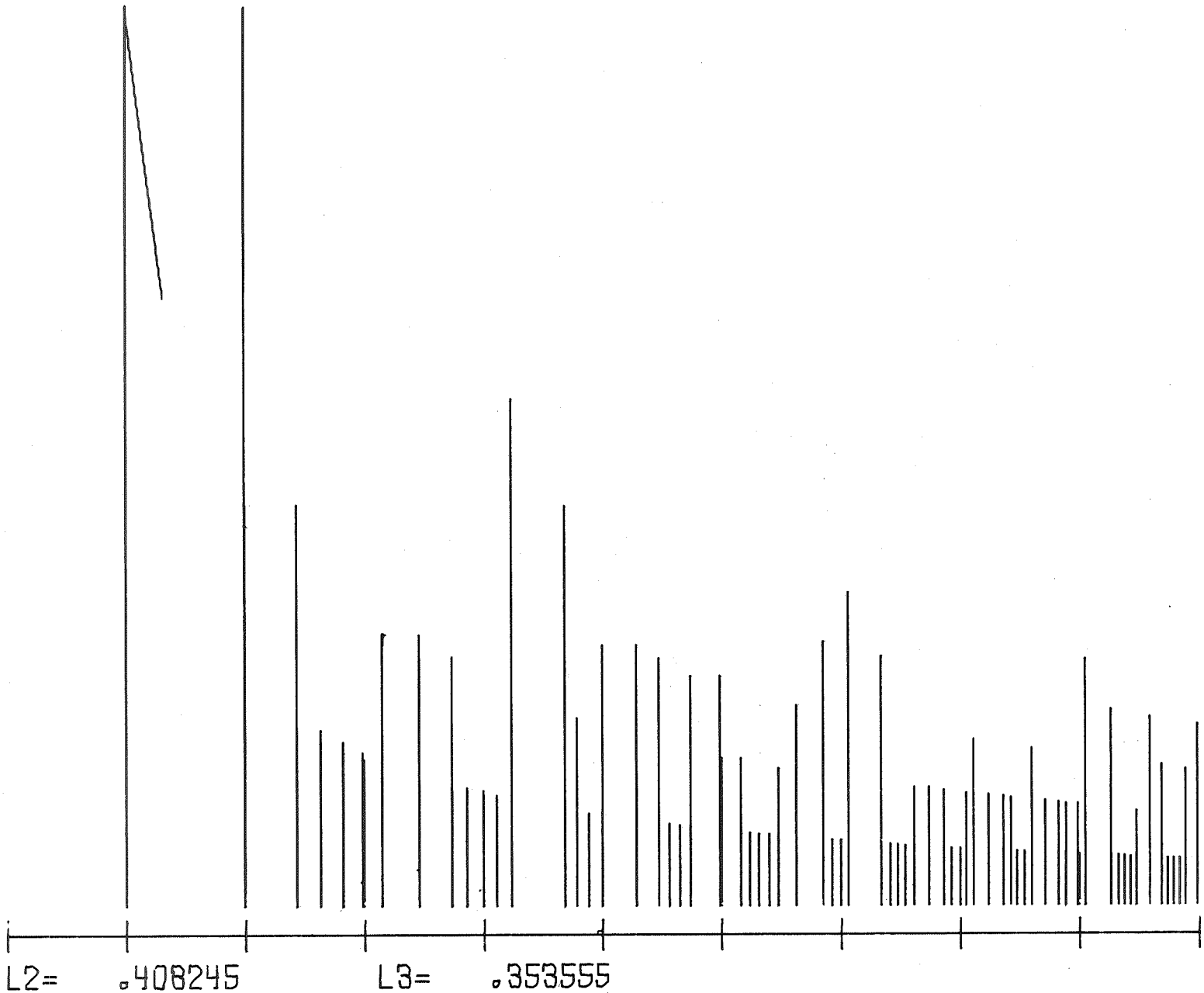

Figure 15. MODAL DENSITY FOR A ROOM HAVING DIMENSION RATIOS 1 : 0.408245 : 0.353555

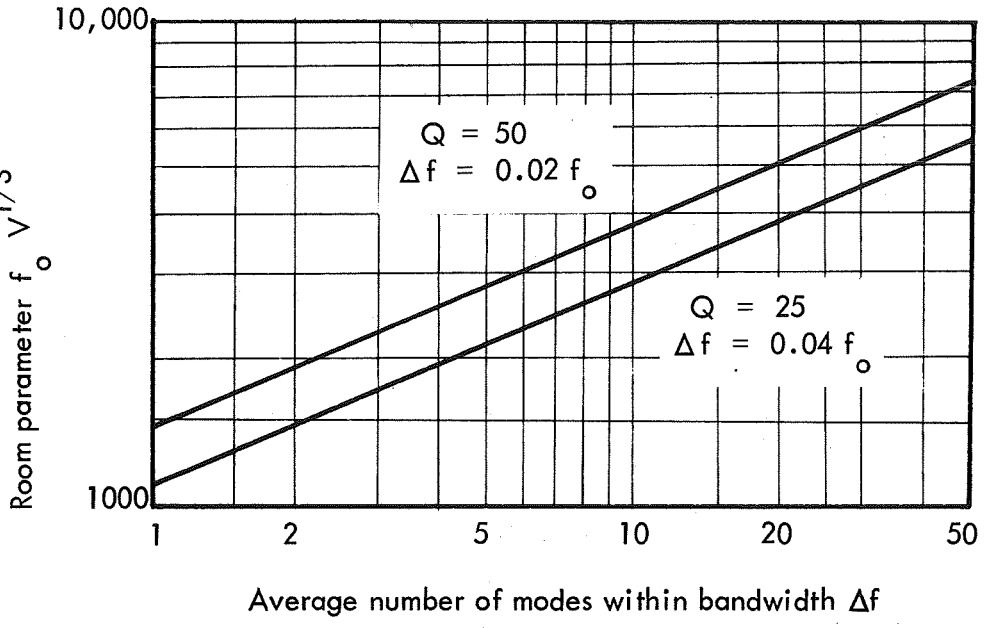

The average number of modes within the resonance bandwidth of a specimen for Q = 25 and 50, as a function of the room parameter $f_o V^{1/3}$, where f_o is the center frequency and V the volume of the reverberation chamber in $feet^3$. (Reprinted from Reference 17.)

Figure 16. MODAL DENSITY IN REVERBERATION ROOM

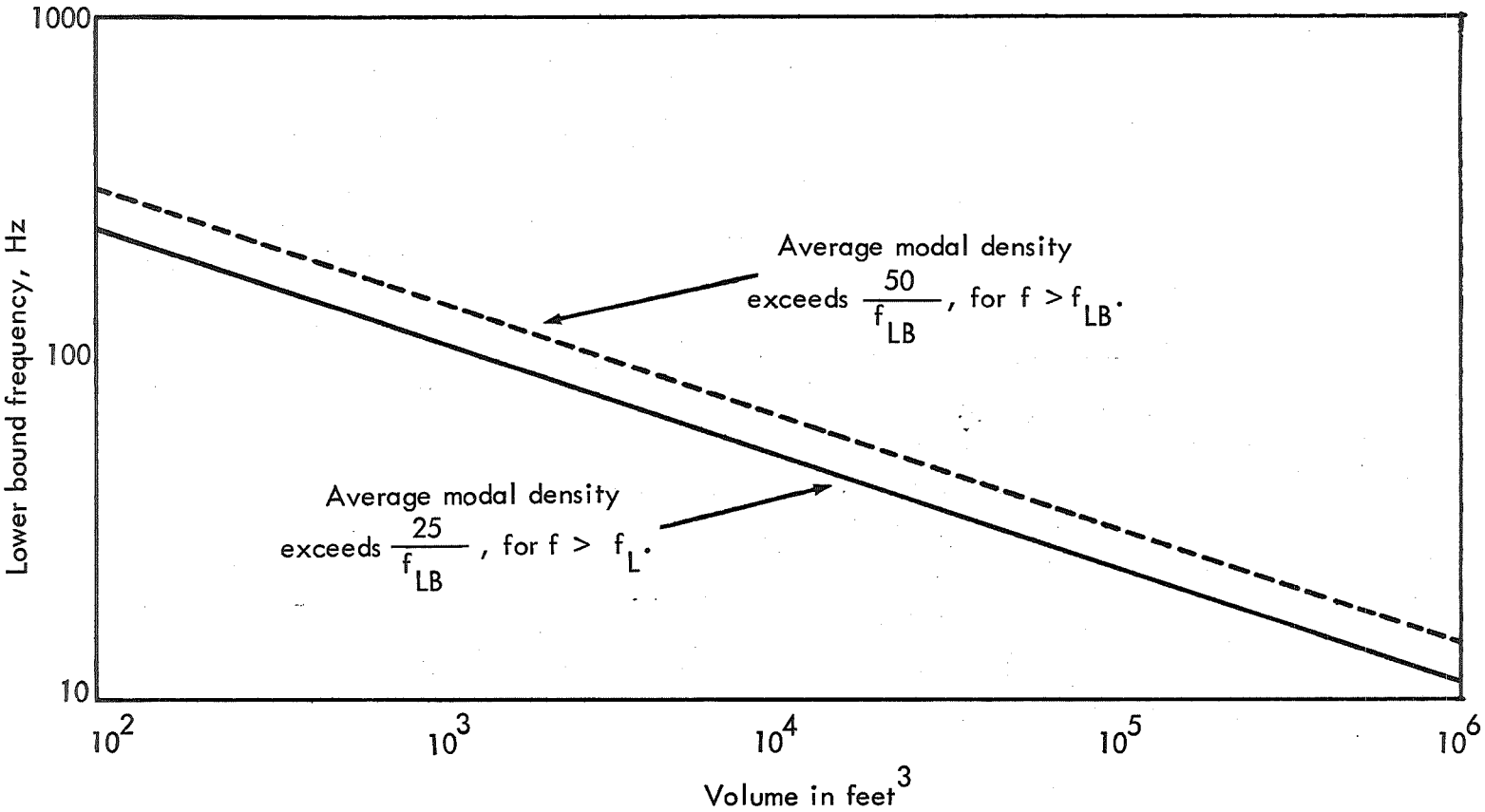

Figure 17. COMPARISON OF REVERBERANT ROOM VOLUME AND LOWER BOUND FREQUENCY (REPRINTED FROM REFERENCE 17.)

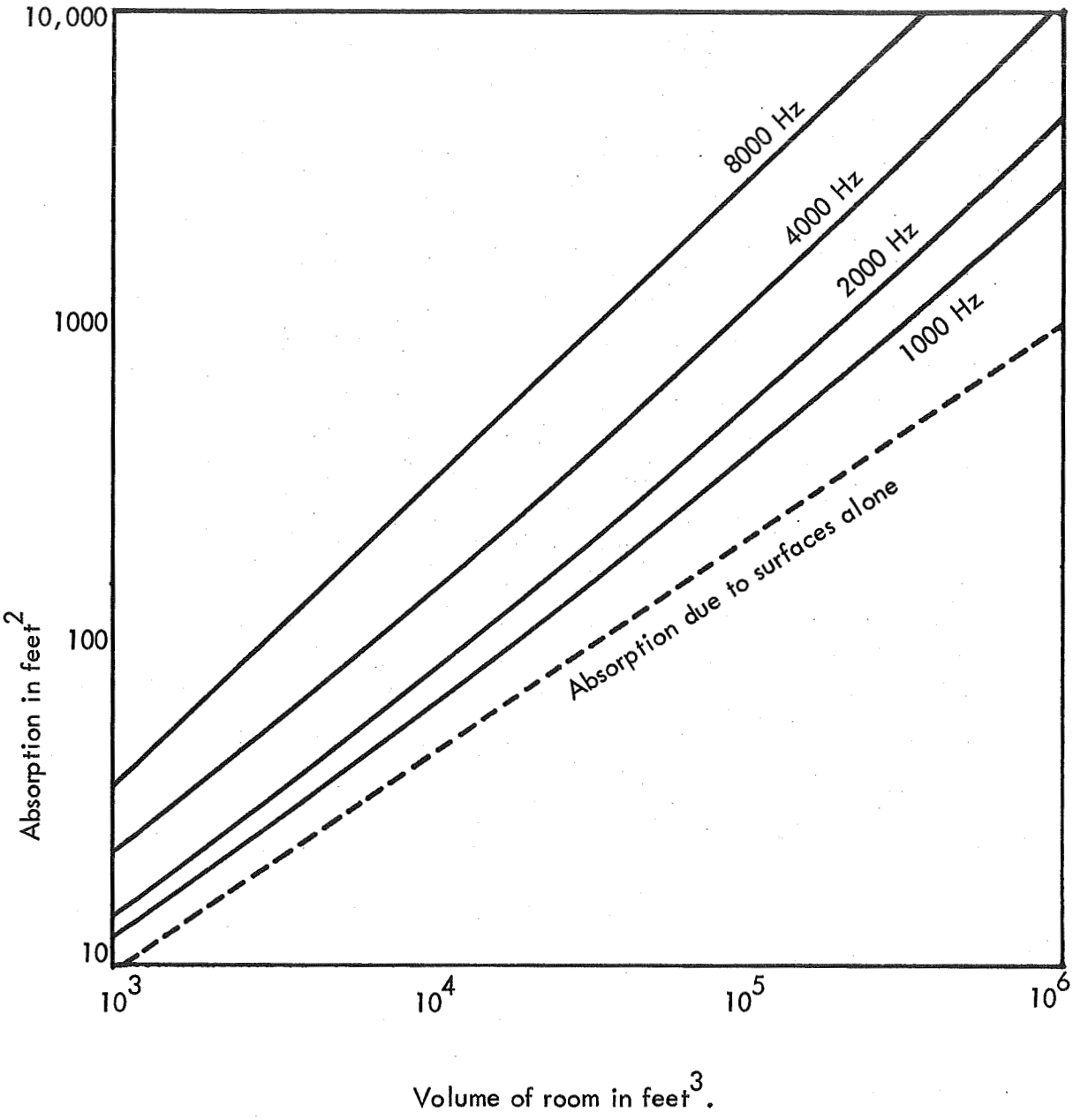

Figure 18. ABSORPTION AS A FUNCTION OF VOLUME FOR A REVERBERATION CHAMBER WITH FREQUENCY AS A PARAMETER, ASSUMING AN AVERAGE ABSORPTION COEFFICIENT OF 0.015 FOR THE SURFACES AND AIR AT 40 PERCENT R.H. AS THE MEDIUM

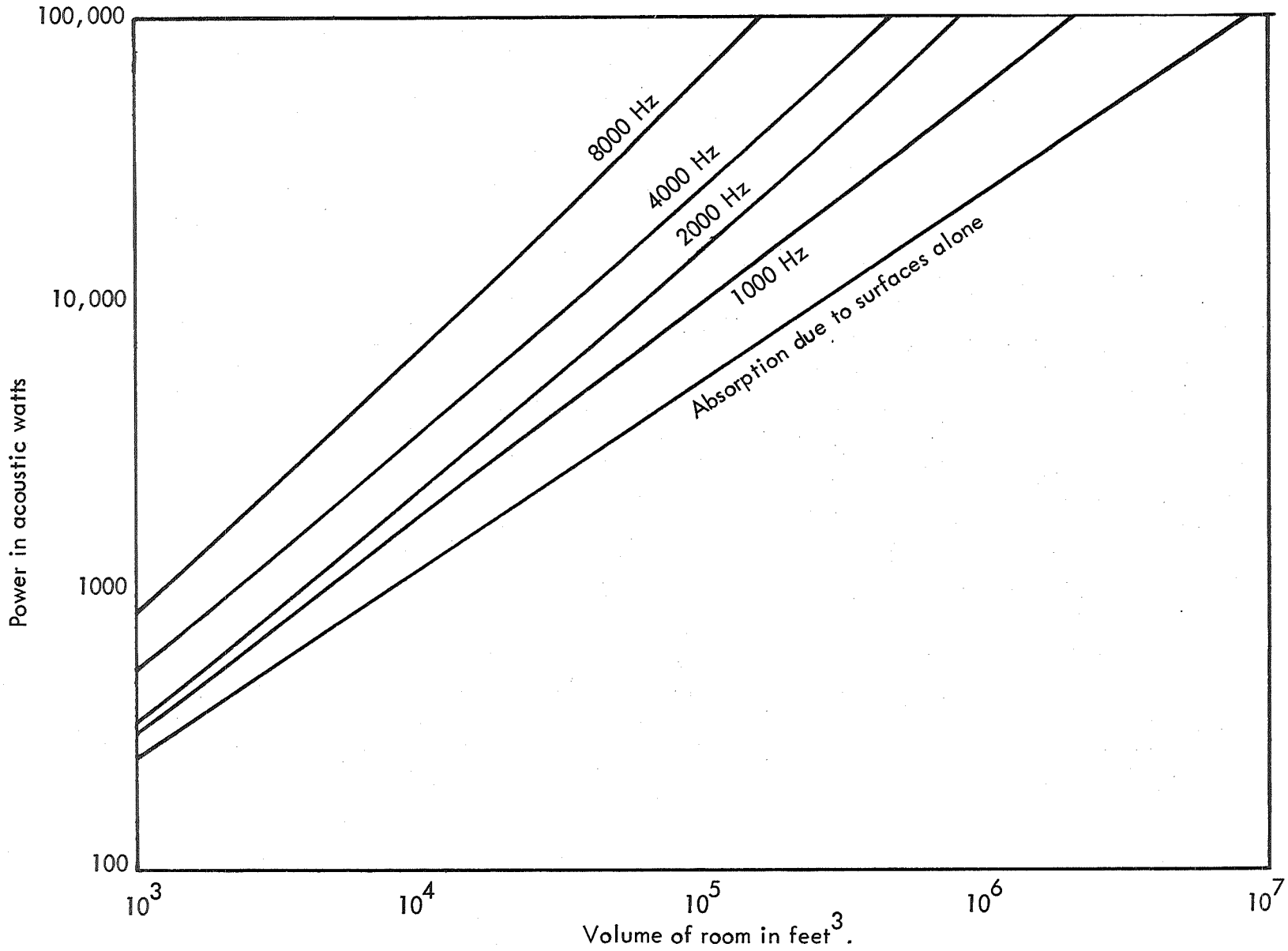

Figure 19. EFFECTIVE POWER REQUIRED TO PRODUCE AN SPL OF 150 dB IN AIR AS A FUNCTION OF ROOM VOLUME WITH IDEAL COUPLING

NOTE: The actual power rating of air modulation will generally have to be three times the required effective power because of coupling inefficiencies.

a) 15" spacing

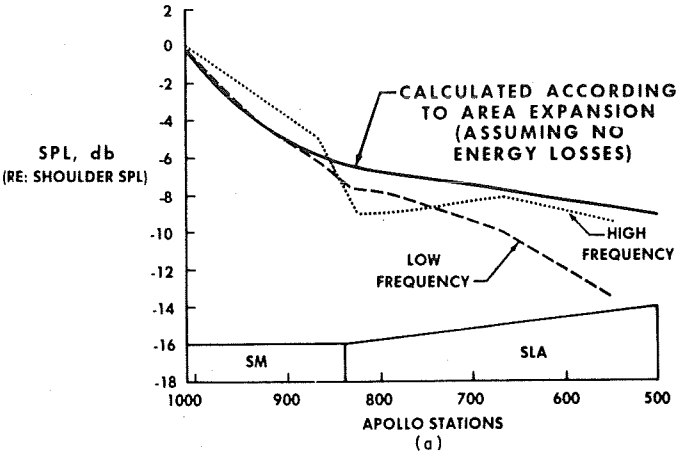

b) 4-1/2" spacing

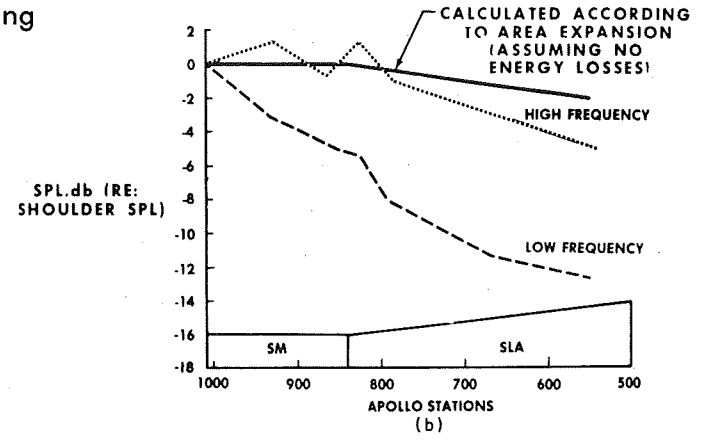

Axial variation in sound pressure level along a progressive wave duct on an Apollo vehicle for a duct depth of (a) 15" and (b) 4-1/2".

The terms high and low frequency regions refer to frequencies greater and less than 500 Hz respectively. (Reprinted from Reference 18).

Figure 20. AXIAL VARIATION IN SOUND PRESSURE LEVEL IN A PROGRESSIVE WAVE DUCT

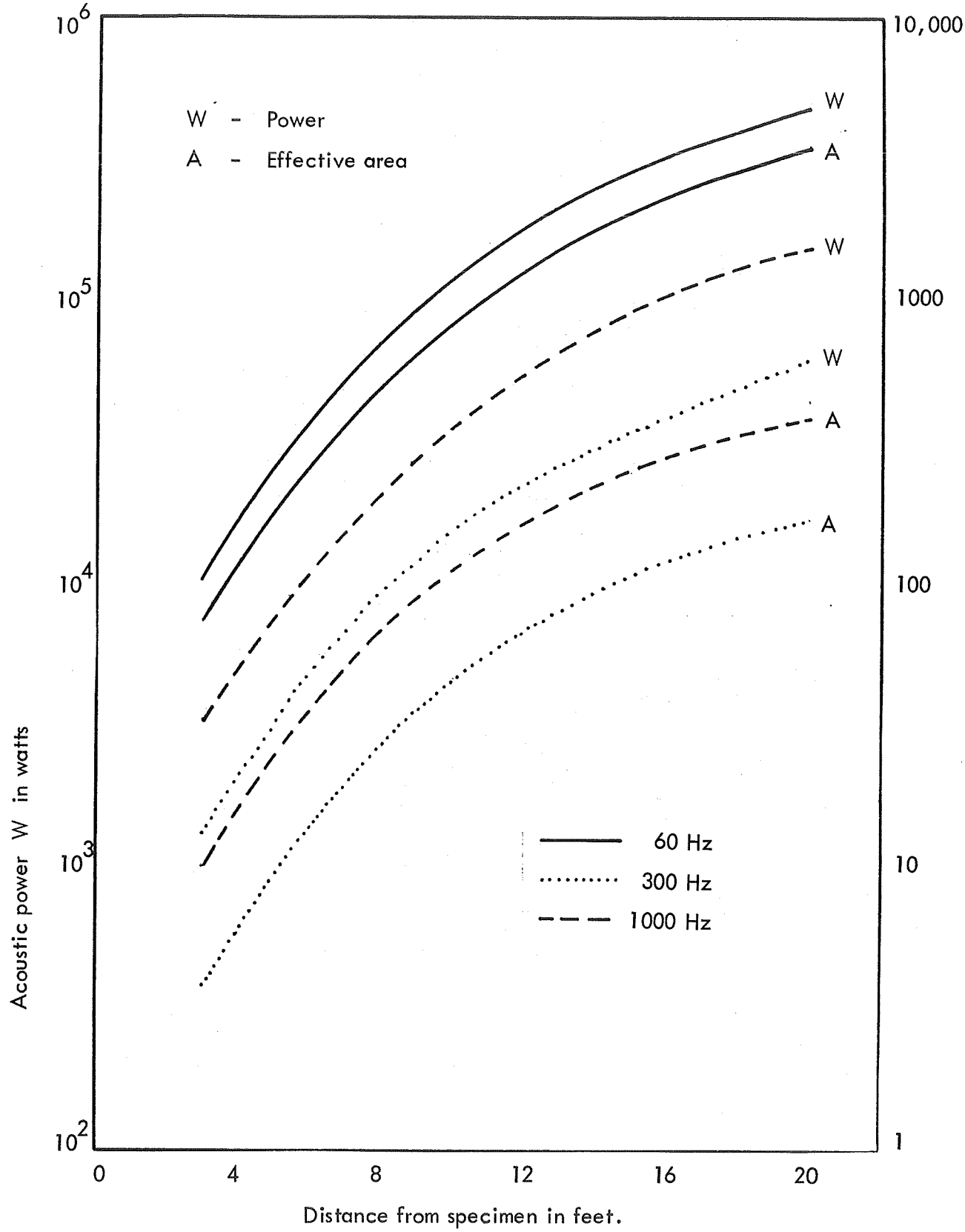

Figure 21. POWER REQUIRED TO PRODUCE A SOUND PRESSURE LEVEL OF 160 dB ON THE SURFACE OF A SPECIMEN, TOGETHER WITH THE EFFECTIVE AREA COVERED. AS A FUNCTION OF SOURCE DISTANCE, FOR DIRECT RADIATION

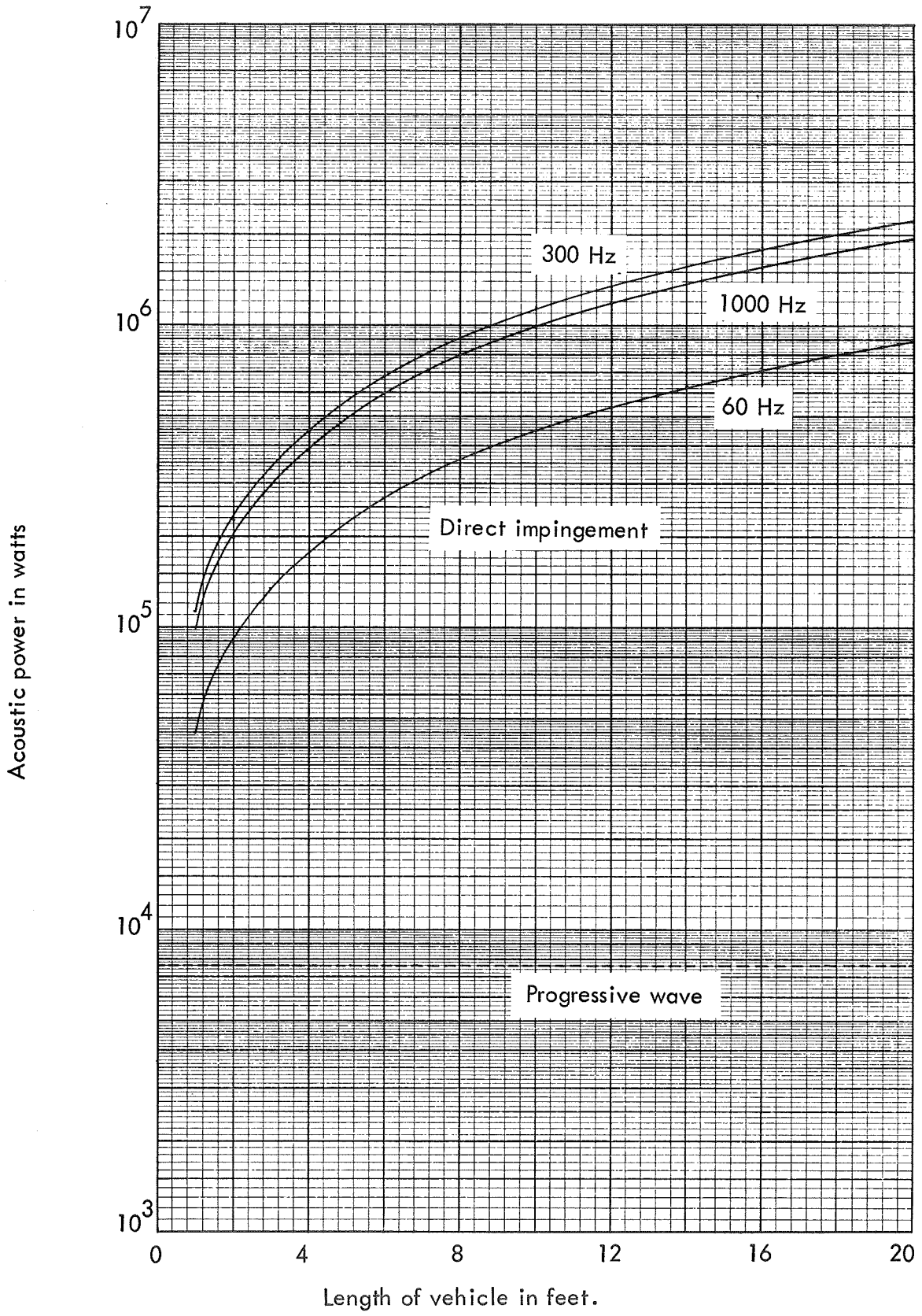

Figure 22. ACOUSTIC POWER IN WATTS REQUIRED TO PRODUCE A SOUND PRESSURE LEVEL OF 160 dB OVER THE SURFACE OF A 10 FT DIAMETER CYLINDER AS A FUNCTION OF CYLINDER LENGTH, FOR THE DIRECT IMPINGEMENT AND PROGRESSIVE WAVE METHODS OF EXCITATION

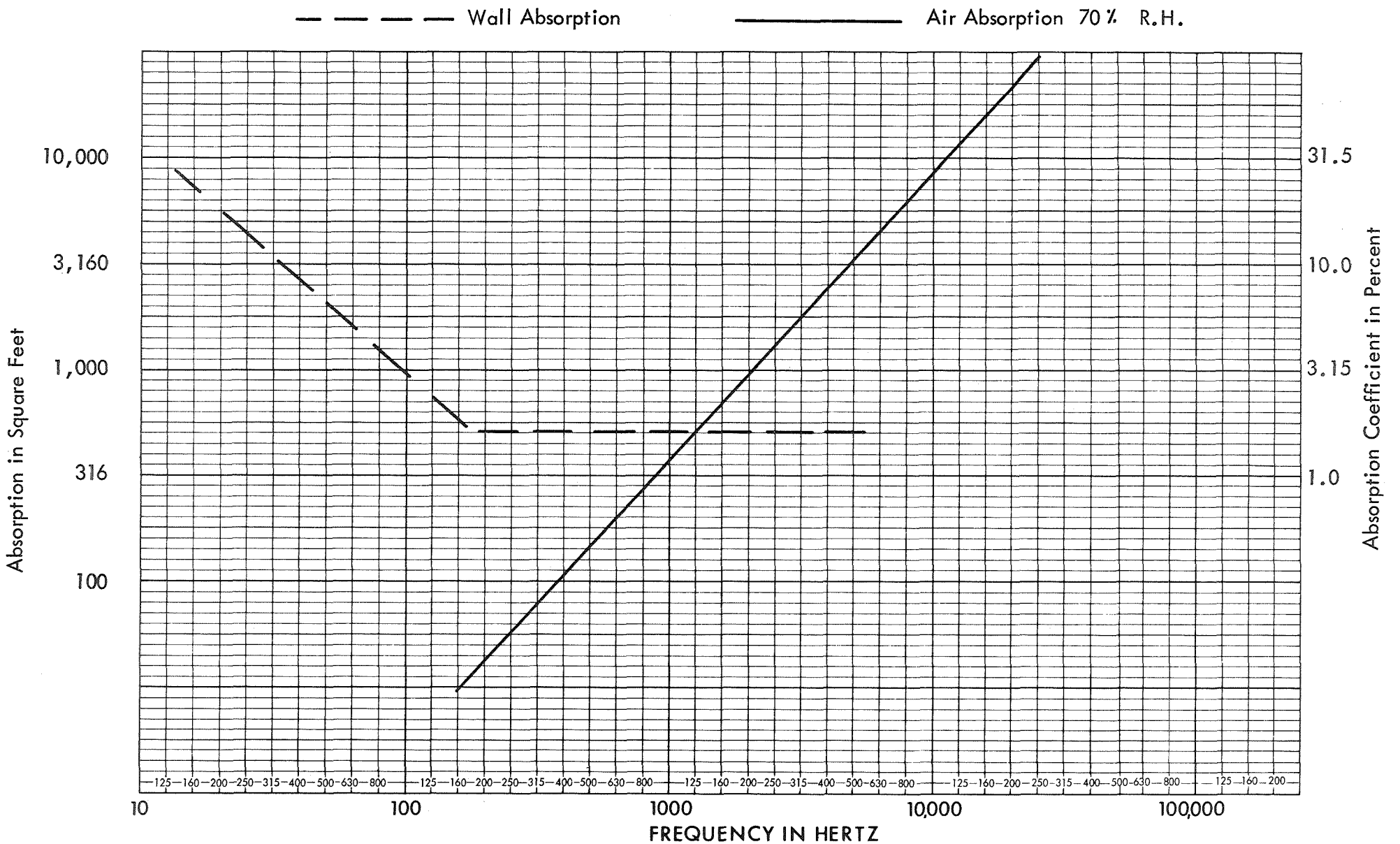

Figure 23. ESTIMATED ABSORPTION IN PROPOSED REVERBERATION ROOM BUILDING 49A

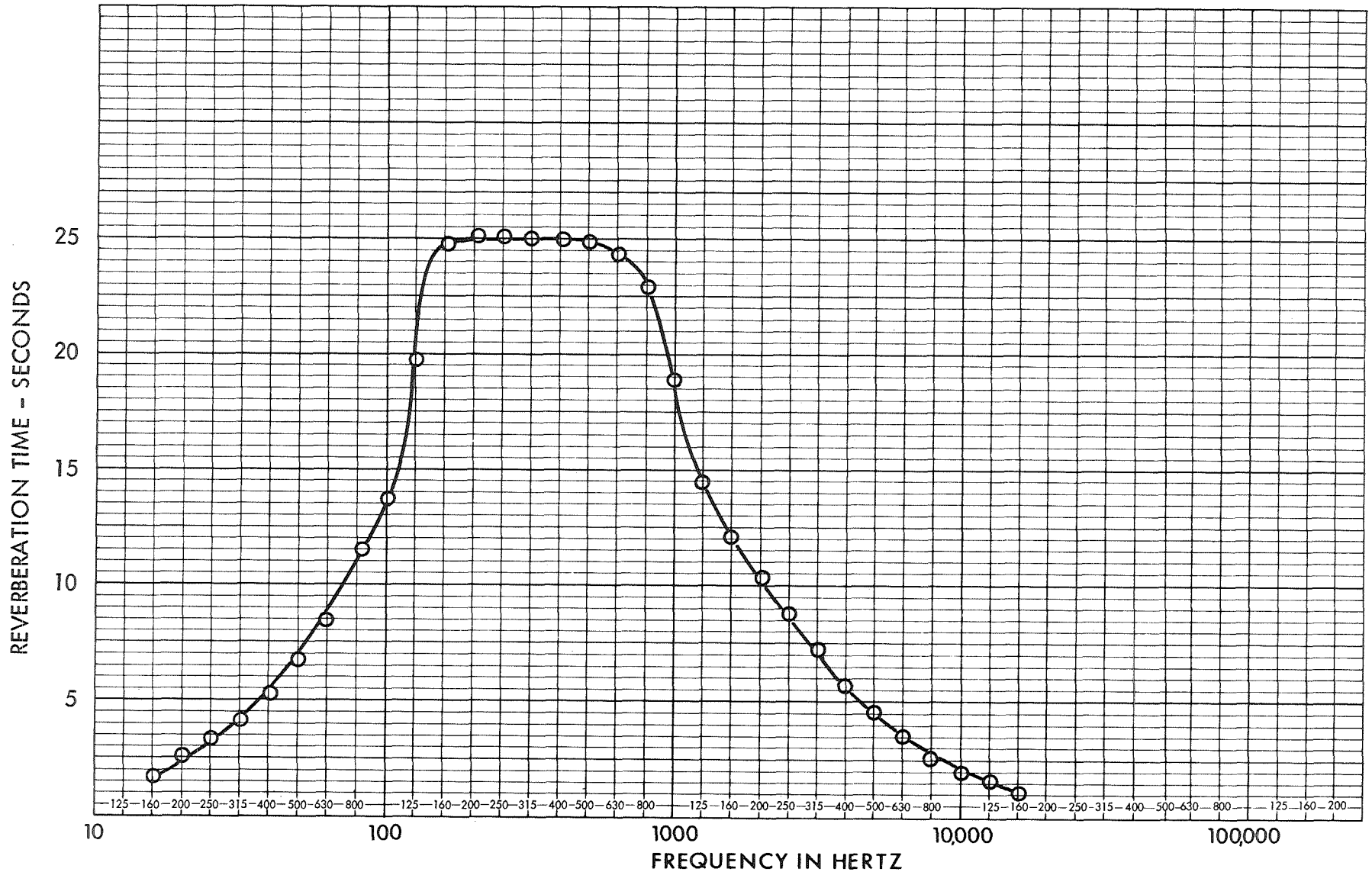

Figure 24. ESTIMATED REVERBERATION TIME - BUILDING 49A WITH AIR

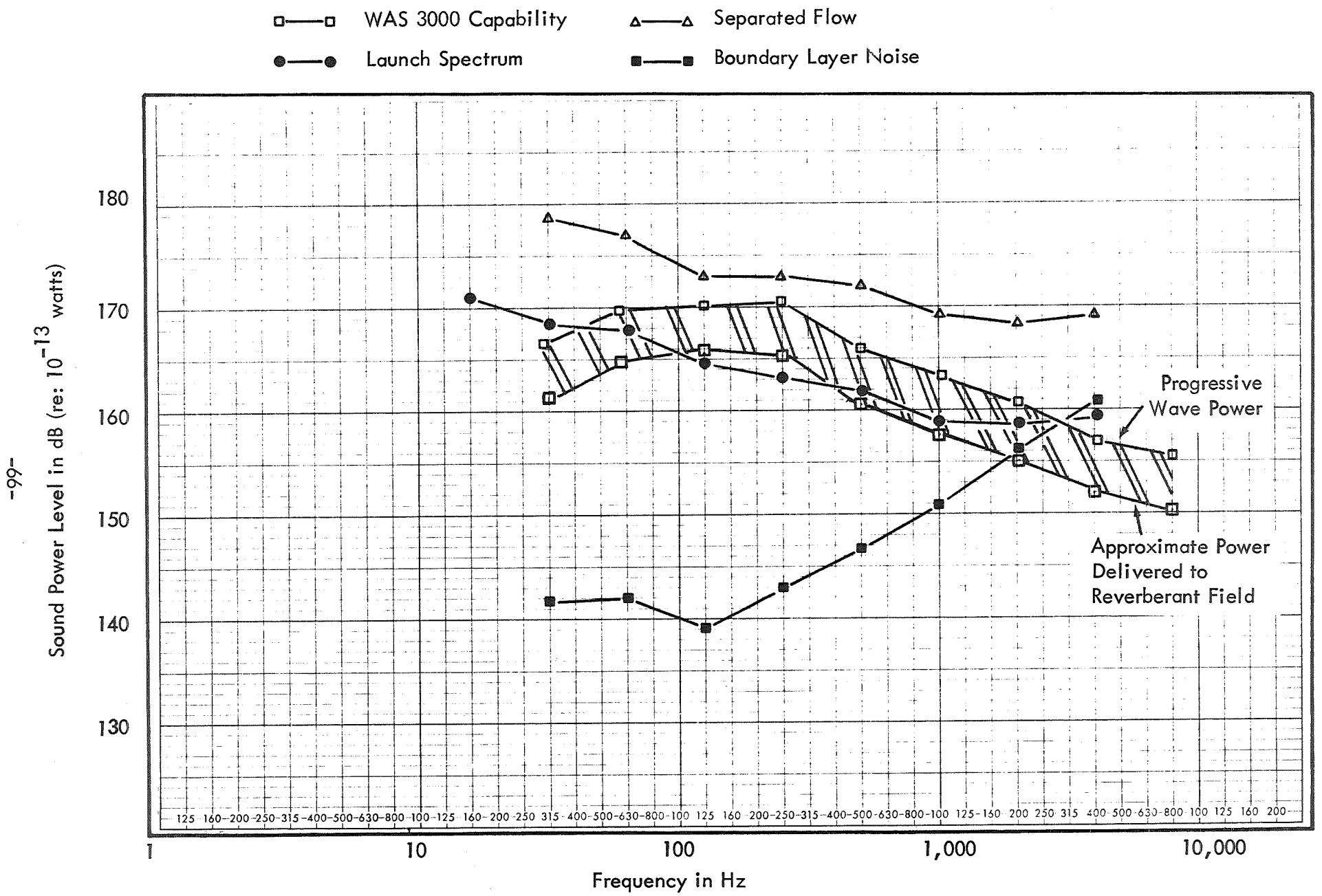

Figure 25. POWER LEVELS FOR BUILDING 49A

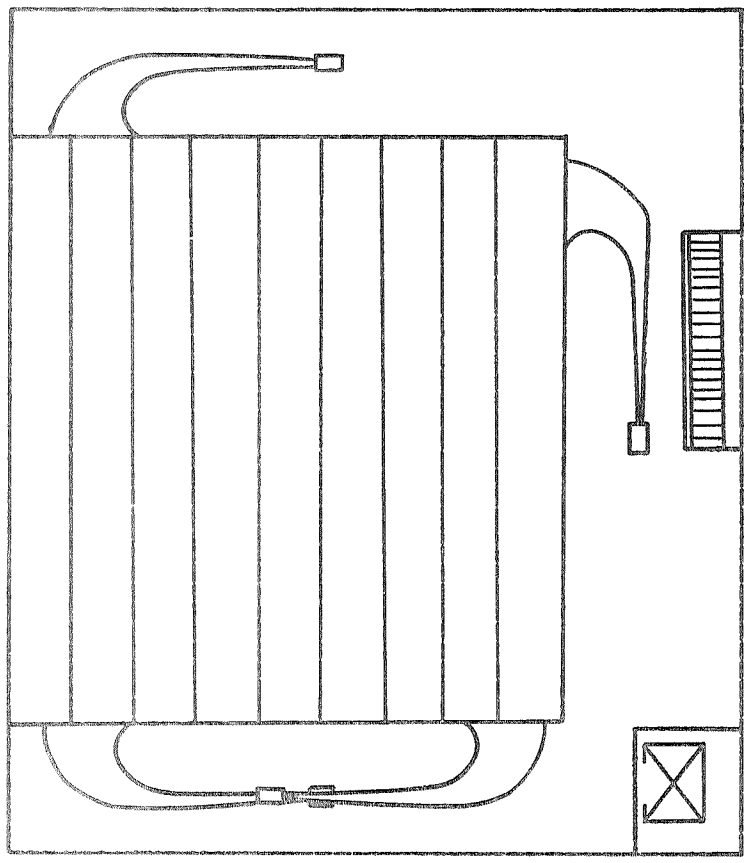

PLATFORM PLAN AT EL 30'-0"

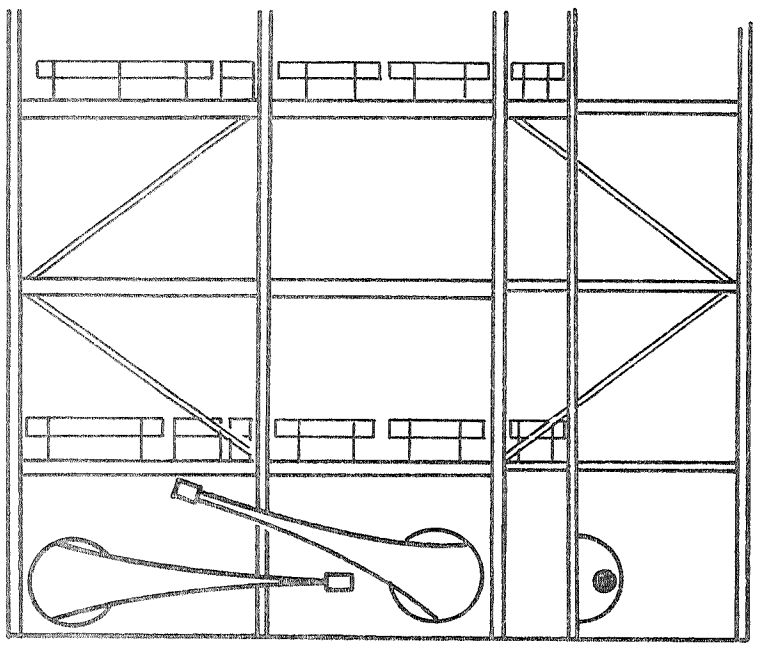

SECTION LOOKING EAST

TABLE I. COUPLING HORN MOLD DIMENSIONS

Station No. on Axis in Feet	Angle of Curvature of Axis	Horn Diameter Inches
0	0	4.2
1	0	4.8
2	0	5.6
3	0	6.4
4	0	7.4
5	0	8.5
6	0	9.8
7	0	11.3
8	0	12.8
9	0	14.8
10	0	17.0
11	0	19.5
12	0	22.3
12.6	0	24.2
13.64	10	28.0
14.68	20	32.5
15.72	30	38.0
16.77	40	43.0
17.82	50	50.5
18.86	60	58.0
19.90	70	67.0
20.95	80	78.0
22	90	90.0

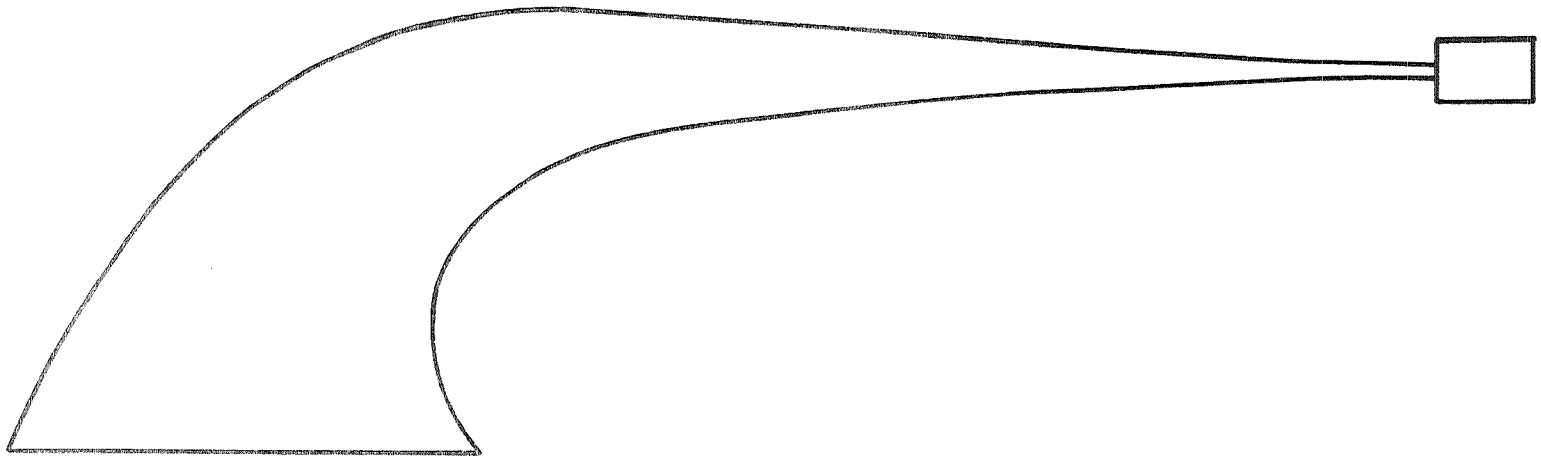

COUPLING HORN MOLD LINE 1" - 3'

Figure 26. PROPOSED HORN SYSTEM

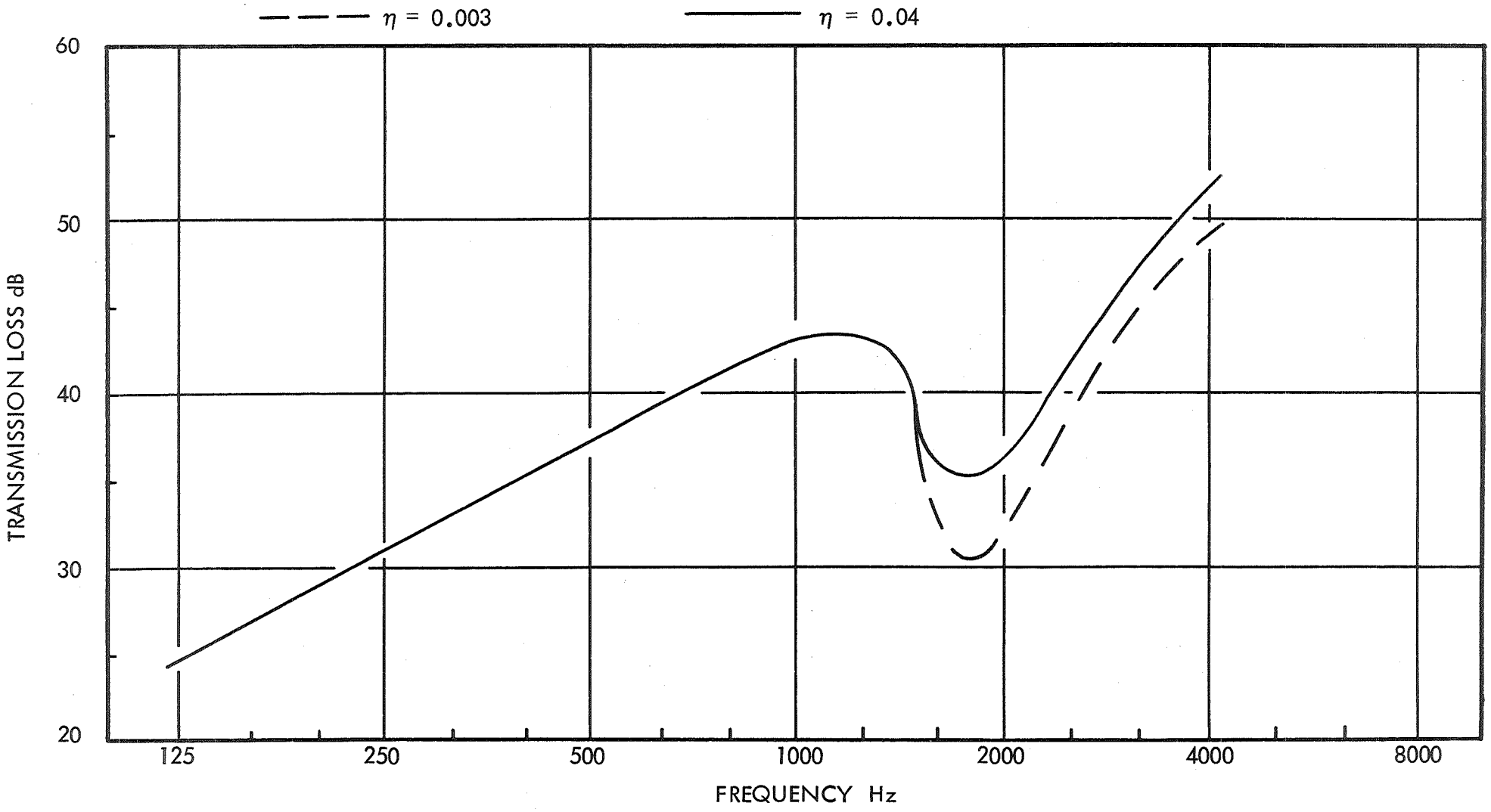

Figure 27. MEASURED TRANSMISSION LOSS FOR DAMPED STEEL PANELS 1/4" THICK

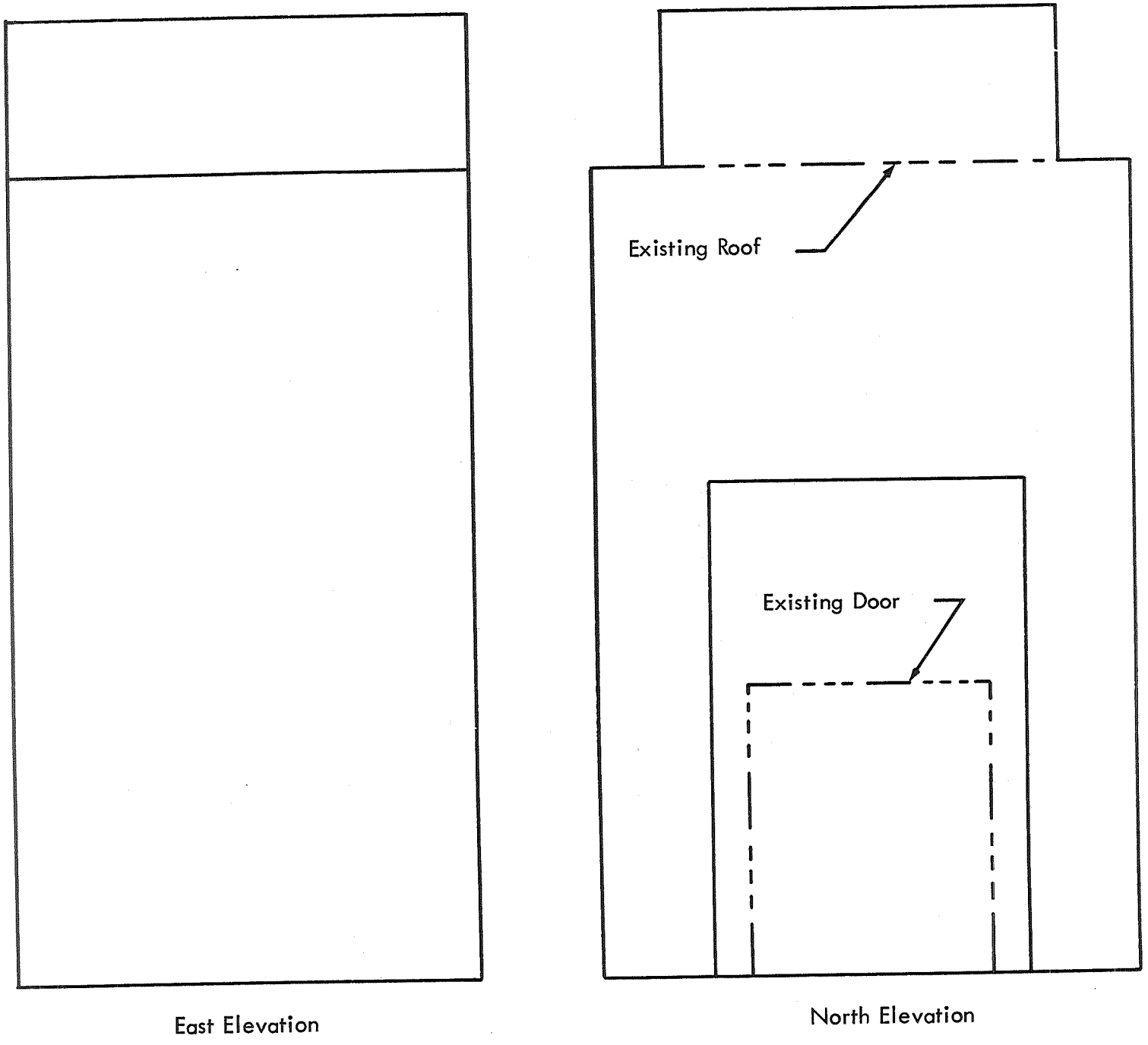

Figure 28. ELEVATION OUTLINES OF BUILDING 49A

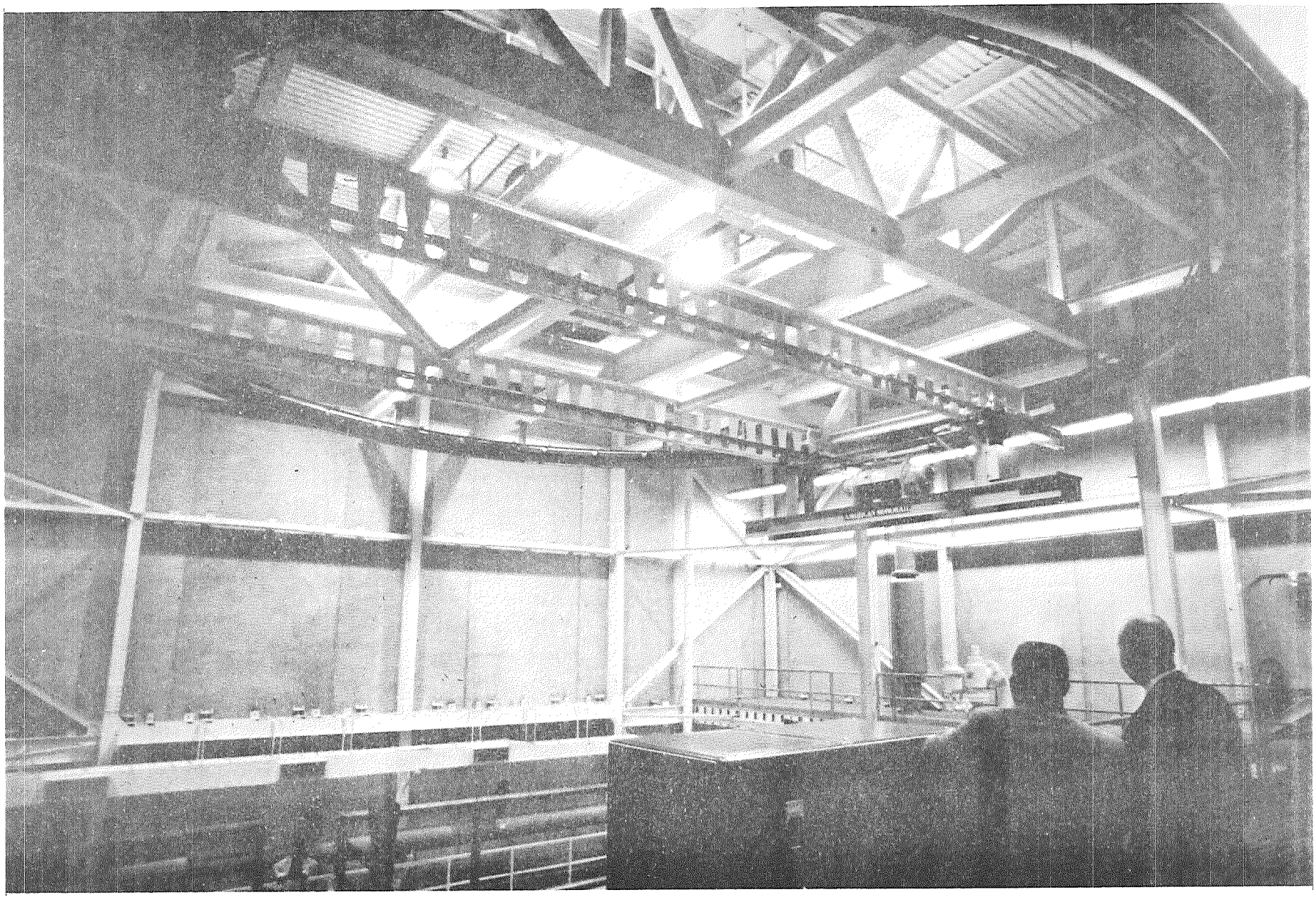

Figure 29. EXISTING CRANE IN BUILDING 49A

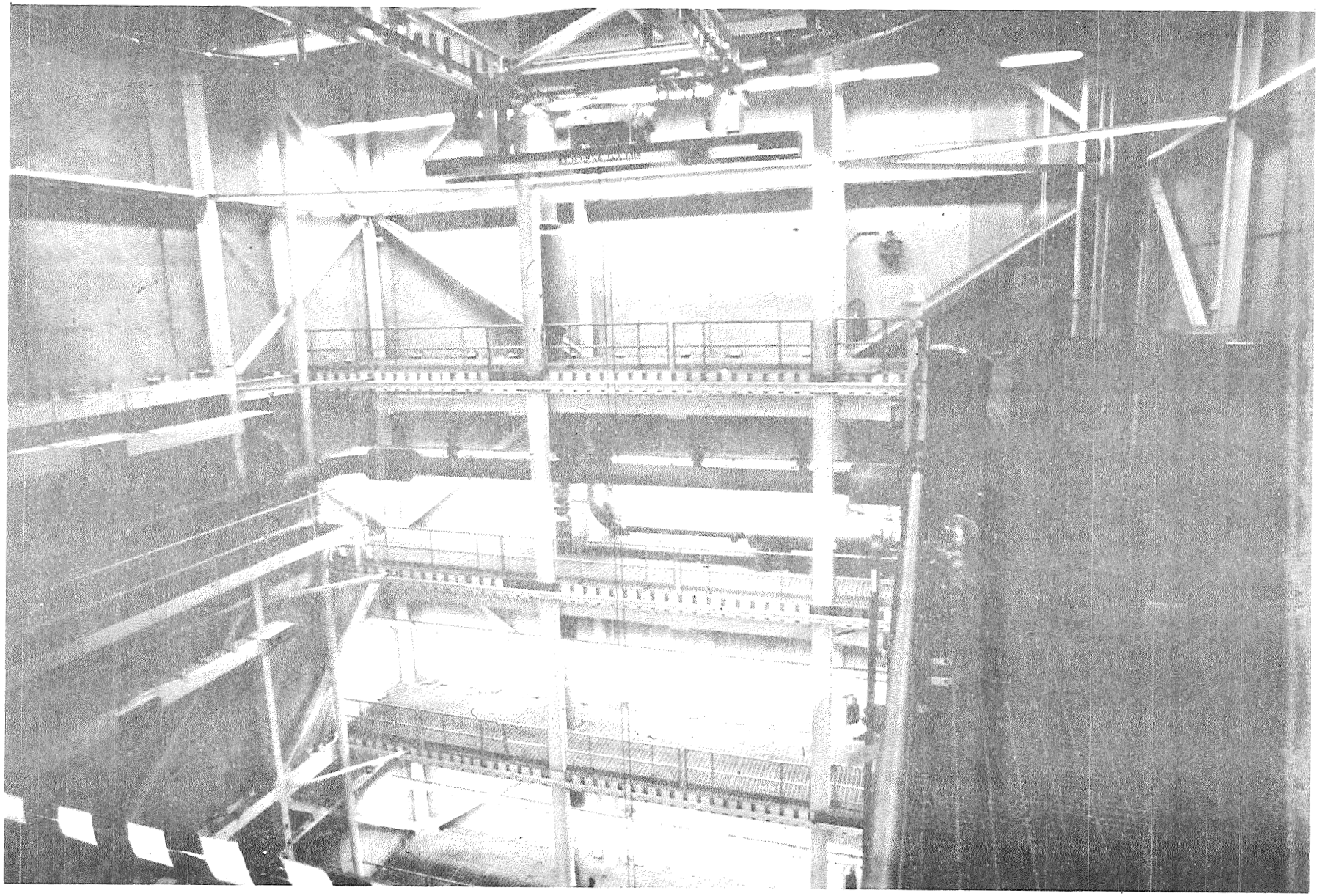

Figure 30. EAST WALL OF BUILDING 49A

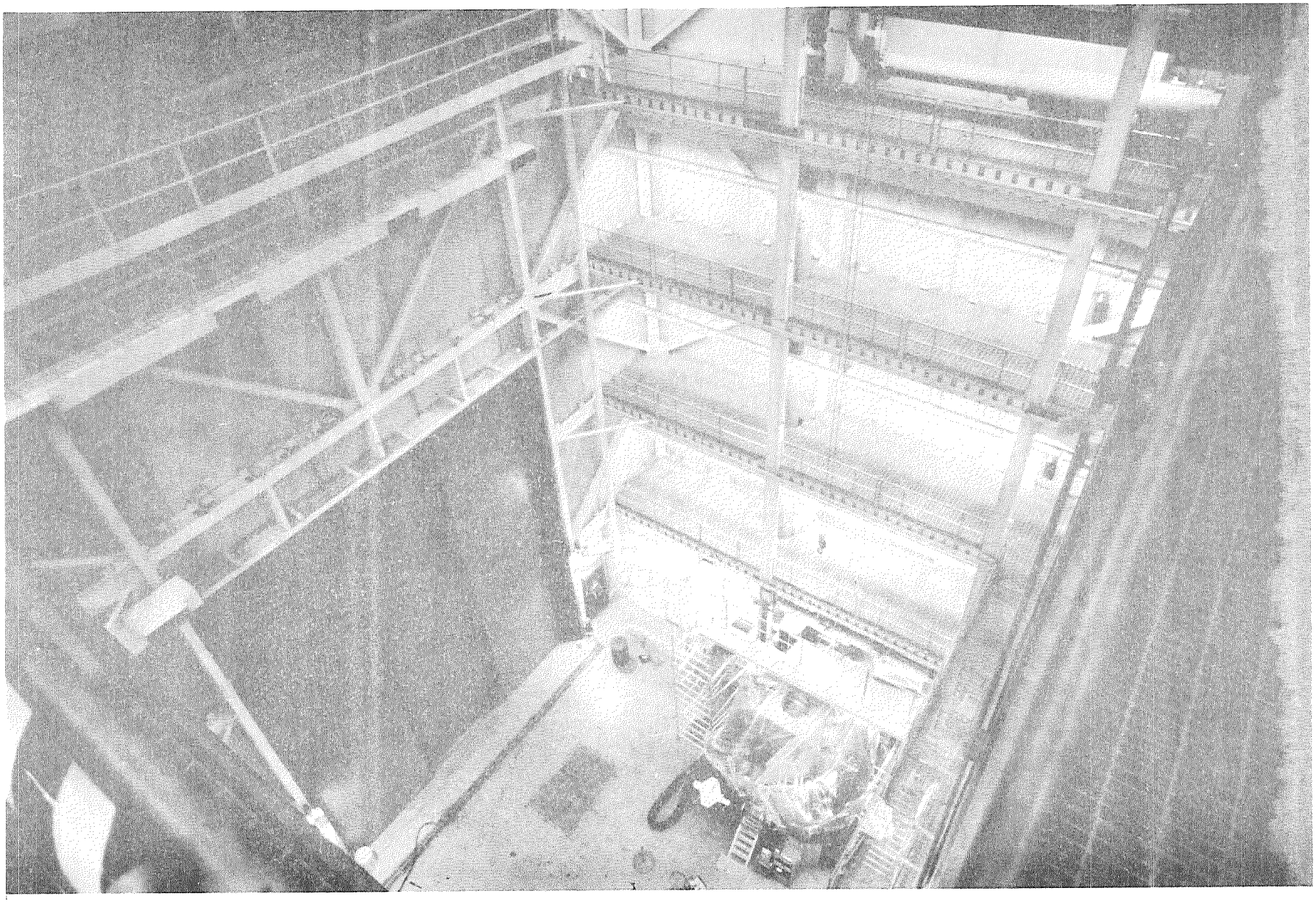

Figure 31. INTERIOR VOLUME OF BUILDING 49A

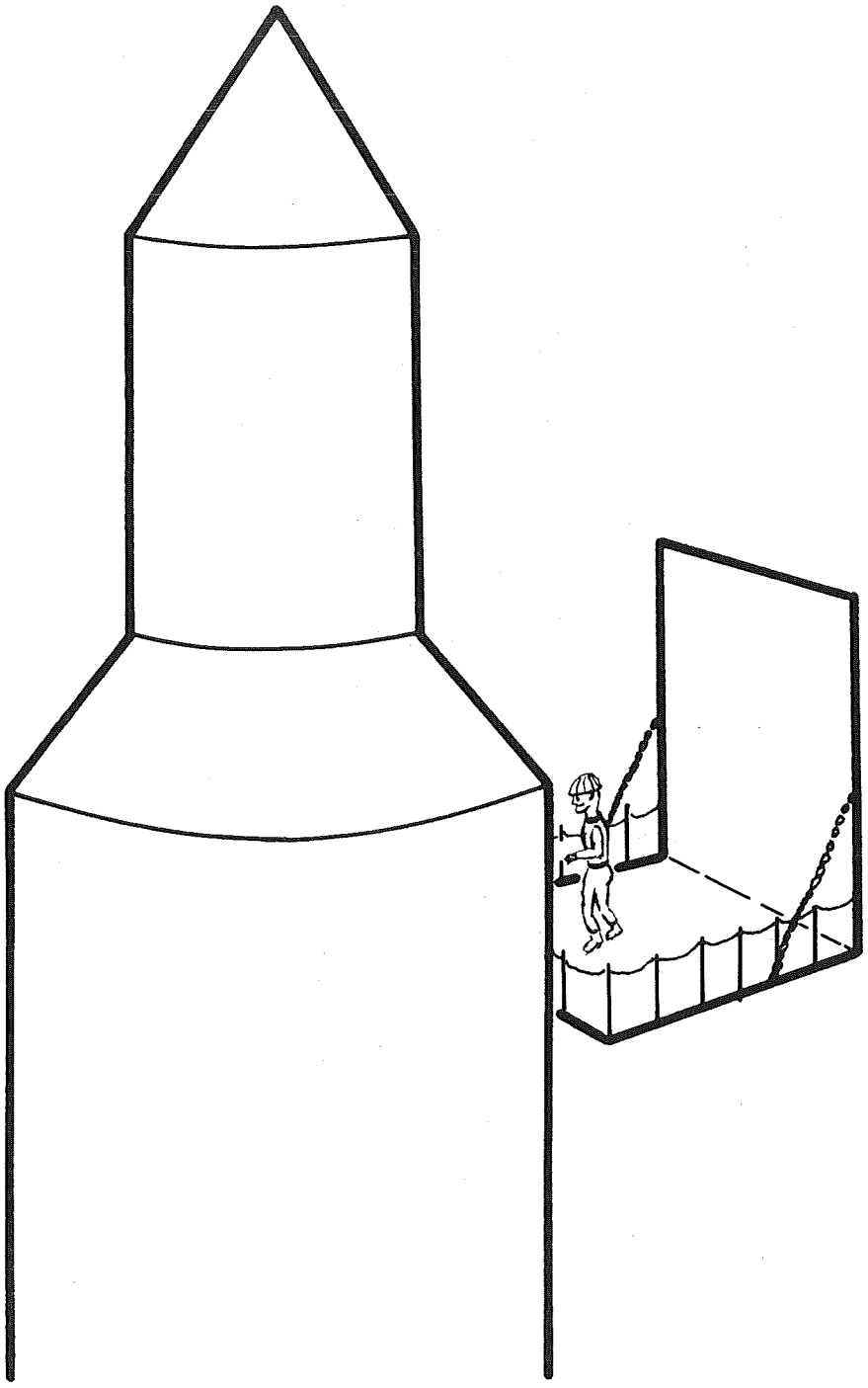

Figure 32. "DRAWBRIDGE" SPECIMEN ACCESS DOOR

REFERENCES

1. Eldred, K.M., Roberts, W.M., and White, R.W., "Structural Vibrations in Space Vehicles," WADD Technical Report 61-62, WPAFB, 1962.

2. Crede, C.E., "Failures Resulting from Vibration," Random Vibration, Vol. 2, Chapter 5, Cambridge: The MIT Press, 1963.

3. Piersol, A.G., "Study of the Interaction of Combined Static and Dynamic Loads," Journal of Sound and Vibration, Vol. 7, p. 319, 1968.

4. Eldred, K.M., and Spice, B.J., "Effect of Static Loads on Structural Vibration Characteristics," Wyle Laboratories Research Staff Report WR 67-11, NASA Contract # NAS8-5384 1967.

5. Weingarten, V.I., "On the Free Vibration of a Thin-Walled Cylindrical Shell Subjected to a Bending Moment," Aerospace Corporation Report No. TRD-269 (4560-40)-4, 1964.

6. Bozich, W.F., "The Vibration and Buckling Characteristics of Cylindrical Shells Under Axial Load and External Pressure," Air Force Flight Dynamics Laboratory, WPAFB, Report No. AFFDL-TR-67-28, 1967.

7. Mixson, J.S., and Naumann, E.C., "Effects of Compressive Load on Shell Frequencies of Isotropic and Foam-Core Sandwich Conical Shell Frustrums," NASA Langley Research Center Working Paper LWP-658.

8. Kennedy, D.R., and Saint, L.D., "Reverberation Room Testing of Space Vehicle Structures," 75th Meeting of Acoustical Society of America, Ottawa, 1968.

9. Eldred, K.M., "Vibroacoustic Environmental Simulation for Aerospace Vehicles," Shock and Vibration Bulletin, No. 37, Part 5, 1968.

10. Potter, R.C., and Crocker, M.J., "Acoustic Prediction Methods for Rocket Engines, Including the Effects of Clustered Engines and Deflected Exhaust Flow," NASA CR-566, October 1966.

11. Lowson, M.V., "Prediction of the Inflight Fluctuating Pressures on Space Vehicles," Wyle Report WR 65-26, NASA Contract No. NAS8-11308, December 1965.

12. Eldred, K.M., Roberts W., White, R., "Structural Vibrations in Space Vehicles," WADD TR 61-62, March 1961.

13. Kinsler, L.E., and Frey, A.R., "Fundamentals of Acoustics," John Wiley and Sons, Inc., 1967.

14. Eldred, K.M., "20,000 Watt High Intensity Noise Facility, Bldg. 262, NASA, MSC, Houston, Wyle Laboratories Research Report WR65-7, NASA Contract No. NAS9-2130, March 1966.

15. Morse, P.M., "Vibration and Sound," McGraw-Hill Book Compnay, Inc. 1948.

16. Sepmeyer, L.W., "Computed Frequency and Angular Distribution of the Normal Modes of Vibration in Rectangular Rooms," Journal of the Acoustical Society of America, 37, 413; 1965.

17. Eldred, K.M., "Problems in the Laboratory Qualification of Structures and Equipment Exposed to Intense Acoustic Environments," IES Symposium, 1964.

18. Wren, R.J., Dorland, W.D., Johnston, J.D., Jr., & Eldred, K.M., "Concept, Design and Performance of the Spacecraft Acoustic Laboratory, Shock and Vibration Bulletin, No. 37, Part 5, 1968.

19. Murray, F.M., "Operational Characteristics of a 100,000 Cubic Foot Acoustic Reverberation Room," Shock and Vibration Bulletin No. 37, Part 5, 1968.

20. Harris, C.M.,"Absorption of Sound in Air in the Audio Frequency Range," JASA Vol. 35, No. 1, p.11, January 1963.

21. Murray, F.M., "Considerations Affecting Modifications to Bldg. 49A, NASA, MSC, Clear Lake, Texas, for Reverberant Testing of Lunar Module LTA-11, Wyle Laboratories Research Report WR69-24, NASA Contract No. NAS9-7484, December 1969.

22. Sharp, B.H., Beauchamp, J.W., "The Transmission Loss of Multilayer Structures," J.Sound Vib. (1969) 9 (3), 383-392.

APPENDIX A

ABSORPTION OF SOUND BY A PANEL IN A REVERBERATION ROOM WALL

The absorption coefficient of a wall panel is given by the ratio of the power absorbed by the panel to the power incident on the panel. Thus:

$$\alpha = \frac{W_p}{W_i} \tag{1}$$

where α is the absorption coefficient,

W is the power,

and p and i subscripts refer to panel and incident, respectively.

The power incident on the wall mounted panel in an ideal diffuse reverberation room is given by:

$$W_i = \frac{\overline{P_r^2}\, S_p}{4\, \rho C} \tag{2}$$

where $\overline{P_r^2}$ is the mean square space average pressure in the reverberant field,

S_p is the area of the panel,

and ρC is the characteristic impedance of air.

The power absorbed by the panel may be divided into two parts, internal and edge structural damping, and radiation damping. At low frequencies, when the panel's bending wavelengths are small relative to an acoustic wavelength, structural damping predominates. At higher frequencies, particularly above coincidence, the situation may be reversed.

The power absorbed by the panel is:

$$W_p = \overline{F_{mn} \cdot V_{mn}} = \frac{\overline{F_{mn}^2}\ \omega \left| H\left(\omega/\omega_{mn}\right) \right| \sin \phi_{mn}}{\omega_{mn}^2\ M_{mn}} \tag{3}$$

where F is the generalized force in the m, n mode,

V is the maximum velocity in the m, n mode,

ω_{mn} is the resonant frequency of the m, n mode,

$$\left|H\left(\omega/\omega_{mn}\right)\right| = \left[\left\{ 1 - \left(\frac{\omega}{\omega_{mn}} \right)^2 \right\}^2 + \left\{ \frac{\omega}{Q\,\omega_{mn}} \right\}^2 \right]^{-1/2}$$

$$\phi_{mn} = \tan^{-1} \left\{ \frac{\frac{\omega}{Q\,\omega_{mn}}}{1 - \left(\frac{\omega}{\omega_{mn}} \right)^2} \right\}$$

Q is the dynamic magnification factor,

and M_{mn} is the generalized mass of the panel in the m, n mode.

For a simply supported panel, whose modes may be expressed in a sine expansion, the generalized mass is one-fourth the total mass, or:

$$M_{mn} = M = \frac{m\,S_p}{4} \tag{4}$$

where m is the mass per unit area.

The generalized force may be written in terms of the pressure acting on the panel, the area and the joint acceptance, or coupling factor, as:

$$\overline{F_{mn}^2} = \overline{p_p^2}\, S_p^2\, j_m^2\, j_n^2 \tag{5}$$

The absorption coefficient equation resulting from a suitable combination of the previous equation is:

$$\alpha_{mn} = 16\left(\frac{\overline{p_p^2}}{\overline{p_r^2}}\right)\left(\frac{\omega\,\rho\,C}{\omega_{mn}^2\, m}\right) j_m^2\, j_n^2 \left| H\,(\omega/\omega_{mn}) \right| \sin\phi \tag{6}$$

For the diffuse field, the mean square panel pressure is twice that of the reverberant field when it can be assumed that the panel motion is small relative to the acoustic particle velocity. With this assumption, Equation (6) becomes:

$$\alpha_{mn} = 32\,\frac{\omega\,\rho\,C}{\omega_{mn}^2\, m}\, j_m^2\, j_n^2 \left| H\,(\omega/\omega_{mn}) \right| \sin\phi \tag{7}$$

The above result enables direct calculation of the absorption coefficient of any panel, utilizing the values of j^2 given in Figure 1 from Reference 1, together with values of $\left| H\,(\omega/\omega_{mn}) \right| \sin\phi$, appropriate to the panel. Whenever the panel's impedance is much greater than the impedance of air, the reaction of the air on both sides of the panel may be ignored in calculating $|H|$. However, when this condition is not fulfilled, the air reactions must be included, and it is convenient to take an impedance approach to the calculation.

The most elementary case is given by a stiff, frictionless piston in an infinite duct as shown in Figure 2. In this case, all motion is parallel to the duct axis, and is assumed of equal amplitude and constant phase in any plane perpendicular to the axis. The equivalent circuit of Figure 2 satisfies the boundary conditions and enables direct calculation of the absorption coefficient from Equation (1).

The impedance of the circuit is:

$$Z = \frac{\rho C}{S} + Z_2 = \frac{2\rho C}{S} + \frac{i\omega M}{S^2} \tag{8}$$

The power dissipated in Z_2 for a sinusoidal wave of amplitude P is given by:

$$W_2 = \frac{2P_1^2 \rho C}{|Z|^2 S} = \frac{2\rho C P_1^2}{S\left[\left(\frac{2\rho C}{S}\right)^2 + \left(\frac{\omega M}{S^2}\right)^2\right]} \tag{9}$$

The absorption coefficient from 1 and 8 is then:

$$\alpha = \frac{W_2}{W_i} = \frac{W_2}{\frac{S P_1^2}{2\rho C}} = \frac{1}{1 + \left(\frac{\omega M}{2\rho C S}\right)^2} \tag{10}$$

This result is identical to that computed for the transmission loss of an infinite limp mass wall, and gives a lower bound to the absorption of sound by a wall panel.

The next more complex case is to add stiffness and structural damping to the piston, as shown in Figure 2b. Then the impedance becomes:

$$Z = \frac{\rho C}{S} + Z_2 = \left(\frac{2\rho C}{S} + \frac{\omega_2 M_2}{QS^2} \right) + i \left(\frac{\omega M_2}{S^2} - \frac{k_2}{\omega S^2} \right)$$

$$= \frac{M_2 \omega_2^2}{\omega S^2} \left\{ \left[\frac{2\rho C \omega S}{M_2 \omega_2^2} + \frac{\omega}{\omega_2 Q} \right] - i \left[1 - \left(\frac{\omega}{\omega_2} \right)^2 \right] \right\} \qquad (11)$$

when

the equation for absorption is:

$$\alpha = \frac{4\rho C \omega S \left[\frac{\rho C \omega S}{M_2 \omega_2^2} + \frac{\omega}{\omega_2 Q} \right]}{M_2 \omega_2^2 \left\{ \left[\frac{2\rho C \omega S}{M_2 \omega_2^2} + \frac{\omega}{\omega_2 Q} \right]^2 + \left[1 - \left(\frac{\omega}{\omega_2} \right)^2 \right]^2 \right\}} \qquad (12)$$

This equation may be used for both a rigid sliding piston restrained by springs and dampers, and an edge constrained flexible piston with bending stiffness and damping. For the first condition, M_2 is the exact value of the piston's mass M_o. However, for the bending case, M_2 is given by:

$$M_2 = \frac{M_o}{4 j_2^2} \qquad (13)$$

where j_2^2 is the standard joint acceptance calculated for the appropriate boundary conditions.

This equation gives a useful prediction of the absorption seen by standing waves which are normal to the panel surface. The value of α for this case is less than that calculated for

the ideal reverberant case. The ratio of the absorption in the diffuse reverberant field to that for normal incidence ranges from 1.0 at low frequencies to 2.0 at higher frequencies when the panel impedance becomes large with respect to the air. This asymptotic higher frequency behavior can be seen in comparing Equation (12) and (13) with Equation (7).

An exact solution for the diffuse reverberant room absorption is given by Morse (Reference 2) in terms of the specific admittance of the panel. The specific admittance (η), using Equation (11), is:

$$\eta = \frac{C}{SZ_2}$$

$$= \frac{\left[\frac{1}{\beta} + \frac{\alpha}{Q}\right] + i\left[1 - \alpha^2\right]}{\beta\left\{\left[\frac{1}{\beta} + \frac{\alpha}{Q}\right]^2 + \left[1 - \alpha^2\right]^2\right\}} \qquad (14)$$

$$= K + i\sigma$$

where $\alpha = \frac{\omega}{\omega_2}$

and $\beta = \frac{M_2 \omega_2^2}{C\omega S}$

The absorption (Reference 2) for the ideal diffuse field is then:

$$\alpha = 8K\left\{1 + \left(\frac{K^2 - \sigma^2}{\sigma}\right) \tan^{-1}\left[\frac{\sigma}{\sigma^2 + K^2 + K}\right] - K\ell n\left[\frac{(K+1)^2 + \sigma^2}{K^2 + \sigma^2}\right]\right\} \qquad (15)$$

The preceding development has resulted in four (4) equations for calculation of the absorption coefficient of a panel, for various boundary conditions and assumptions, as summarized below:

Equation No.	Boundary Conditions and Assumptions
10	Rigid frictionless piston in infinite duct - normal incidence.
12	Flexible damped piston in infinite duct - normal incidence.
7	Flexible damped panel in reverberation room wall, assuming panel impedance is greater than air.
15	Flexible damped panel in reverberation room wall.

The preceding equations have been applied to calculate the absorption coefficient of a typical damped steel wall panel in the LMSC Acoustic Facility. The panel is assumed simply supported and damped by a visco-elastic layer applied to its surface and by friction in the gaskets at the edge. The damping is estimated sufficient to give a Q of 10 or less, and the resonant frequencies will probably be somewhat lower than those calculated because of compliance in the edge mounting. The mode shapes are assumed sinusoidal with mode numbers m and n.

The values utilized for calculation are:

Area (S)	$1.47\ m^2$
Mass (M_o)	87.5 Kg
ρC	$420\ Kg - sec/m^2$
Q	10
j^2	Figure 1

Resonant frequencies

m \ n	1	2	3	4	5
1	21	52.5*	105	178*	272
2		84*	136*	210*	304*
3			188	264*	356
4				335*	430*
5					525

The results are summarized in Figure 3. The upper and lower curves give the general boundaries based on a $Q = 10$ for each type of excitation. An increase in Q would result in a shift of the straight line segments of these curves in the direction of the change.

Two resonances are evident. These are the only ones of those investigated which came in the range of the graph. The fundamental resonance at 21 Hz does not appear to offer difficulty since its absorption is very low at 31 Hz and above. The 3, 1 resonance at 105 Hz does, however, intrude into the operating range. However, the maximum absorption, obtained from both Equations (7) and (15), is .0415 and it does not exceed .02 except in a narrow bandwidth. The normal absorption coefficient fares even better, with a maximum of .028. This result can be lowered somewhat by increasing panel damping, thus lowering Q. However, it appears adequate for the intended purpose.

* Modes whose coupling is theoretically zero for normal incidence and very small for reverberant field excitation.

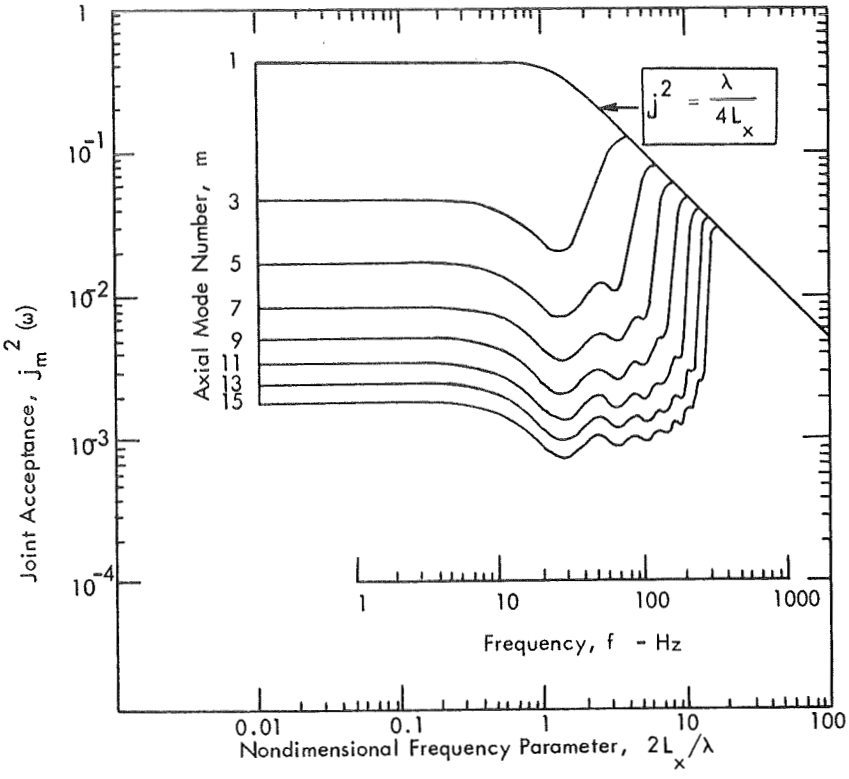

Figure 1. JOINT ACCEPTANCE FOR ODD NUMBERED MODES OF A SIMPLY SUPPORTED PANEL FOR AN IDEAL DIFFUSE REVERBERANT FIELD

a) Normal Incidence Progressive Wave in Infinite Duct of Area S with Stiff Frictionless Piston.

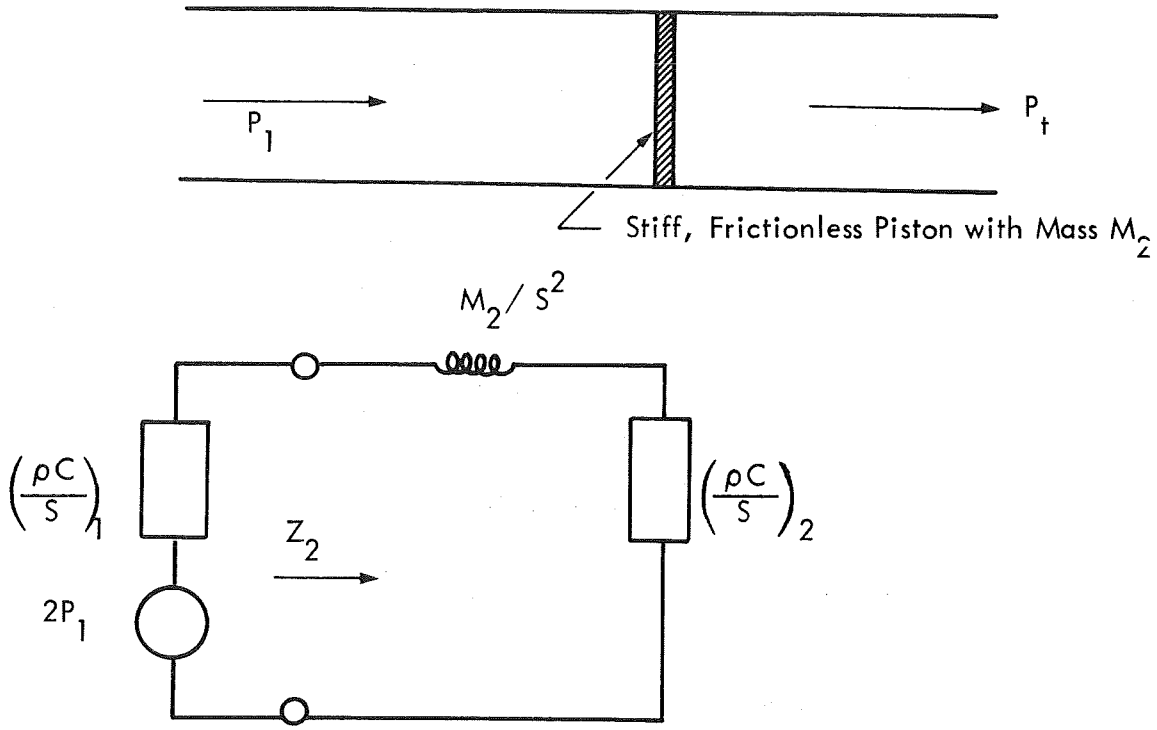

b) Normal Incidence Progressive Wave in Infinite Duct of Area S with Resonant Piston with a Q= 10

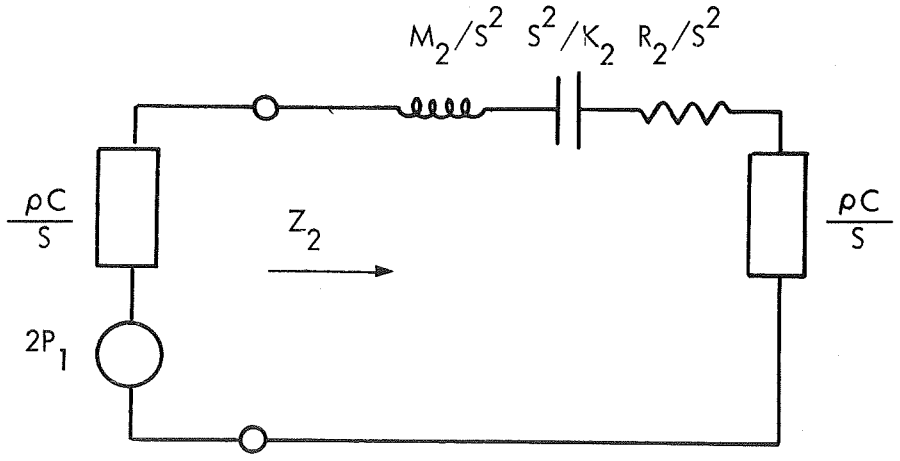

Figure 2

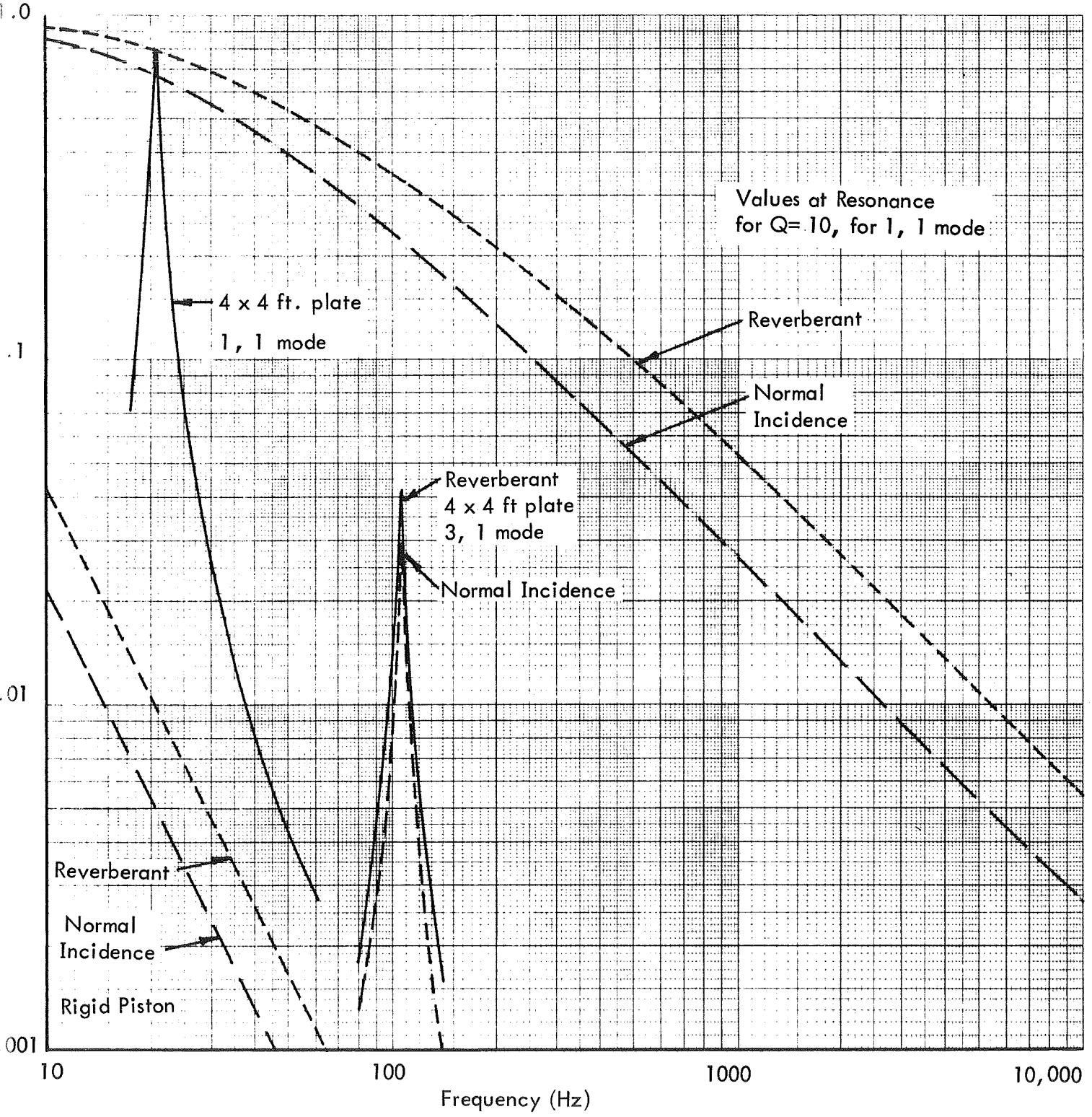

Figure 3. ACOUSTIC ABSORPTION RESULTING FROM 4 x 4 FOOT PANEL UNDER VARIOUS BOUNDARY CONDITIONS

REFERENCES

1. White, R. W., "Predicted Vibration Responses of Apollo Structure and Effects of Pressure Correlation Lengths on Response," Report No. WR 67-4, Contract No. NAS9-5810, (March 1967), Wyle Laboratories - Research Staff.

2. Morse, P. M., Vibration and Sound, Second Edition, McGraw-Hill Book Company, Inc., (1948), pp. 366, 388.